Review Article

phys. stat. sol. (b) **177**, 9 (1993)

Subject classification: 71.36 and 71.45; 71.25; 73.40; S7.15

Fachbereich Physik, Martin-Luther-Universität Halle[1]) *(a) and*
Institut für Halbleiter- und Mikrosystemtechnik, Technische Universität Dresden[2]) *(b)*

Intra- and Intersubband Plasmon-Polaritons in Semiconductor Quantum Wells

By

L. WENDLER (a) and E. KÄNDLER (b)

Contents

---

[1]) Friedemann-Bach-Platz 6, D-06099 Halle, Federal Republic of Germany.
[2]) Mommsenstr. 13, D-01069 Dresden, Federal Republic of Germany.

1. Introduction

Advances in nanometer technologies, i.e. epitaxial layer growth techniques, high-resolution submicrometer lithography, and etching techniques make it possible to realize electronic systems in which the synthesized carrier gases have a dimensionality varying between three and zero. This progress has stimulated enormous activities in the study of low-dimensional systems.

In semiconductor microstructures such as metal–oxide–semiconductor (MOS) systems, single heterostructure (HS) and semiconductor quantum wells (QW), and on the surface of liquid helium, electrons can be confined in very narrow one-dimensional potential wells [1]. Following, in single quantum wells (SQW), the motion of the carriers (electrons, holes) is quasi-free parallel to the heterointerfaces, but confined within a narrow channel perpendicular to the heterointerfaces. Hence, the electrons or holes of these systems form a quasi-two-dimensional electron or hole gas (Q2DEG or Q2DHG). Because the width of this channel is usually in the order of the de Broglie wavelength of the carriers and at low temperatures much smaller than their elastic mean free path, the size-quantization of the carrier motion perpendicular to the heterointerfaces becomes important. Hence, the spectrum of the carriers consists of discrete subbands. This is true because the subband spacing is much larger than the energy broadening induced by scattering processes.

Besides of size-quantization there is still another property, typical for semiconductor microstructures. With the modulation-doping technique it is possible to separate the carriers spatially from the parent ionized impurities. This separation drastically reduces ionized impurity scattering and, consequently, gives rise to very high carrier mobilities at low temperatures. A new device concept called high electron mobility transistor (HEMT) [2] has been developed on the base of these structures. Because of their novel properties semiconductor microstructures represent a large potential for applications. Furthermore, semiconductor microstructures are related to new fundamental physical problems [3 to 5].

Most of the work was done with the III–V compound semiconductors. Among all possible combinations of semiconductors, the lattice-matched (or at least closely matched) system GaAs-$Ga_{1-x}Al_xAs$ has attracted most interest.

With sufficiently fine confinement within the plane of a Q2DEG, the motion of the carriers will become quantized in the layer plane as well as perpendicular to the plane. Simultaneous confinement perpendicular and in one direction parallel to the layer will produce a so-called quantum-well wire (QWW). Confinement perpendicular to the plane and in both directions parallel to the plane results in a quantum dot (QD). These low-dimensional systems, called semiconductor nanostructures, are typified by novel physical properties including both, mesoscopic coherence phenomena, such as universal conductance fluctuations in the electron transport [6] as well as ballistic-transport phenomena, such as the quantization of the conductance [7, 8]. The manufacturing of these structures is only possible because of the recent considerable efforts in high-resolution nanometer-scale lithography.

Many aspects of the physics of low-dimensional electron systems have been studied. Much attention has been focused on the electronic collective excitations of the Q2DEG. Most of the work was done for the strictly two-dimensional model of the electron gas. The dispersion of two-dimensional plasmons of a very thin metallic layer has first been derived by Ritchie [9] and Ferrell [10]. Stern [11] derived the polarization function and the 2D plasmon dispersion in the self-consistent field (SCF) approximation [12]. In these works it was found out that in the long-wavelength limit, neglecting retardation the frequency of the

2D plasmon is $\omega \sim \sqrt{q_\parallel}$,where $q_\parallel = |\boldsymbol{q}_\parallel|$ is the absolute value of the wave vector in the plane parallel to the heterointerface. Chaplik [13] calculated the dispersion relation of 2D plasmons for Si-MOS systems including the perfectly screening property of the gate.

Consideration of multiple-layer systems has also usually been restricted to one-dimensional arrays of strict 2DEG's. Visscher and Falicov [14] have discussed the static dielectric function of this so-called layered electron gas (LEG) model in the random-phase approximation (RPA). Fetter [15] has given a detailed discussion of the plasmons of the LEG in a hydrodynamic approximation. A similar calculation using the equation-of-motion method to obtain the RPA was done by Apostol [16]. The plasmons were also investigated for semi-infinite LEG systems by Giuliani and Quinn [17], Jain [18], and for finite LEG systems by Grecu [19] and Jain and Allen [20].

The effects of a perpendicular quantizing magnetic field on the collective excitations of a strict 2DEG, the 2D magnetoplasmons, were first discussed by Chaplik [13] and Chiu and Quinn [21] followed by a lot of works [22 to 24]. The magnetoplasmons of the LEG model are discussed by Kobayashi et al. [25], Das Sarma and Quinn [26], Bloss and Brody [27], Tselis and Quinn [28], and Gasser and Täuber [29]. Since semiconductor microstructures are mostly composed of the weakly polar compound semiconductor materials of the III–V series, optical phonons occur, which interact with the plasmons. In most of all papers only the ordinary 3D bulk longitudinal optical (LO) phonon is considered to interact with the 2D plasmons [27, 28, 30 to 32].

For a range of phenomena the strict-2DEG model is a good approximation. However, there are phenomena for which the small but finite thickness of the electron system cannot be neglected. In this case the electronic subband structure becomes important. The effect of the finite layer thickness on the collective excitations was considered by Chen et al. [33], Dahl and Sham [34], Eguiluz and Maradudin [35], and others [36 to 41]. Taking into account the finite thickness of the electron system, two types of plasmons, intra- and intersubband plasmons, occur. The intrasubband plasmon is the analog to the 2D plasmons. It is connected with electron motion within one subband. But the intersubband plasmon is connected with electron motion between two different subbands. Wendler and coworkers [42 to 49] considered the plasmon–phonon and magnetoplasmon–phonon coupling including the confined LO phonons and the interface optical phonons [50 to 52] of the layered systems using the full RPA polarization function of the Q2DEG.

In most of these works the coupling between the intra- and intersubband modes is neglected. Das Sarma [53], Jain and Das Sarma [54], and Wendler et al. [46] considered the intersubband mixing and obtained the result that the effect on the dispersion curves is small for the usual thickness of the quantum wells. Landau damping of the plasmons is considered by Xiaoguang et al. [31, 32] for a strict 2DEG interacting with ordinary 3D bulk LO phonons and by Wendler [45] for a Q2DEG interacting with the complete set of optical phonon modes of a double heterostructure (DHS).

In going beyond the RPA, Jonson [55], Rajagopal [56], and Czachor et al. [57] considered the effects of exchange and correlation on the 2D plasmons and Wendler and Grigoryan [47] investigated these effects for a Q2DEG interacting with the optical phonons of a DHS. The collective expitations in a spin-polarized Q2DEG are considered by Ryan [58].

First results about plasmons in QWW's [59 to 63] and arrays of QD's [64, 65] are published.

2D plasmons have been observed first by Grimes and Adams [66] for electrons on the surface of liquid helium. For Si-MOS systems 2D plasmons have been firstly investigated by Allen et al. [67] and by Theis et al. [68], using far-infrared (FIR) transmission

spectroscopy. FIR emission of 2D plasmons has been observed by Tsui et al. [69]. Experiments on 2D plasmons in the electron space-charge layers of GaAs-$Ga_{1-x}Al_xAs$ HS's have also been performed [70]. Further, Raman scattering is used to probe the intra- and intersubband plasmons of GaAs-$Ga_{1-x}Al_xAs$ SL's [71 to 74]. Review articles on 2D plasmons are published, e.g., by Theis [75], Höpfel and Gornik [76], Chaplik [77], Heitmann [78], and Batke et al. [70, 79].

The interest in the experimental study of the plasmons of the Q2DEG arises in particular from the possibility that the charge density can be varied over several orders of magnitude in these systems. With the charge density, many related physical properties, e.g. Fermi energy, Fermi wave vector, etc., can be varied. This and the possible variation of the thickness of the quantum well allows a detailed investigation of different mechanisms that determine the plasmon resonance itself and interactions of plasmons with different types of excitations such as the optical phonons [42 to 49], acoustic phonons [80], and piezoelectric waves [81]. With the remotely doped parabolic quantum wells it is possible to produce a new very interesting physical system containing a Q2DEG. In remotely doped parabolic quantum wells it is possible to synthesize a Q2DEG which is almost three-dimensional but with much weaker electron–impurity interactions than in conventionally doped bulk semiconductors [82 to 84]. Further, in these so-called wide parabolic quantum wells it might be possible to observe broken-symmetry ground states [85 to 87]. The plasmons in such systems are observed recently with FIR transmission spectroscopy using a grating coupler technique [88, 89].

In the many-particle theory dynamical properties can be treated within the framework of linear response theory. In principle, there are two different response formalisms used to calculate the properties of the collective excitations. In the density-response treatment the response of the system to an external charge density is considered. In the current-response treatment, however, the response of the system to an external current density is considered. The plasmons resulting from the density-response treatment are unretarded, because the equations of electrostatics are used to relate the densities with the fields. In the case of the current-response, the modes are retarded, i.e. they are modes of the solid coupled to photons and hence they are plasmon-polaritons. However, in the case of a homogeneous three-dimensional electron gas (3DEG) of an isotropic solid the longitudinal part of the current-response is strictly the same as in the density-response. As shown by Wendler and Kändler [90] this is not valid for a Q2DEG. In this case the collective excitations of the density response are only correct in the unretarded limit.

The retardation effects on the collective excitations are considered by Chen et al. [33], Dahl and Sham [34], Eguiluz and Maradudin [35], Rajagopal [56], Tselis and Quinn [91], Toyoda et al. [92], King-Smith and Inkson [93] and by other workers.

The aim of this paper is to review the density- and current-response of the Q2DEG and to give a detailed investigation of the collective excitations for both density- and current-response within a full RPA treatment. In our calculations no simplifying approximations for the RPA response functions are made. This allows the comparison of the results for all wave vectors. Further, for the first time we have included in the calculations, represented in this review article, the image effects on the scalar and vector potential arising from the different polarizabilities of the different semiconductors forming the quantum well structure. Hence, this paper generalizes the earlier works of Dahl and Sham [34], Eguiluz and Maradudin [35], and King-Smith and Inkson [93] on both, electrodynamics as well as quantum mechanics. Our aim, first, is to give a rigorous comparison between the density-

and the current response and, second, to investigate the effects of the image terms on both density- as well as current-response for the configuration used in experiments.

This review paper is organized as follows. At first we discuss the electrodynamics of the layered semiconductor system including the case of electrostatics in Section 3. After this we consider the ground state and the response properties of the Q2DEG confined within the quantum well using many-particle theory in Section 4. We then calculate the dispersion curves of intra- and intersubband plasmons and plasmon-polaritons in Sections 3 and 5. These collective excitations are discussed in detail in Section 5.

2. General Consideration

Many experiments in condensed matter physics measure the linear response to an external perturbation. In principle, there are two different response formalisms used to calculate the electromagnetic response properties of an electron gas. In the density-response formalism the response of the system to an external charge density is calculated. The corresponding response function is the density-response or polarization function. The collective excitations connected with the density-response are the plasmons. Because the physical system is perturbed by an external charge density, usually the electrodynamics of the system is represented by Maxwell's equations of electrostatics, i.e., Poisson's equation is used to relate the charge density to the electric field. Following, the plasmons are unretarded collective excitations.

On the other hand, in the current-response formalism the response of the system to an external current density is calculated. The corresponding response function is the current-response or polarization tensor. The collective excitations connected with the current-response are the plasmon-polaritons. The presence of an external current density indicates that the electrodynamics of the system is represented by the full set of Maxwell's equations. Therefore, the plasmon-polaritons are coupled excitations of the electron gas and of photons.

In the well-known case of a homogeneous 3DEG of an isotropic solid, the current-response tensor consists of two parts: the longitudinal and the transverse ones. The longitudinal part is essentially the same as the density-response function. But this is, in general, not true for a Q2DEG in a layered semiconductor quantum well structure [90]. The physical reason is that in layered structures of isotropic materials the electromagnetic fields are p- or s-polarized and hence, purely longitudinal fields cannot exist.

For the calculation of the dispersion relation of the electronic collective excitations it is therefore necessary to consider both the electrostatics and the electrodynamics of the layered systems. The electromagnetic response theory consists of two parts. The first part is the electrodynamics (or electrostatics) which gives an answer to the question which fields are produced by the sources. The resonances in the resulting equations describe the dispersion relation of the collective excitations. But in these equations there are unknown functions, the response functions. These response functions must be calculated using quantum theory. Hence, the equations describing the response of the electron gas in a layered quantum well structure represent a combination of a Kubo formula with Maxwell's equations [94].

In this paper we consider the linear response of the Q2DEG of a DHS. The DHS (Fig. 1) which is under consideration in this paper consists of a smaller gap semiconductor ($\nu = 1$) for $a > z > 0$ (for instance GaAs) which is embedded between a wider gap semiconductor ($\nu = 2$) for $a + b > z > a$ and $0 > z$ ($\nu = 3$) (for instance $Ga_{1-x}Al_xAs$). With respect to a real DHS and experiments the region $z > a + b$ is filled by vacuum ($\nu = 0$). Due to the

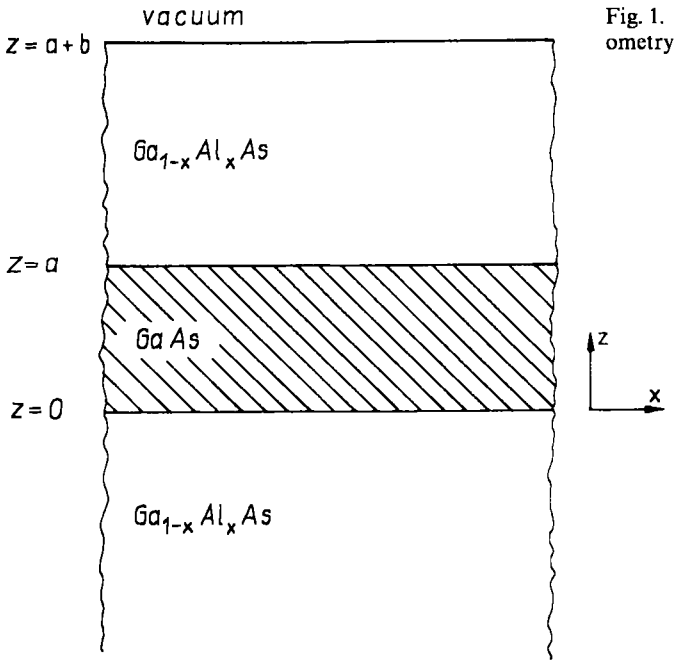

Fig. 1. Schematic arrangement of the geometry of a double heterostructure

conduction band discontinuity at the two heterointerfaces at $z = 0$ and $z = a$ a one-dimensional potential well arises to confine the electron motion to the smaller gap semiconductor layer.

3. Electrodynamics of Layered Semiconductor Quantum Well Structures

3.1 Electrostatics

The Maxwell equations of electrostatics are

$$\nabla \cdot (\varepsilon_0 \varepsilon_b(z)\, \boldsymbol{E}(\boldsymbol{x})) = \varrho^{\mathrm{ind}}(\boldsymbol{x}) + \varrho^{\mathrm{ext}}(\boldsymbol{x}), \tag{1}$$

$$\nabla \times \boldsymbol{E}(\boldsymbol{x}) = \boldsymbol{0}, \tag{2}$$

where $\boldsymbol{E} = \boldsymbol{E}^{\mathrm{total}}$ is the total electric field that appears in the usual version of Maxwell's equations, $\varepsilon_b(z)$ is the background dielectric function which is the constant ε_{b_v} in each semiconductor of the layered system, and ϱ^{ind} and ϱ^{ext} are the induced and the external macroscopic charge densities, respectively. Defining the total scalar potential Φ as $\boldsymbol{E} = -\nabla\Phi$, (1) and (2) produce the following Poisson equation:

$$\nabla \cdot (\varepsilon_b(z)\, \nabla\Phi(\boldsymbol{x})) = -\frac{1}{\varepsilon_0} (\varrho^{\mathrm{ind}}(\boldsymbol{x}) + \varrho^{\mathrm{ext}}(\boldsymbol{x})). \tag{3}$$

For a layered system it is convenient to solve Poisson's equations with the help of the Green's function $D(\boldsymbol{x}, \boldsymbol{x}')$. This Green's function describes the electrostatic problem for the non-magnetic background semiconductor characterized by the dielectric function $\varepsilon_b(z)$, without the Q2DEG. It satisfies the boundary conditions at $z = 0, a, a + b$, and at $z = \pm\infty$

(see Fig. 1) and is calculated in Appendix A. For a layered system in which the materials have different polarizabilities the Green's function of the Poisson equation contains two parts, the direct Coulomb and image parts. The formal solution for the scalar potential is

$$\Phi(\boldsymbol{x}) = \frac{1}{\varepsilon_0} \int \mathrm{d}^3x'\, D(\boldsymbol{x}, \boldsymbol{x}')\, (\varrho^{\mathrm{ind}}(\boldsymbol{x}') + \varrho^{\mathrm{ext}}(\boldsymbol{x}'))\,. \tag{4}$$

A time-dependent external charge density ϱ^{ext}, or the corresponding external scalar potential Φ^{ext}, induces a redistribution of the charge within the system, the induced charge density ϱ^{ind} which is related to the induced electron number density n_{ind} by $\varrho^{\mathrm{ind}} = -en_{\mathrm{ind}}$ (electron charge $-e$). If the perturbation is weak, the system will respond linearly. Linear response means that the signal is directly proportional to the intensity of the external perturbation. The response function describing the linear response of the system to the external scalar potential is the quasi-density response, or reducible polarization function $\Pi(\boldsymbol{x}, \boldsymbol{x}' \mid t, t')$, defined by

$$\varrho^{\mathrm{ind}}(\boldsymbol{x}, t) = \int \mathrm{d}^3x' \int \mathrm{d}t'\, \Pi(\boldsymbol{x}, \boldsymbol{x}' \mid t, t')\, \Phi^{\mathrm{ext}}(\boldsymbol{x}, t')\,. \tag{5}$$

The induced charge density is a source of the induced scalar potential. The summation of all the scalar potentials is the total scalar potential entering Poisson's equation. This potential is also called in response theory the self-consistent potential $V^{\mathrm{sc}} = -e\Phi$. The response function describing the linear response of the system to the total scalar potential is the density-response, or irreducible (proper) polarization function, $P(\boldsymbol{x}, \boldsymbol{x}' \mid t, t')$ defined by

$$\varrho^{\mathrm{ind}}(\boldsymbol{x}, t) = \int \mathrm{d}^3x' \int \mathrm{d}t'\, P(\boldsymbol{x}, \boldsymbol{x}' \mid t, t')\, \Phi(\boldsymbol{x}', t')\,. \tag{6}$$

We note that often the density-response function is defined by $n_{\mathrm{ind}} = PV^{\mathrm{sc}}$ with the result that this function differs by a factor of e^2 from that defined in (6). But if we want to consider both, the density- and current-response, it seems the definition (6) is the more convenient one.

Using (6) in the formal solution (4) of Poisson's equation we obtain

$$\Phi(\boldsymbol{x}, t) = \Phi^{\mathrm{ext}}(\boldsymbol{x}, t) + \frac{1}{\varepsilon_0} \int \mathrm{d}^3x' \int \mathrm{d}^3x'' \int \mathrm{d}t''\, D(\boldsymbol{x}, \boldsymbol{x}')\, P(\boldsymbol{x}', \boldsymbol{x}'' \mid t, t'')\, \Phi(\boldsymbol{x}'', t'')\,. \tag{7}$$

Because we investigate stationary problems in systems which are spatially homogeneous in the x–y plane it is convenient to introduce two-dimensional Fourier series,

$$\Phi(\boldsymbol{x}, t) = \frac{1}{2\pi A} \sum_{\boldsymbol{q}_\parallel} \int \mathrm{d}\omega\, \mathrm{e}^{i(\boldsymbol{q}_\parallel \boldsymbol{x}_\parallel - \omega t)}\, \Phi(\boldsymbol{q}_\parallel; z \mid \omega)\,, \tag{8}$$

$$\Phi(\boldsymbol{q}_\parallel; z \mid \omega) = \int \mathrm{d}^2x_\parallel \int \mathrm{d}t\, \mathrm{e}^{-i(\boldsymbol{q}_\parallel \boldsymbol{x}_\parallel - \omega t)}\, \Phi(\boldsymbol{x}, t)\,, \tag{9}$$

where $\boldsymbol{x}_\parallel = (x, y, 0)$ and $\boldsymbol{q}_\parallel = (q_x, q_y, 0)$ are the two-dimensional position and wave vector in the x–y plane. We have applied Born-von Kármán periodic boundary conditions in this plane with the unit area A. Using (9) the scalar potential is given by

$$\Phi(\boldsymbol{q}_\parallel; z \mid \omega) = \Phi^{\mathrm{ext}}(\boldsymbol{q}_\parallel; z \mid \omega) + \frac{1}{\varepsilon_0} \int \mathrm{d}z' \int \mathrm{d}z''\, D(\boldsymbol{q}_\parallel; z, z')\, P(\boldsymbol{q}_\parallel; z', z'' \mid \omega)\, \Phi(q_\parallel; z'' \mid \omega)\,. \tag{10}$$

From (10) and the corresponding equation containing $\Pi(\boldsymbol{q}_\parallel; z, z' \mid \omega)$ it is possible to derive a relation between Π and P. It follows:

$$\Pi(\boldsymbol{q}_\parallel; z, z' \mid \omega) = P(\boldsymbol{q}_\parallel; z, z' \mid \omega) + \int \mathrm{d}z'' \int \mathrm{d}z''' \, P(\boldsymbol{q}_\parallel; z, z'' \mid \omega) \times D(\boldsymbol{q}_\parallel; z'', z''') \, \Pi(\boldsymbol{q}_\parallel; z''', z' \mid \omega) . \tag{11}$$

From the point of view of the density-response formalism it is usual to define the total longitudinal dielectric response function $\varkappa_\mathrm{L}(\boldsymbol{x}, \boldsymbol{x}' \mid \omega)$ and its inverse $\varkappa_\mathrm{L}^{-1}(\boldsymbol{x}, \boldsymbol{x}' \mid \omega)$ which are defined in the sense of screening functions by

$$\Phi^{\mathrm{ext}}(\boldsymbol{x}, \omega) = \int \mathrm{d}^3x' \, \varkappa_\mathrm{L}(\boldsymbol{x}, \boldsymbol{x}' \mid \omega) \, \Phi(\boldsymbol{x}', \omega) , \tag{12}$$

$$\Phi(\boldsymbol{x}, \omega) = \int \mathrm{d}^3x' \, \varkappa_\mathrm{L}^{-1}(\boldsymbol{x}, \boldsymbol{x}' \mid \omega) \, \Phi^{\mathrm{ext}}(\boldsymbol{x}', \omega) . \tag{13}$$

From the last two equations and (9) and (10) it follows:

$$\varkappa_\mathrm{L}(\boldsymbol{q}_\parallel; z, z' \mid \omega) = \delta(z - z') - \frac{1}{\varepsilon_0} \int \mathrm{d}z'' \, D(\boldsymbol{q}_\parallel; z, z'') \, P(\boldsymbol{q}_\parallel; z'', z' \mid \omega) \tag{14}$$

and

$$\varkappa_\mathrm{L}^{-1}(\boldsymbol{q}_\parallel; z, z' \mid \omega) = \delta(z - z') + \frac{1}{\varepsilon_0} \int \mathrm{d}z'' \, D(\boldsymbol{q}_\parallel; z, z'') \, \Pi(\boldsymbol{q}_\parallel; z'', z' \mid \omega) . \tag{15}$$

We note that the meaning longitudinal arises from $\nabla \times \boldsymbol{E} = \boldsymbol{0}$. For a 3D homogeneous and isotropic solid this implies that $\boldsymbol{E} \parallel \boldsymbol{q}$, where $\boldsymbol{q}$ is the 3D wave vector. But for a layered system the word "longitudinal" does not necessarily mean parallel to $\boldsymbol{q}_\parallel$. From the point of view of the classical macroscopic electrodynamics it is usual to define the dielectric tensor $\varepsilon_{\alpha\beta}(\boldsymbol{x}, \boldsymbol{x}' \mid \omega)$ where $\alpha, \beta = x, y, z$. This dielectric tensor relates the electric field $\boldsymbol{E}$ with the displacement field $\boldsymbol{D}$ according to

$$D_\alpha(\boldsymbol{x}, \omega) = \varepsilon_0 \sum_\beta \int \mathrm{d}^3x' \, \varepsilon_{\alpha\beta}(\boldsymbol{x}, \boldsymbol{x}' \mid \omega) \, E_\beta(\boldsymbol{x}', \omega) = \varepsilon_0 \varepsilon_\mathrm{b}(z) \, E_\alpha(\boldsymbol{x}, \omega) + P_\alpha(\boldsymbol{x}, \omega) , \tag{16}$$

where the dielectric polarization field $\boldsymbol{P}$ is related to the induced charge density according to

$$\varrho^{\mathrm{ind}}(\boldsymbol{x}, \omega) = -\sum_\alpha \frac{\partial}{\partial x_\alpha} P_\alpha(\boldsymbol{x}, \omega) . \tag{17}$$

Using these definitions and (6) it follows:

$$P(\boldsymbol{x}, \boldsymbol{x}' \mid \omega) = \varepsilon_0 \sum_{\alpha, \beta} \frac{\partial^2}{\partial x_\alpha \partial x'_\beta} \left(\varepsilon_\mathrm{b}(z) \, \delta(\boldsymbol{x} - \boldsymbol{x}') \, \delta_{\alpha\beta} - \varepsilon_{\alpha\beta}(\boldsymbol{x}, \boldsymbol{x}' \mid \omega) \right) . \tag{18}$$

It is important to note that for layered systems there is a basic difference between $\varkappa_\mathrm{L}$ and $\varepsilon_{\alpha\beta}$. Whereas $\varepsilon_{\alpha\beta}$ only incorporates the sources, $\varkappa_\mathrm{L}$ in addition contains as a screening function all information about the geometry. Only for isotropic and homogeneous 3D systems (14) and (18) give the same result: $\varkappa_\mathrm{L}(\boldsymbol{q}, \omega) = \varepsilon_\mathrm{L}(\boldsymbol{q}, \omega)$, where $\varepsilon_\mathrm{L}(\boldsymbol{q}, \omega)$ is the longitudinal part of $\varepsilon_{\alpha\beta}(\boldsymbol{q}, \omega)$.

The dispersion relation for the plasmons of the quantum-well structure is obtained using (10) for a finite total scalar potential with no applied external potential. The condition for the existence of collective excitations reads

$$\delta(z - z') - \frac{1}{\varepsilon_0} \int \mathrm{d}z'' \, D(\boldsymbol{q}_\parallel; z, z'') \, P(\boldsymbol{q}_\parallel; z'', z' \mid \omega) = 0 . \tag{19}$$

3.2 Electrodynamics

The full set of Maxwell's equations is

$$\nabla \cdot (\varepsilon_0 \varepsilon_b(z)\, \boldsymbol{E}(\boldsymbol{x}, t)) = \varrho^{\mathrm{ind}}(\boldsymbol{x}, t) + \varrho^{\mathrm{ext}}(\boldsymbol{x}, t)\,, \tag{20}$$

$$\nabla \times \boldsymbol{E}(\boldsymbol{x}, t) = -\frac{\partial}{\partial t} \boldsymbol{B}(\boldsymbol{x}, t)\,, \tag{21}$$

$$\nabla \cdot \boldsymbol{B}(\boldsymbol{x}, t) = 0\,, \tag{22}$$

$$\nabla \times \boldsymbol{B}(\boldsymbol{x}, t) = \mu_0 \varepsilon_0 \varepsilon_b(z) \frac{\partial}{\partial t} \boldsymbol{E}(\boldsymbol{x}, t) + \mu_0 \boldsymbol{j}^{\mathrm{ind}}(\boldsymbol{x}, t) + \mu_0 \boldsymbol{j}^{\mathrm{ext}}(\boldsymbol{x}, t)\,, \tag{23}$$

where $\boldsymbol{j}^{\mathrm{ind}}$ and $\boldsymbol{j}^{\mathrm{ext}}$ are the induced and external macroscopic current densities, respectively. We assume the media to be non-magnetic and notice that both types of current and charge densities must satisfy the equation of continuity, e.g.

$$\nabla \cdot \boldsymbol{j}^{\mathrm{ind}}(\boldsymbol{x}, t) + \frac{\partial}{\partial t} \varrho^{\mathrm{ind}}(\boldsymbol{x}, t) = 0\,. \tag{24}$$

The total vector potential $\boldsymbol{A}$ is defined by $\boldsymbol{B} = \nabla \times \boldsymbol{A}$ and the total scalar potential Φ by $\boldsymbol{E} = -\nabla\Phi - \frac{\partial}{\partial t}\boldsymbol{A}$. Because of the gauge invariance of the potentials: $\boldsymbol{A} \to \boldsymbol{A}' = \boldsymbol{A} + \nabla\Lambda$ and $\Phi \to \Phi' = \Phi - \frac{\partial}{\partial t}\Lambda$, with Λ a scalar field, it is necessary to use a gauge fixing condition. In the following we use the gauge $\Phi = 0$. From Maxwell's equations and the definition of the vector potential the inhomogeneous wave equation follows:

$$\Delta \boldsymbol{A}(\boldsymbol{x}, t) - \nabla(\nabla \cdot \boldsymbol{A}(\boldsymbol{x}, t)) + \varepsilon_b(z) \frac{\omega^2}{c^2} \boldsymbol{A}(\boldsymbol{x}, t) = -\mu_0 \boldsymbol{j}^{\mathrm{ind}}(\boldsymbol{x}, t) - \mu_0 \boldsymbol{j}^{\mathrm{ext}}(\boldsymbol{x}, t)\,. \tag{25}$$

For a layered system it is useful to solve this equation with help of the Green's tensor $D_{\alpha\beta}(\boldsymbol{x}, \boldsymbol{x}' \mid t, t')$. This Green's tensor expresses the propagation of electromagnetic waves in the background semiconductors without the Q2DEG. It contains direct and image parts for layered systems, in which the materials have different polarizabilities, and satisfies the boundary conditions at the heterointerfaces and at infinity. The components of the Green's tensor are calculated in Appendix A. The formal solution for the vector potential is

$$A_\alpha(\boldsymbol{x}, t) = \mu_0 \sum_\beta \int \mathrm{d}^3x' \int \mathrm{d}t'\, D_{\alpha\beta}(\boldsymbol{x}, \boldsymbol{x}' \mid t, t') [j_\beta^{\mathrm{ind}}(\boldsymbol{x}', t') + j_\beta^{\mathrm{ext}}(\boldsymbol{x}', t')]\,. \tag{26}$$

The external current density $\boldsymbol{j}^{\mathrm{ext}}$, or correspondingly, the external vector potential $\boldsymbol{A}^{\mathrm{ext}}$, induces a redistribution of the current density within the system, $\boldsymbol{j}^{\mathrm{ind}}$. The response function describing the linear response of the system to the external vector potential is the quasi-current response or reducible polarization tensor $\Pi_{\alpha\beta}(\boldsymbol{x}, \boldsymbol{x}' \mid t, t')$ defined by

$$j_\alpha^{\mathrm{ind}}(\boldsymbol{x}, t) = \sum_\beta \int \mathrm{d}^3x' \int \mathrm{d}t'\, \Pi_{\alpha\beta}(\boldsymbol{x}, \boldsymbol{x}' \mid t, t')\, A_\beta^{\mathrm{ext}}(\boldsymbol{x}', t')\,. \tag{27}$$

The response function describing the linear response of the system to the total vector potential $\boldsymbol{A}$, which is the actual vector potential acting in the solid, is the current-response or irreducible (proper) polarization tensor $P_{\alpha\beta}(\boldsymbol{x}, \boldsymbol{x}' \mid t, t')$ defined by

$$j_\alpha^{\mathrm{ind}}(\boldsymbol{x}, t) = \sum_\beta \int \mathrm{d}^3x' \int \mathrm{d}t'\, P_{\alpha\beta}(\boldsymbol{x}, \boldsymbol{x}' \mid t, t')\, A_\beta(\boldsymbol{x}, t')\,. \tag{28}$$

Using this equation in the formal solution (26) of the inhomogeneous wave equation it follows after Fourier transforming according to (9):

$$A_\alpha(\boldsymbol{q}_\parallel; z \mid \omega) = A_\alpha^{\mathrm{ext}}(\boldsymbol{q}_\parallel; z \mid \omega) + \mu_0 \sum_{\beta,\gamma} \int \mathrm{d}z' \int \mathrm{d}z'' \, D_{\alpha\beta}(\boldsymbol{q}_\parallel; z, z' \mid \omega) \times P_{\beta\gamma}(\boldsymbol{q}_\parallel; z', z'' \mid \omega) \, A_\gamma(\boldsymbol{q}_\parallel; z'' \mid \omega) \,. \tag{29}$$

The relation between $\Pi_{\alpha\beta}$ and $P_{\alpha\beta}$ is found to be

$$\Pi_{\alpha\beta}(\boldsymbol{q}_\parallel; z, z' \mid \omega) = P_{\alpha\beta}(\boldsymbol{q}_\parallel; z, z' \mid \omega) + \sum_{\gamma,\delta} \int \mathrm{d}z'' \int \mathrm{d}z''' \times P_{\alpha\gamma}(\boldsymbol{q}_\parallel; z, z'' \mid \omega) \, D_{\gamma\delta}(\boldsymbol{q}_\parallel; z'', z''' \mid \omega) \, \Pi_{\delta\beta}(\boldsymbol{q}_\parallel; z''', z' \mid \omega) \,. \tag{30}$$

In the current-response theory it is convenient to define the total dielectric response tensor $\varkappa_{\alpha\beta}(\boldsymbol{x}, \boldsymbol{x}' \mid \omega)$ which relates the total vector potential in the system to the applied external vector potential through the relationship

$$A_\alpha^{\mathrm{ext}}(\boldsymbol{x}, \omega) = \sum_\beta \int \mathrm{d}^3x' \, \varkappa_{\alpha\beta}(\boldsymbol{x}, \boldsymbol{x}' \mid \omega) \, A_\beta(\boldsymbol{x}', \omega) \,. \tag{31}$$

From (29) and (31) it follows that

$$\varkappa_{\alpha\beta}(\boldsymbol{x}, \boldsymbol{x}' \mid \omega) = \delta(\boldsymbol{x} - \boldsymbol{x}') \, \delta_{\alpha\beta} - \mu_0 \sum_\gamma \int \mathrm{d}^3x'' \, D_{\alpha\gamma}(\boldsymbol{x}, \boldsymbol{x}'' \mid \omega) \, P_{\gamma\beta}(\boldsymbol{x}'', \boldsymbol{x}' \mid \omega) \,. \tag{32}$$

In the classical macroscopic electrodynamics it is more familar to use the conductivity tensor $\sigma_{\alpha\beta}(\boldsymbol{x}, \boldsymbol{x}' \mid \omega)$ or the dielectric tensor $\varepsilon_{\alpha\beta}(\boldsymbol{x}, \boldsymbol{x}' \mid \omega)$. The conductivity tensor is defined by the equation

$$j_\alpha^{\mathrm{ind}}(\boldsymbol{x}, \omega) = \sum_\beta \int \mathrm{d}^3x' \, \sigma_{\alpha\beta}(\boldsymbol{x}, \boldsymbol{x}' \mid \omega) \, E_\beta(\boldsymbol{x}', \omega) \tag{33}$$

and hence

$$\sigma_{\alpha\beta}(\boldsymbol{x}, \boldsymbol{x}' \mid \omega) = \frac{1}{i\omega} P_{\alpha\beta}(\boldsymbol{x}, \boldsymbol{x}' \mid \omega) \tag{34}$$

is valid. The dielectric tensor relates the electric field $\boldsymbol{E}$ with the displacement field $\boldsymbol{D}$ according to (16), where now the polarization field of the non-magnetic solid is given by $\boldsymbol{P} = (i/\omega) \, \boldsymbol{j}^{\mathrm{ind}}$. Combining (16) with (34) the dielectric tensor is obtained as

$$\varepsilon_{\alpha\beta}(\boldsymbol{x}, \boldsymbol{x}' \mid \omega) = \varepsilon_{\mathrm{b}}(z) \, \delta(\boldsymbol{x} - \boldsymbol{x}') \, \delta_{\alpha\beta} + \frac{1}{\varepsilon_0 \omega^2} P_{\alpha\beta}(\boldsymbol{x}, \boldsymbol{x}' \mid \omega) \,. \tag{35}$$

We note that, as in the case of electrostatics there is the same basic difference between $\varkappa_{\alpha\beta}$ and $\varepsilon_{\alpha\beta}$. The dispersion relation of the coupled plasmon-photons, the plasmon-polaritons of the quantum well structure, will be obtained using (29) for $\boldsymbol{A} \neq \boldsymbol{0}$ with no applied external potential: $\boldsymbol{A}^{\mathrm{ext}} = \boldsymbol{0}$. Under this condition we obtain

$$\sum_{\beta\gamma} \int \mathrm{d}z' \int \mathrm{d}z'' [\delta(z - z'') \, \delta_{\alpha\gamma} - \mu_0 D_{\alpha\beta}(\boldsymbol{q}_\parallel; z, z' \mid \omega) \, P_{\beta\gamma}(\boldsymbol{q}_\parallel; z', z'' \mid \omega)] \, A_\gamma(\boldsymbol{q}_\parallel; z'' \mid \omega) = 0 \,. \tag{36}$$

The dispersion relation follows as the condition for non-trivial solutions of A_γ.

4. Linear Response of the Quasi-Two-Dimensional Electron Gas

4.1 Ground state: electronic subbands

According to the quantum well structure of the DHS (Fig. 1) the electrons of the conduction band can move quasi-free in the x–y plane with the wave vector component $\boldsymbol{k}_{\parallel}$ but their motion is quantum-confined in z-direction. In the effective-mass approximation the one-electron motion is given by the effective Schrödinger equation

$$\left(-\frac{\hbar^2}{2m}\Delta + V_{\text{eff}}(\boldsymbol{x}) \right) \psi_{K\boldsymbol{k}_{\parallel}}(\boldsymbol{x}) = \mathscr{E}_K(\boldsymbol{k}_{\parallel})\, \psi_{K\boldsymbol{k}_{\parallel}}(\boldsymbol{x}) , \tag{37}$$

where $V_{\text{eff}}(\boldsymbol{x})$ is the effective confining potential. According to the symmetry of the DHS the single-particle electronic wave function $\psi_{K\boldsymbol{k}_{\parallel}}(\boldsymbol{x})$ can be written in the form

$$\langle \boldsymbol{x} \mid K\boldsymbol{k}_{\parallel} \rangle \equiv \psi_{K\boldsymbol{k}_{\parallel}}(\boldsymbol{x}) = \frac{1}{\sqrt{A}}\, \mathrm{e}^{i\boldsymbol{k}_{\parallel}\boldsymbol{x}_{\parallel}}\, \varphi_K(z) . \tag{38}$$

The quantum confinement of the electron motion in z-direction leads to the occurrence of the electronic subbands characterized as

$$\mathscr{E}_K(\boldsymbol{k}_{\parallel}) = \mathscr{E}_K + \frac{\hbar^2 k_{\parallel}^2}{2m}, \qquad K = 0, 1, 2, 3, \ldots \tag{39}$$

The envelope wave function $\varphi_K(z)$ for an electron in the K-th subband is given by the one-dimensional effective Schrödinger equation

$$\left(-\frac{\hbar^2}{2m}\frac{\mathrm{d}^2}{\mathrm{d}z^2} + V_{\text{eff}}(z) \right) \varphi_K(z) = \mathscr{E}_K \varphi_K(z) . \tag{40}$$

The simplest model potential for the DHS is given by infinite barriers, neglecting any band-bending and exchange-correlation effects. In this case we obtain

$$\varphi_K(z) = \sqrt{\frac{2}{a}}\, \sin\left(\frac{\pi(K+1)\, z}{a} \right) \tag{41}$$

and

$$\mathscr{E}_K = \frac{\hbar^2 \pi^2}{2ma^2} (K+1)^2 . \tag{42}$$

We use these simple results in the numerical calculations discussed in the following sections.

The width of the narrow channel to which the electrons are confined is usually of the order of their de Broglie wavelength $\lambda_0 = 2\pi/k_{\text{F}}$, with $k_{\text{F}} = (2\pi n_{2\text{DEG}})^{1/2}$ the 2D Fermi wave number and $n_{2\text{DEG}}$ is the sheet carrier concentration. Because the sheet carrier concentration of a Q2D electronic system at $T = 0$ K

$$n_{2\text{DEG}} = \frac{m}{\pi\hbar^2} \sum_K (E_{\text{F}} - \mathscr{E}_K)\, \theta(E_{\text{F}} - \mathscr{E}_K) , \tag{43}$$

with E_{F} being the Fermi energy and $\theta(x)$ being the unit step function ($\theta(x) = +1$ for $x > 0$ and $\theta(x) = 0$ for $x < 0$), varies for usual quantum wells in the region $1 \times 10^{10}\,\text{cm}^{-2} < n_{2\text{DEG}} < 5 \times 10^{12}\,\text{cm}^{-2}$ corresponding to $0.24 < r_{\text{S}} < 5.5$ for the dimensionless Wigner-Seitz parameter $r_{\text{S}} = r_0/a_0^*$ ($r_0 = (\pi n_{2\text{DEG}})^{-1/2}$ is the mean radius between the

electrons, $a_0^* = 4\pi\varepsilon_0\varepsilon_{s1}\hbar^2/(me^2)$ is the effective Bohr radius; for GaAs $a_0^* = 10.29$ nm with the effective electron mass $m = 0.06624m_0$ and the static dielectric constant $\varepsilon_{s1} = 12.87$), the de Broglie wavelength varies between 10 nm $< \lambda_0 <$ 250 nm. The usual thickness of the quantum wells is below 100 nm. Further, at low temperatures for which the electron mobility μ can reach values up to 2×10^7 cm^2/Vs, this width is much smaller than the elastic mean free path of the electrons ($l = v_F\tau \approx 1000$ nm, $\tau = m\mu/e$), i.e. the motion of the electrons between the boundaries of the channel is ballistic. Following, the subband spacing, typical in the range $\Delta\mathscr{E} = 20$ to 100 meV, is much larger than the energy broadening $\Gamma = \hbar/\tau$ induced by scattering processes. According to (39) and (40), the size-quantization becomes experimentally observable and, hence, becomes important for describing the physical properties of semiconductor microstructures. For typical III–V semiconductor quantum wells only few subbands $\mathscr{E}_K$ are occupied.

4.2 Density-response of a Q2DEG

Now we consider the interacting many-particle system of the Q2DEG in the presence of a perturbation. The many-particle Hamiltonian of this system in second quantized form reads

$$\hat{H} = \hat{H}_0 + \hat{H}_1(t), \tag{44}$$

where $\hat{H}_0$ is the unperturbed part,

$$\hat{H}_0 = \sum_{K\boldsymbol{k}_\parallel} \mathscr{E}_K(\boldsymbol{k}_\parallel)\, \hat{C}^+_{K\boldsymbol{k}_\parallel} \hat{C}_{K\boldsymbol{k}_\parallel}. \tag{45}$$

Herein $\hat{C}_{K\boldsymbol{k}_\parallel}(\hat{C}^+_{K\boldsymbol{k}_\parallel})$ is the destruction (creation) operator of an electron with the quantum number $\{K\boldsymbol{k}_\parallel\}$. The interacting part $\hat{H}_1(t)$ has for the density-response the form

$$\hat{H}_1(t) = \int \mathrm{d}^3x\, \hat{\varrho}(\boldsymbol{x})\, \Phi(\boldsymbol{x}, t), \tag{46}$$

where

$$\hat{\varrho}(\boldsymbol{x}) = -e\hat{\psi}^+(\boldsymbol{x})\, \hat{\psi}(\boldsymbol{x}) \tag{47}$$

is the charge density operator, Φ is the total scalar potential and the electron field operators are given by

$$\hat{\psi}(\boldsymbol{x}) = \sum_{K\boldsymbol{k}_\parallel} \psi_{K\boldsymbol{k}_\parallel}(\boldsymbol{x})\, \hat{C}_{K\boldsymbol{k}_\parallel}, \tag{48}$$

$$\hat{\psi}^+(\boldsymbol{x}) = \sum_{K\boldsymbol{k}_\parallel} \psi^*_{K\boldsymbol{k}_\parallel}(\boldsymbol{x})\, \hat{C}_{K\boldsymbol{k}_\parallel}. \tag{49}$$

Note that the system is perturbed at $t = -\infty$ by turning on the time-dependent Hamiltonian $\hat{H}_1(t)$. It is assumed that this perturbation is switched on adiabatically. The first-order change in the ensemble average of an operator $\hat{O}$ is given by [94]

$$\delta\langle\hat{O}\rangle = -\frac{i}{\hbar}\int \mathrm{d}t'\, \mathrm{Tr}\,\{\hat{\varrho}_G[\hat{O}(t), \hat{H}_1(t')]\}, \tag{50}$$

where the operators are in the Heisenberg picture. The trace (Tr) is evaluated in the equilibrium grand canonical ensemble with $\hat{\varrho}_G$ the grand canonical statistical operator. From (50) we find the first-order change in the ensemble average of the charge density

operator $\delta\langle\hat{\varrho}\rangle \equiv \varrho^{\text{ind}}$, the induced charge density, according to

$$\varrho^{\text{ind}}(\boldsymbol{x}, t) = -\frac{i}{\hbar}\int \mathrm{d}^3x' \int_{-\infty}^{t} \mathrm{d}t' \,\mathrm{Tr}\,\{\hat{\varrho}_{\mathrm{G}}[\hat{\varrho}(\boldsymbol{x}, t), \hat{\varrho}(\boldsymbol{x}', t')]\}\, \Phi(\boldsymbol{x}', t')\,. \tag{51}$$

Comparing this Kubo formula [95] with (6) we found for the density-response function

$$P(\boldsymbol{x}, \boldsymbol{x}' \mid t, t') = -\frac{i}{\hbar}\,\mathrm{Tr}\,\{\hat{\varrho}_{\mathrm{G}}[\hat{\varrho}(\boldsymbol{x}, t), \hat{\varrho}(\boldsymbol{x}', t')]\}\,\theta(t - t')\,, \tag{52}$$

which is a retarded density–density correlation function. Since such a function cannot easily be calculated directly with the Feynman-Dyson perturbation series because Wick's theorem applies only to a time-ordered product of operators, an associated time-ordered correlation function is introduced. The time-ordered correlation function in the Matsubara formalism can be calculated according to [96, 97]

$$P(\boldsymbol{x}, \boldsymbol{x}' \mid i\omega_n) = -\frac{1}{\hbar}\int_0^{\beta\hbar} \mathrm{d}\tau\, \mathrm{e}^{i\omega_n\tau}\,\mathrm{Tr}\,\{\hat{\varrho}_{\mathrm{G}} T_\tau \hat{\varrho}(\boldsymbol{x}, \tau)\,\hat{\varrho}(\boldsymbol{x}', 0)\}\,, \tag{53}$$

where $\omega_n = 2\pi n/\beta\hbar$ (n is an integer) is the Matsubara frequency. After the evaluation of $P(\boldsymbol{x}, \boldsymbol{x}' \mid i\omega_n)$ using the diagrammatic techniques we obtain the retarded correlation function $P(\boldsymbol{x}, \boldsymbol{x}' \mid \omega)$ by the analytic continuation $i\omega_n \to \omega + i\delta;\ \delta \to 0^+$ in the usual way.

Here we are concerned with the random-phase approximation (RPA) for the irreducible polarization function (52). Using this single-loop approximation in the Matsubara expression, (53), with the wave function $|K\boldsymbol{k}_\parallel\rangle$ and subband energies $\mathscr{E}_K(\boldsymbol{k})$ of non-interacting electrons we found after analytic continuation and Fourier transformation in the x–y plane [42]

$$P(\boldsymbol{q}_\parallel; z, z' \mid \omega) = \sum_{KK'} P_{KK'}(\boldsymbol{q}_\parallel, \omega)\,\eta_{KK'}(z)\,\eta^*_{KK'}(z')\,, \tag{54}$$

$$P_{KK'}(\boldsymbol{q}_\parallel, \omega) = \sum_{\boldsymbol{k}_\parallel} P_{KK'}(\boldsymbol{q}_\parallel, \boldsymbol{k}_\parallel \mid \omega)\,, \tag{55}$$

$$P_{KK'}(\boldsymbol{q}_\parallel, \boldsymbol{k}_\parallel \mid \omega) = \frac{2e^2}{A}\,\frac{n_{\mathrm{F}}(\mathscr{E}_{K'}(\boldsymbol{k}_\parallel)) - n_{\mathrm{F}}(\mathscr{E}_K(\boldsymbol{k}_\parallel + \boldsymbol{q}_\parallel))}{(\hbar\omega + i\delta) + \mathscr{E}_{K'}(\boldsymbol{k}_\parallel) - \mathscr{E}_K(\boldsymbol{k}_\parallel + \boldsymbol{q}_\parallel)}\,, \tag{56}$$

and

$$\eta_{KK'}(z) = \varphi_K(z)\,\varphi^*_{K'}(z)\,. \tag{57}$$

Herein $n_{\mathrm{F}}(\mathscr{E}_K(\boldsymbol{k}_\parallel))$ denotes the Fermi occupancy factor of electrons. Using (54) for the RPA polarization function in (19) we can derive the dispersion relation. To do this we make two assumptions. For simplicity, we want to discuss the dispersion relation for $T = 0$ K and in the electric quantum limit (EQL). It means that in equilibrium the electrons only occupy the lowest ($K = 0$) subband. This is valid within the usual concentrations of carrier densities and at low temperatures in the most common III–V semiconductor microstructures. The matrix polarization function $P_{KK'}(\boldsymbol{q}_\parallel, \omega)$ has at zero temperature only the non-vanishing elements P_{00}, P_{0K}, and P_{K0}. Hence, (54) can be written in the form

$$P(\boldsymbol{q}_\parallel; z, z' \mid \omega) = \sum_K \chi_K(\boldsymbol{q}_\parallel, \omega)\,\eta_{K0}(z)\,\eta_{K0}(z')\,, \tag{58}$$

where we have now assumed that the $\varphi_K(z)$ are real functions. The RPA polarization function $\chi_K(q_\parallel, \omega)$ in der EQL is defined by

$$\chi_K(q_\parallel, \omega) = \begin{cases} P_{00}(q_\parallel, \omega) & \text{if} \quad K = 0\,, \\ P_{K0}(q_\parallel, \omega) + P_{0K}(q_\parallel, \omega) & \text{if} \quad K > 0\,. \end{cases} \tag{59}$$

The polarization function $\chi_K(q_\parallel, \omega)$ contains two physically different contributions:

(i) the intrasubband contribution for $K = 0$ arising from the electron excitation above the Fermi surface within the lowest subband and

(ii) the intersubband contribution for $K > 0$ arising from the electron excitation to higher subbands.

With the approximations described above the dispersion relation reads

$$\det\left\{\delta_{KL} - \frac{1}{\varepsilon_0} D_{KL}(q_\parallel)\, \chi_L(q_\parallel, \omega)\right\} = 0\,, \tag{60}$$

where $D_{KK'}(q_\parallel)$ is given by

$$\begin{aligned} D_{KK'}(q_\parallel) &= \int \mathrm{d}z \int \mathrm{d}z'\, \eta_{K0}(z)\, D(q_\parallel; z, z')\, \eta_{K'0}(z') \\ &= \frac{1}{2\varepsilon_{b1} q_\parallel} [f^{\mathrm{dir}}_{KK'}(q_\parallel) + f^{\mathrm{im}}_{KK'}(q_\parallel)]\,. \end{aligned} \tag{61}$$

The matrix elements of the Green's function (61) are calculated in Appendix B. The dispersion relation (60) describes intra- and intersubband plasmons. Because only the lowest subband is assumed to be occupied, the once intrasubband plasmon is the (0–0) intrasubband plasmon, which is in general coupled to all (K–0) intersubband plasmons. For a spatially symmetric quantum well, such as the rectangular quantum well in the case of a DHS, the modes are split into two independent sets, the symmetric modes: (0–0), (2–0), (4–0), ... and the antisymmetric modes: (1–0), (3–0), (5–0), ... Symmetric and antisymmetric modes are not coupled. We note that the usual Coulomb matrix element $V^{\mathrm{b}}_{KK'}$ is related to (61) by $V^{\mathrm{b}}_{KK'} = e^2/\varepsilon_0 D_{KK'}$. In (61) $f^{\mathrm{dir}}_{KK'}(q_\parallel)$ is the form factor of the direct Coulomb interaction potential and $f^{\mathrm{im}}_{KK'}(q_\parallel)$ that of the image part.

For the numerical calculation of the dispersion relation (60), it is necessary to make one further approximation. One possibility is to neglect the off-diagonal elements of (60). Hence, the dispersion relation is given in the diagonal approximation by

$$1 - \frac{1}{\varepsilon_0} D_{KK}(q_\parallel)\, \chi_K(q_\parallel, \omega) = 0 \tag{62}$$

under the condition that the imaginary part of the polarization function vanishes. This dispersion relation describes

(i) intrasubband plasmons if $K = 0$ and

(ii) intersubband plasmons if $K > 0$.

The neglect of the off-diagonal elements is equivalent to neglecting the mixing between the intra- and intersubband plasmons.

The second possibility for the further approximation is if we retain the off-diagonal elements but use a two- or three-subband model [46, 48].

The RPA polarization function of a Q2DEG in the electric quantum limit is calculated in [42] to be

$$\chi_K(\boldsymbol{q}_\parallel, \omega) = -\frac{m^2 e^2}{\pi \hbar^3 \boldsymbol{q}_\parallel^2}\left(2\Omega_{K0} + \frac{\hbar \boldsymbol{q}_\parallel^2}{m} - W_1^K(\boldsymbol{q}_\parallel, \omega) - W_2^K(\boldsymbol{q}_\parallel, \omega)\right) \tag{63}$$

with

$$W_1^K(\boldsymbol{q}_\parallel, \omega) = \left\{\left(\omega + i\delta - \Omega_{K0} - \frac{\hbar q_\parallel^2}{2m}\right)^2 - (v_F q_\parallel)^2\right\}^{1/2}$$

$$= \begin{cases} -\left\{\left(\omega - \Omega_{K0} - \dfrac{\hbar q_\parallel^2}{2m}\right)^2 - (v_F q_\parallel)^2\right\}^{1/2} \\ \text{for} \quad (v_F q_\parallel)^2 < \left(\omega - \Omega_{K0} - \dfrac{\hbar q_\parallel^2}{2m}\right)^2 \quad \text{and} \quad \dfrac{\hbar q_\parallel^2}{2m} + Q_{K0} < \omega\,; \\ \left\{\left(\omega - \Omega_{K0} - \dfrac{\hbar q_\parallel^2}{2m}\right)^2 - (v_F q_\parallel)^2\right\}^{1/2} \\ \text{for} \quad (v_F q_\parallel)^2 < \left(\omega - \Omega_{K0} - \dfrac{\hbar q_\parallel^2}{2m}\right)^2 \quad \text{and} \quad \dfrac{\hbar q_\parallel^2}{2m} + \Omega_{K0} > \omega\,; \\ -i\left\{(v_F q_\parallel)^2 - \left(\omega - \Omega_{K0} - \dfrac{\hbar q_\parallel^2}{2m}\right)^2\right\}^{1/2} \quad \text{for} \quad (v_F q_\parallel)^2 > \left(\omega - \Omega_{K0} - \dfrac{\hbar q_\parallel^2}{2m}\right)^2, \end{cases} \tag{64}$$

$$W_2^K(\boldsymbol{q}_\parallel, \omega) = \left\{\left(\omega + i\delta + \Omega_{K0} + \frac{\hbar q_\parallel^2}{2m}\right)^2 - (v_F q_\parallel)^2\right\}^{1/2}$$

$$= \begin{cases} \left\{\left(\omega + \Omega_{K0} + \dfrac{\hbar q_\parallel^2}{2m}\right)^2 - (v_F q_\parallel)^2\right\}^{1/2} \quad \text{for} \quad (v_F q_\parallel)^2 < \left(\omega + \Omega_{K0} + \dfrac{\hbar q_\parallel^2}{2m}\right)^2; \\ i\left\{(v_F q_\parallel)^2 - \left(\omega + \Omega_{K0} + \dfrac{\hbar q_\parallel^2}{2m}\right)^2\right\}^{1/2} \quad \text{for} \quad (v_F q_\parallel)^2 > \left(\omega + \Omega_{K0} + \dfrac{\hbar q_\parallel^2}{2m}\right)^2. \end{cases} \tag{65}$$

Herein $\Omega_{KK'} = (\mathscr{E}_K - \mathscr{E}_{K'})/\hbar$ denotes the subband separation frequency and $v_F = \hbar k_F/m$ is the Fermi velocity. For explicit analytic calculation we use long-wavelength approximations (LWA) of the polarization function. If we expand all quantities in the RPA polarization function in a power series of $q_\parallel = |\boldsymbol{q}_\parallel|$ we obtain

$$\chi_0(\boldsymbol{q}_\parallel, \omega) = \frac{n_{2DEG} e^2 q_\parallel^2}{m\omega^2}\left(1 + \frac{3}{4}\frac{v_F^2 q_\parallel^2}{\omega^2}\right) \tag{66}$$

for $K = 0$, and for $K > 0$ it follows:

$$\chi_K(\boldsymbol{q}_\parallel, \omega) = \frac{2n_{2DEG} e^2}{\hbar^2}\frac{1}{\omega^2 - \Omega_{K0}^2} \times \left\{\hbar\Omega_{K0} + q_\parallel^2\left[\frac{\hbar^2}{2m} + \frac{1}{\omega^2 - \Omega_{K0}^2}\left(\frac{3}{4}v_F^2\hbar\Omega_{K0} + \frac{\hbar^2\Omega_{K0}^2}{m}\right) + \frac{v_F^2\hbar\Omega_{K0}^3}{(\omega^2 - \Omega_{K0}^2)^2}\right]\right\}. \tag{67}$$

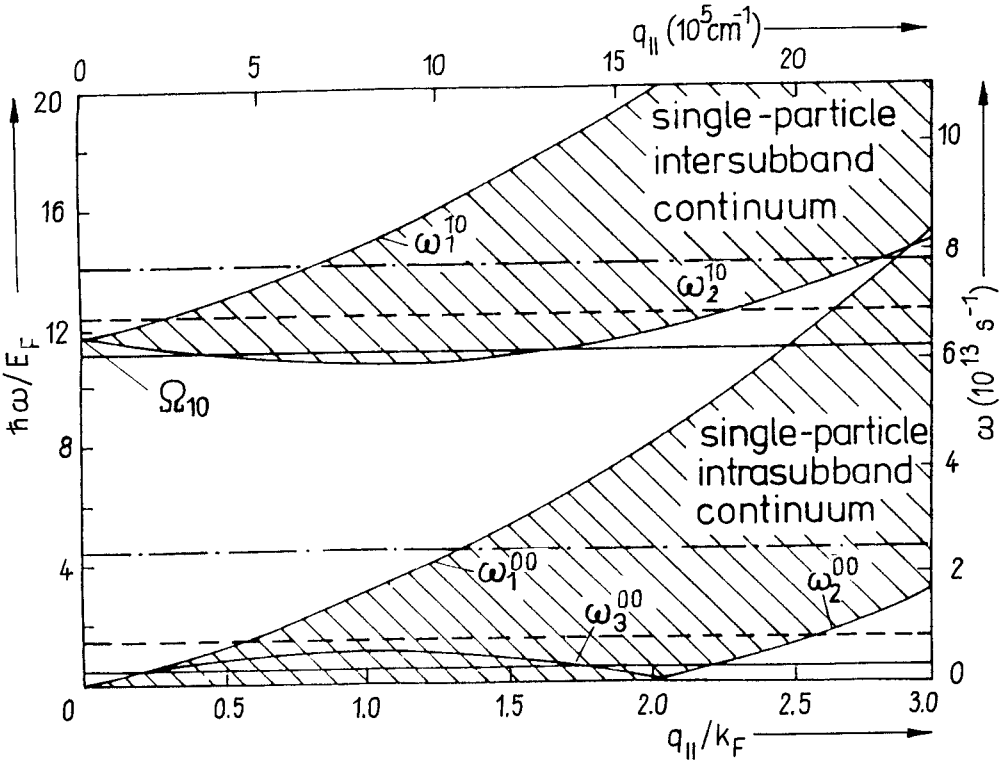

Fig. 2. Regions of the single-particle intra- and intersubband excitations in the ω–$q_{\parallel}$ plane. These regions are characterized by Im $\chi_K(\boldsymbol{q}_{\parallel}, \omega) \neq 0$ and Im $\chi^K_{xx}(\boldsymbol{q}_{\parallel}, \omega) \neq 0$, Im $\chi^K_{yy}(\boldsymbol{q}_{\parallel}, \omega) \neq 0$, Im $\chi^K_{zz}(\boldsymbol{q}_{\parallel}, \omega) \neq 0$, Re $\chi^K_{xz}(\boldsymbol{q}_{\parallel}, \omega) \neq 0$, and Re $\chi^K_{zx}(\boldsymbol{q}_{\parallel}, \omega) \neq 0$, and shown by the shaded areas. The boundaries of the regions are given by $\omega_1^{00} = v_F q_{\parallel}(1 + q_{\parallel}/(2k_F))$, $\omega_2^{00} = v_F q_{\parallel}(-1 + q_{\parallel}/(2k_F))$, $\omega_3^{00} = v_F q_{\parallel}(1 - q_{\parallel}/(2k_F))$, $\omega_1^{10} = v_F q_{\parallel}(1 + q_{\parallel}/(2k_F)) + \Omega_{10}$, and $\omega_2^{10} = v_F q_{\parallel}(-1 + q_{\parallel}/(2k_F)) + \Omega_{10}$. The lines $\hbar\omega/E_F = 0.5$, 1.5, 4.5 and $\omega/\Omega_{10} = -0.95$, 1.05, and 1.20 correspond to the frequencies at which the real and imaginary parts of $\chi_0(\boldsymbol{q}_{\parallel}, \omega)$, $\chi_1(\boldsymbol{q}_{\parallel}, \omega)$, $\chi^0_{\alpha\beta}(\boldsymbol{q}_{\parallel}, \omega)$, and $\chi^1_{\alpha\beta}(\boldsymbol{q}_{\parallel}, \omega)$ are calculated; $n_{2\,\mathrm{DEG}} = 10^{11}$ cm^{-2}, $a = 20$ nm

In Fig. 2 we have plotted the regions in the ω–$q_{\parallel}$ plane in which Im $\chi_K(\boldsymbol{q}_{\parallel}, \omega) \neq 0$. Outside these regions Im $\chi_K(\boldsymbol{q}_{\parallel}, \omega) = 0$ is valid. Im $\chi_K(\boldsymbol{q}_{\parallel}, \omega) \neq 0$ means that the single-particle excitations of the Q2DEG occur. These are transitions of single electrons from states below the Fermi surface to an empty state above it.

Fig. 3 and 4 demonstrate the calculated RPA results for $\chi_0(\boldsymbol{q}_{\parallel}, \omega)$ and $\chi_1(\boldsymbol{q}_{\parallel}, \omega)$. The polarization functions are calculated at three fixed frequencies which are also plotted in Fig. 2.

From Fig. 3 is to be seen that the real part of $\chi_0(\boldsymbol{q}_{\parallel}, \omega)$ has a sharp peak for this wave vector for which the boundary of the single-particle intrasubband continuum (curve ω_1^{00} in Fig. 2) is crossed. For lower frequencies the sharpness of the peak increases. If the boundaries ω_3^{00} and ω_2^{00} are crossed, an edge occurs in the curve of Re $\chi_0(\boldsymbol{q}_{\parallel}, \omega)$. The imaginary part of $\chi_0(\boldsymbol{q}_{\parallel}, \omega)$ shows sharp minima if crossing the boundaries ω_1^{00} and ω_3^{00} and is only different from zero between the boundaries ω_1^{00} and ω_2^{00}. For $\chi_1(\boldsymbol{q}_{\parallel}, \omega)$ the analogous characteristics are depicted in Fig. 4.

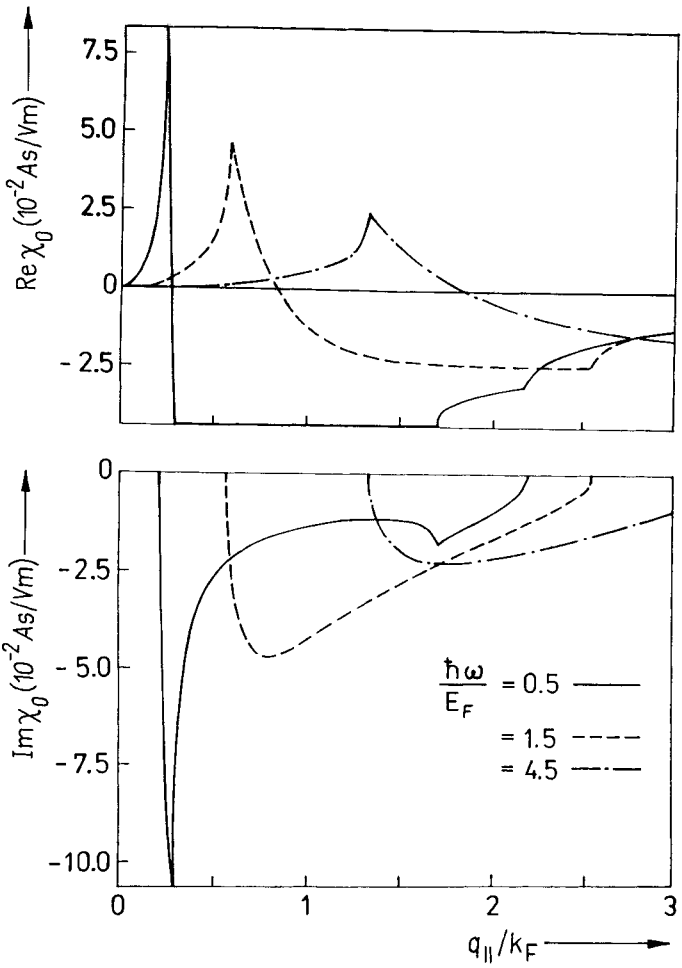

Fig. 3. Plot of the intrasubband contributions Re $\chi_0(\boldsymbol{q}_{\parallel}, \omega)$ and Im $\chi_0(\boldsymbol{q}_{\parallel}, \omega)$ of the RPA polarization function for three different frequencies

4.3 Current-response of a Q2DEG

The interacting part $\hat{H}_1(t)$ of the Hamiltonian $\hat{H}$ of the Q2DEG in presence of an external current is

$$\hat{H}_1(t) = -\sum_{\alpha} \int \mathrm{d}^3x \, \hat{j}_{\alpha}(\boldsymbol{x}) \, A_{\alpha}(\boldsymbol{x}, t) , \tag{68}$$

where A_{α} is the α-th component of the total vector potential and the α-th component of the current density operator is given by

$$\hat{j}_{\alpha}(\boldsymbol{x}) = \frac{i\hbar e}{2m} \left(\hat{\psi}^{+}(\boldsymbol{x}) \frac{\partial}{\partial x_{\alpha}} \hat{\psi}(\boldsymbol{x}) - \frac{\partial}{\partial x_{\alpha}} \hat{\psi}^{+}(\boldsymbol{x}) \, \hat{\psi}(\boldsymbol{x}) \right) . \tag{69}$$

We note that the expection value of this current operator, the paramagnetic current, used in the Hamiltonian differs from the real current density by a term proportional to $\boldsymbol{A}$, the

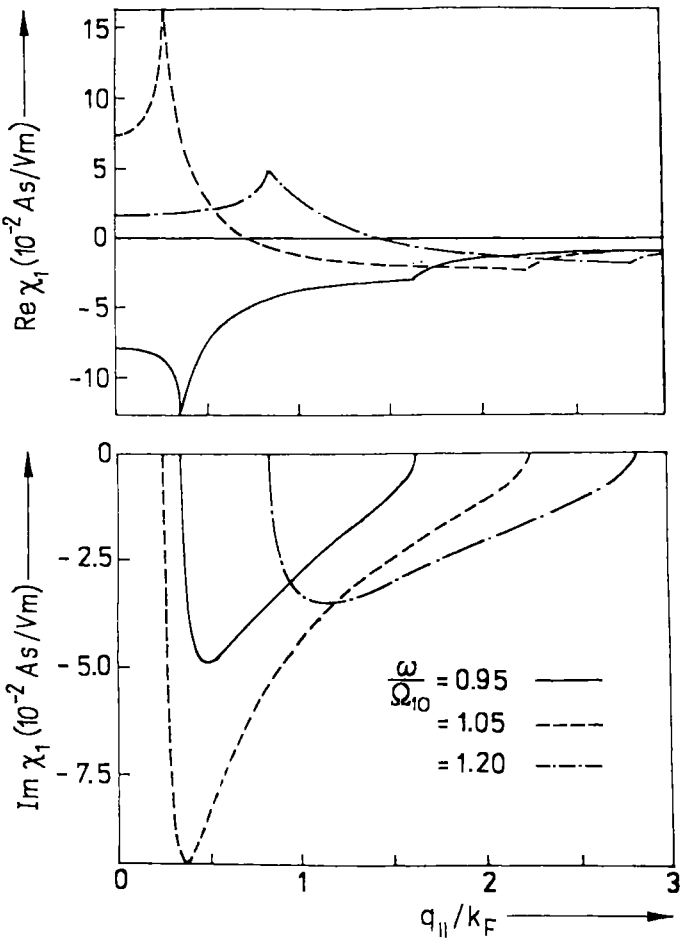

Fig. 4. Plot of the (1–0) intersubband contributions $\mathrm{Re}\,\chi_1(\boldsymbol{q}_{\parallel}, \omega)$ and $\mathrm{Im}\,\chi_1(\boldsymbol{q}_{\parallel}, \omega)$ of the RPA polarization function for three different frequencies

diamagnetic current given by

$$\hat{j}_\alpha^{\mathrm{D}}(\boldsymbol{x}) = -\frac{e^2}{m}\hat{\psi}^+(\boldsymbol{x})\,\hat{\psi}(\boldsymbol{x})\,A_\alpha(\boldsymbol{x}, t)\,. \tag{70}$$

Hence, the paramagnetic current must be used in the Hamiltonian of the linear response alone and the contribution from the diamagnetic current must be added at the end of the calculation. Only the paramagnetic current can be derived directly by the Kubo formula [96]. Using this circumstance in (50) we have for the induced current density

$$j_\alpha^{\mathrm{ind}}(\boldsymbol{x}, t) = \frac{i}{\hbar}\sum_\beta \int \mathrm{d}^3x' \int_{-\infty}^{t} \mathrm{d}t'\,\mathrm{Tr}\,\{\hat{\varrho}_{\mathrm{G}}[\hat{j}_\alpha(\boldsymbol{x}, t), \hat{j}_\beta(\boldsymbol{x}', t')]\}$$

$$\times A_\beta(\boldsymbol{x}', t') - \frac{e^2}{m}\,\mathrm{Tr}\,\{\hat{\varrho}_{\mathrm{G}}\hat{\psi}^+(\boldsymbol{x})\,\hat{\psi}(\boldsymbol{x})\}\,A_\alpha(\boldsymbol{x}, t)\,, \tag{71}$$

where we have used the gauge fixing condition $\Phi = 0$. The gauge invariance of the theory is discussed in detail in Appendix C. Comparing the Kubo formula (71) with (28) we found for the current-response function

$$P_{\alpha\beta}(\boldsymbol{x}, \boldsymbol{x}' \mid t, t') = \frac{i}{\hbar} \operatorname{Tr} \{\hat{\varrho}_G[\hat{j}_\alpha(\boldsymbol{x}, t), \hat{j}_\beta(\boldsymbol{x}', t')]\} \, \theta(t - t')$$

$$- \frac{e^2}{m} \operatorname{Tr} \{\hat{\varrho}_G \hat{\psi}^+(\boldsymbol{x}) \hat{\psi}(\boldsymbol{x})\} \, \delta(t - t') \, \delta(\boldsymbol{x} - \boldsymbol{x}') \, \delta_{\alpha\beta} \,. \tag{72}$$

The first term is the retarded current–current correlation function which is a two-particle function and is calculated using the Matsubara formalism. The second term is transformed in a single-particle Green's function according to

$$\operatorname{Tr} \{\hat{\varrho}_G \hat{\psi}^+(\boldsymbol{x}) \hat{\psi}(\boldsymbol{x})\} = - \lim_{\substack{\boldsymbol{x}' \to \boldsymbol{x} \\ \tau \to 0^-}} \operatorname{Tr} \{\hat{\varrho}_G T_\tau \hat{\psi}(\boldsymbol{x}, \tau) \, \hat{\psi}^+(\boldsymbol{x}', 0)\} \,. \tag{73}$$

Here we are again concerned with the RPA for the irreducible polarization tensor (72). Using this single-loop approximation in the Matsubara expression with the state vector $|K\boldsymbol{k}_\parallel\rangle$ and subband energies $\mathscr{E}_K(\boldsymbol{k}_\parallel)$ of non-interacting electrons we found, after analytic continuation and Fourier transformation in the x–y plane, by similar calculations as in the case of the density-response for the polarization tensor,

$$P_{\alpha\beta}(\boldsymbol{q}_\parallel; z, z' \mid \omega) = - \frac{\hbar^2}{4m^2} \sum_{KK'} \sum_{\boldsymbol{k}_\parallel} P_{KK'}(\boldsymbol{q}_\parallel, \boldsymbol{k}_\parallel \mid \omega) \, F_\alpha^{KK'}(\boldsymbol{q}_\parallel, \boldsymbol{k}_\parallel \mid z)$$

$$\times F_\beta^{KK'}(\boldsymbol{q}_\parallel, \boldsymbol{k}_\parallel \mid z')^* - \delta(z - z') \, \delta_{\alpha\beta} \frac{2e^2}{mA} \sum_K \sum_{\boldsymbol{k}_\parallel} n_F(\mathscr{E}_K(\boldsymbol{k}_\parallel)) \mid \varphi_K(z)|^2 \tag{74}$$

with

$$F_\alpha^{KK'}(\boldsymbol{q}_\parallel, \boldsymbol{k}_\parallel \mid z) = (1 - \delta_{\alpha z}) \, (2k_\alpha + q_\alpha) \, \eta_{KK'}(z) + i\delta_{\alpha z} g_{KK'}(z) \tag{75}$$

and

$$g_{KK'}(z) = \varphi_K(z) \frac{\mathrm{d}}{\mathrm{d}z} \varphi_{K'}^*(z) - \varphi_{K'}^*(z) \frac{\mathrm{d}}{\mathrm{d}z} \varphi_K(z) \,. \tag{76}$$

Using the RPA polarization tensor in (36) we can derive the dispersion relation. We make here the same two assumptions: $T = 0$ K and the EQL, as in the case of the density-response. For convenience, we choose a Cartesian coordinate system for which $\boldsymbol{q}_\parallel = (q_x, 0, 0)$, without loss of generality, because the medium is isotropic in the x–y plane. In such a coordinate system the only non-vanishing components of the Green's tensor are D_{xx}, D_{xz}, D_{yy}, D_{zx}, and D_{zz} (see Appendix A). Hence, (36) separates into two disconnected sets: one for the p-polarization (TM-modes) for $\boldsymbol{A} = (A_x, 0, A_z)$ and one for the s-polarization (TE-modes) for $\boldsymbol{A} = (0, A_y, 0)$. For convenience, we write the polarization tensor (74) in the form

$$P_{\alpha\beta}(\boldsymbol{q}_\parallel; z, z' \mid \omega) = \sum_{KK'} P_{\alpha\beta}^{KK'}(\boldsymbol{q}_\parallel, \omega) \, \xi_\alpha^{KK'}(z) \, \xi_\beta^{KK'}(z')^* = P_{\beta\alpha}^*(\boldsymbol{q}_\parallel; z', z \mid \omega) \tag{77}$$

with

$$P_{xx}^{KK'}(\boldsymbol{q}_\parallel, \omega) = -\sum_{\boldsymbol{k}_\parallel} \left(\frac{\hbar^2}{4m^2} P_{KK'}(\boldsymbol{q}_\parallel, \boldsymbol{k}_\parallel \mid \omega) (2k_\parallel \cos\varphi + q_\parallel)^2 + \frac{2e^2}{mA} n_F(\mathscr{E}_K(\boldsymbol{k}_\parallel)) \right), \tag{78}$$

$$P_{xz}^{KK'}(\boldsymbol{q}_\parallel, \omega) = i \sum_{\boldsymbol{k}_\parallel} \frac{\hbar^2}{4m^2} P_{KK'}(\boldsymbol{q}_\parallel, \boldsymbol{k}_\parallel \mid \omega) (2k_\parallel \cos\varphi + q_\parallel) = -P_{zx}^{KK'}(\boldsymbol{q}_\parallel, \omega), \tag{79}$$

$$P_{yy}^{KK'}(\boldsymbol{q}_\parallel, \omega) = -\sum_{\boldsymbol{k}_\parallel} \left(\frac{\hbar^2}{4m^2} P_{KK'}(\boldsymbol{q}_\parallel, \boldsymbol{k}_\parallel \mid \omega) (2k_\parallel \sin\varphi)^2 + \frac{2e^2}{mA} n_F(\mathscr{E}_K(\boldsymbol{k}_\parallel)) \right), \tag{80}$$

$$P_{zz}^{KK'}(\boldsymbol{q}_\parallel, \omega) = -\sum_{\boldsymbol{k}_\parallel} \left(\frac{\hbar^2}{4m^2} P_{KK'}(\boldsymbol{q}_\parallel, \boldsymbol{k}_\parallel \mid \omega) + \frac{e^2\hbar}{m^2 A \Omega_{KK'}} n_F(\mathscr{E}_K(\boldsymbol{k}_\parallel)) \right), \tag{81}$$

and

$$\xi_\alpha^{KK'}(z) = (1 - \delta_{\alpha z}) \eta_{KK'}(z) + \delta_{\alpha z} g_{KK'}(z). \tag{82}$$

Herein φ is the angle between $\boldsymbol{k}_\parallel$ and $\boldsymbol{q}_\parallel$ and $\boldsymbol{k}_\parallel = |\boldsymbol{k}_\parallel|$, $q_\parallel = |\boldsymbol{q}_\parallel|$. In the calculation of (77) we have used the following relations:

$$\sum_K \varphi_K(z) \varphi_K(z') = \delta(z - z'), \tag{83}$$

$$\frac{\mathrm{d}}{\mathrm{d}z} g_{KK'}(z) = \frac{2m\Omega_{KK'}}{\hbar} \eta_{KK'}(z), \tag{84}$$

and

$$\sum_K \eta_{KK'}(z) g_{KK'}(z') = \varphi_{K'}(z') \frac{\mathrm{d}}{\mathrm{d}z} (\varphi_{K'}(z) \delta(z - z')). \tag{85}$$

Assuming that the $\varphi_K(z)$ are real functions and taking into account that the matrix polarization function $P_{KK'}$ has under the assumption of the EQL and at zero temperature only the non-vanishing elements P_{00}, P_{0K}, and P_{K0}, (77) can be written in the form

$$P_{\alpha\beta}(\boldsymbol{q}_\parallel; z, z' \mid \omega) = \sum_K \chi_{\alpha\beta}^K(\boldsymbol{q}_\parallel, \omega) \xi_\alpha^{K0}(z) \xi_\beta^{K0}(z'). \tag{86}$$

The RPA polarization tensor $\chi_{\alpha\beta}^K(\boldsymbol{q}_\parallel, \omega)$ in the EQL is defined by

$$\chi_{\alpha\beta}^K(\boldsymbol{q}_\parallel, \omega) = \begin{cases} P_{\alpha\beta}^{00}(\boldsymbol{q}, \omega) & \text{if } K = 0 \text{ and } \alpha = \beta = x, y, \\ P_{\alpha\beta}^{K0}(\boldsymbol{q}_\parallel, \omega) + P_{\alpha\beta}^{0K}(\boldsymbol{q}_\parallel, \omega) & \text{if } K > 0 \text{ and } \alpha = \beta = x, y, z, \\ P_{\alpha\beta}^{K0}(\boldsymbol{q}_\parallel, \omega) - P_{\alpha\beta}^{0K}(\boldsymbol{q}_\parallel, \omega) & \text{if } K > 0 \text{ and } \alpha = x, \beta = z \\ & \qquad\qquad \text{or } \alpha = z, \beta = x. \end{cases} \tag{87}$$

The polarization tensor $\chi_{\alpha\beta}^K(\boldsymbol{q}_\parallel, \omega)$ contains two physically different contributions, (i) the intrasubband contribution for $K = 0$ which is only present for χ_{xx}^0 and χ_{yy}^0 and (ii) the intersubband contribution for $K > 0$ which is present for all components of $\chi_{\alpha\beta}^K$.

Using these relations above the dispersion relation for the s-polarization reads

$$\det \{\delta_{KL} - \mu_0 D_{yy}^{KL}(\boldsymbol{q}_\parallel, \omega) \chi_{yy}^L(\boldsymbol{q}_\parallel, \omega)\} = 0, \tag{88}$$

and for the p-polarization

$$\det\left\{\delta_{KL} - \mu_0 D_{xx}^{KL}(\boldsymbol{q}_\parallel, \omega)\left[\chi_{xx}^{L}(\boldsymbol{q}_\parallel, \omega) - \frac{iq_\parallel}{\alpha_1^2}\frac{2m\Omega_{L0}}{\hbar}\chi_{zx}^{L}(\boldsymbol{q}_\parallel, \omega)\right]\right.$$
$$\left. - \mu_0 \sum_{MN} D_{xx}^{KM}(\boldsymbol{q}_\parallel, \omega)\left[\chi_{xz}^{M}(\boldsymbol{q}_\parallel, \omega) - \frac{iq_\parallel}{\alpha_1^2}\frac{2m\Omega_{M0}}{\hbar}\chi_{zz}^{M}(\boldsymbol{q}_\parallel, \omega)\right](B_1^{-1})^{MN}B_2^{NL}\right\} = 0 \tag{89}$$

with $\alpha_v = (\boldsymbol{q}_\parallel^2 - \varepsilon_{bv}\omega^2/c^2)^{1/2}$. The intra- and intersubband modes, described by (88) and (89) are coupled in general. For the DHS under consideration we have symmetric and antisymmetric modes. The matrix elements $D_{\alpha\beta}^{KK'}(\boldsymbol{q}_\parallel, \omega)$ are given by

$$D_{\alpha\beta}^{KK'}(\boldsymbol{q}_\parallel, \omega) = \int \mathrm{d}z \int \mathrm{d}z'\, \xi_\alpha^{K0}(z)\, D_{\alpha\beta}(\boldsymbol{q}_\parallel; z, z' \mid \omega)\, \xi_\beta^{K'0}(z') \tag{90}$$

which are calculated in Appendix B. We have further defined

$$B_1^{KK'} = \alpha_1^2\delta_{KK'} - \mu_0 C_{KK'}\chi_{zz}^{K'}(\boldsymbol{q}_\parallel, \omega)\,, \tag{91}$$

$$B_2^{KK'} = iq_\parallel \frac{2m\Omega_{K0}}{\hbar}\delta_{KK'} + \mu_0 C_{KK'}\chi_{zx}^{K'}(\boldsymbol{q}_\parallel, \omega)\,, \tag{92}$$

and

$$C_{KK'} = \int \mathrm{d}z\, g_{K0}(z)\, g_{K'0}(z)\,. \tag{93}$$

The dispersion relation of the s-polarization in the diagonal approximation is given by

$$1 - \mu_0 D_{yy}^{KK}(\boldsymbol{q}_\parallel, \omega)\,\chi_{yy}^{K}(\boldsymbol{q}_\parallel, \omega) = 0 \tag{94}$$

under the condition that the imaginary part of the yy component of the polarization tensor $\mathrm{Im}\,\chi_{yy}^{K}(\boldsymbol{q}_\parallel, \omega) = 0$. This dispersion relation describes (i) s-polarized intrasubband plasmon-polaritons if $K = 0$ and (ii) s-polarized intersubband plasmon-polaritons if $K > 0$.

The dispersion relation of the p-polarization in the diagonal approximation is given by

$$1 - \mu_0 D_{xx}^{00}(\boldsymbol{q}_\parallel, \omega)\,\chi_{xx}^{0}(\boldsymbol{q}_\parallel, \omega) = 0 \tag{95}$$

for $K = 0$ describing the p-polarized intrasubband plasmon-polaritons and by

$$1 - \mu_0 D_{xx}^{KK}(\boldsymbol{q}_\parallel, \omega)\left\{\left[\chi_{xx}^{K}(\boldsymbol{q}_\parallel, \omega) - \frac{iq_\parallel}{\alpha_1^2}\frac{2m\Omega_{K0}}{\hbar}\chi_{zx}^{K}(\boldsymbol{q}_\parallel, \omega)\right]\right.$$
$$\left. + \frac{iq_\parallel\dfrac{2m\Omega_{K0}}{\hbar} + \mu_0 C_{KK}\chi_{zx}^{K}(\boldsymbol{q}_\parallel, \omega)}{\alpha_1^2 - \mu_0 C_{KK}\chi_{zz}^{K}(\boldsymbol{q}_\parallel, \omega)}\left[\chi_{xz}^{K}(\boldsymbol{q}_\parallel, \omega) - \frac{iq_\parallel}{\alpha_1^2}\frac{2m\Omega_{K0}}{\hbar}\chi_{zz}^{K}(\boldsymbol{q}_\parallel, \omega)\right]\right\} = 0 \tag{96}$$

for $K > 0$ describing the p-polarized intersubband plasmon-polaritons. The dispersion relations (95) and (96) describe the modes under the condition that the imaginary parts of xx and zz and the real part of zx components of the polarization tensor vanish.

The components of the RPA polarization tensor of the Q2DEG in the EQL are calculated using the integrals derived in [59]. We have found for $\chi_{xx}^{K}(\boldsymbol{q}_\parallel, \omega)$ the full RPA result to be

$$\chi_{xx}^{K}(\boldsymbol{q}_\parallel, \omega) = -\frac{m^2e^2}{\hbar^3\pi q_\parallel^4}\left\{(\omega - \Omega_{K0})^2\left(W_1^{K}(\boldsymbol{q}_\parallel, \omega) + \omega - \Omega_{K0} - \frac{\hbar q_\parallel^2}{2m}\right)\right.$$
$$\left. + (\omega + \Omega_{K0})^2\left(W_2^{K}(\boldsymbol{q}_\parallel, \omega) - \omega - \Omega_{K0} - \frac{\hbar q_\parallel^2}{2m}\right) + (v_F q_\parallel)^2\,\Omega_{K0}\right\}. \tag{97}$$

The corresponding LWA expression is given by

$$\chi^K_{xx}(\boldsymbol{q}_\parallel, \omega) = -\frac{n_{2\mathrm{DEG}}e^2}{m}\left(1 + \frac{v_\mathrm{F}k_\mathrm{F}}{2}\frac{\Omega_{K0}}{\omega^2 - \Omega^2_{K0}} + \frac{\hbar^2 q^2_\parallel}{2m}\left[\frac{k^4_\mathrm{F}\hbar\Omega_{K0}}{2m^2}\frac{3\omega^2 + \Omega^2_{K0}}{(\omega^2 - \Omega^2_{K0})^3} + \frac{3k^2_\mathrm{F}}{2m}\frac{\omega^2 + \Omega^2_{K0}}{(\omega^2 - \Omega^2_{K0})^2} + \frac{1}{2\hbar}\frac{\Omega_{K0}}{\omega^2 - \Omega^2_{K0}}\right]\right). \tag{98}$$

The component $\chi^K_{yy}(\boldsymbol{q}_\parallel, \omega)$ of the RPA polarization tensor is calculated to be

$$\chi^K_{yy}(\boldsymbol{q}_\parallel, \omega) = -\frac{k^2_\mathrm{F}e^2\Omega_{K0}}{\hbar\pi q^2_\parallel} - \frac{m^2e^2}{3\hbar^3\pi q^4_\parallel}\left\{\left(\omega - \Omega_{K0} - \frac{\hbar q^2_\parallel}{2m}\right)^3 - \left(\omega + \Omega_{K0} + \frac{\hbar q^2_\parallel}{2m}\right)^3 + (W^K_1(\boldsymbol{q}_\parallel, \omega))^3 + (W^K_2(\boldsymbol{q}_\parallel, \omega))^3\right\} \tag{99}$$

and the corresponding LWA result is given by

$$\chi^K_{yy}(\boldsymbol{q}_\parallel, \omega) = -\frac{n_{2\mathrm{DEG}}e^2}{m}\left(1 + \frac{v_\mathrm{F}k_\mathrm{F}}{2}\frac{\Omega_{K0}}{\omega^2 - \Omega^2_{K0}} + \frac{\hbar^2 q^2_\parallel}{2m}\left[\frac{k^2_\mathrm{F}}{2m}\frac{\omega^2 + \Omega^2_{K0}}{(\omega^2 - \Omega^2_{K0})^2} + \frac{k^4_\mathrm{F}\hbar\Omega_{K0}}{6m^2}\frac{3\omega^2 + \Omega^2_{K0}}{(\omega^2 - \Omega^2_{K0})^3}\right]\right). \tag{100}$$

For the component $\chi^K_{xz}(\boldsymbol{q}_\parallel, \omega)$ of the full RPA polarization tensor we have found

$$\chi^K_{xz}(\boldsymbol{q}_\parallel, \omega) = i\frac{\hbar^2e^2}{4\pi m^2}\left\{\frac{2m^3}{\hbar^4 q^3_\parallel}\left((\omega - \Omega_{K0})\times\left(W^K_1(\boldsymbol{q}_\parallel, \omega) + \omega - \Omega_{K0} - \frac{\hbar q^2_\parallel}{2m}\right) - (\omega + \Omega_{K0})\times\left(W^K_2(\boldsymbol{q}_\parallel, \omega) - \omega - \Omega_{K0} - \frac{\hbar q^2_\parallel}{2m}\right)\right) - \frac{2mk^2_\mathrm{F}}{\hbar^2 q_\parallel}\right\} \tag{101}$$

and for the corresponding LWA expression

$$\chi^K_{xz}(\boldsymbol{q}_\parallel, \omega) = iq_\parallel\frac{n_{2\mathrm{DEG}}e^2}{m}\left(\frac{\hbar\Omega_{K0}}{2m(\omega^2 - \Omega^2_{K0})} + \frac{v^2_\mathrm{F}}{4}\frac{\omega^2 + \Omega^2_{K0}}{(\omega^2 - \Omega^2_{K0})^2}\right). \tag{102}$$

The RPA result for $\chi^K_{zz}(\boldsymbol{q}_\parallel, \omega)$ is

$$\chi^K_{zz}(\boldsymbol{q}_\parallel, \omega) = -\frac{\hbar^2e^2}{4\pi m^2}\left\{\frac{k^2_\mathrm{F}}{\hbar\Omega_{K0}} + \frac{m^2}{\hbar^3 q^2_\parallel}\left(W^K_1(\boldsymbol{q}_\parallel, \omega) + W^K_2(\boldsymbol{q}_\parallel, \omega) - 2\Omega_{K0} - \frac{\hbar q^2_\parallel}{m}\right)\right\} \tag{103}$$

and the LWA result reads

$$\chi^K_{zz}(\boldsymbol{q}_\parallel, \omega) = -\frac{n_{2\mathrm{DEG}}e^2}{m}\left(\frac{\hbar}{2m\Omega_{K0}}\frac{\omega^2}{\omega^2 - \Omega^2_{K0}} + \frac{\hbar^2 q^2_\parallel}{4m^2}\frac{\omega^2 + \Omega^2_{K0}}{(\omega^2 - \Omega^2_{K0})^2} + \frac{\hbar^3 q^2_\parallel k^2_\mathrm{F}\Omega_{K0}}{8m^3}\frac{3\omega^2 + \Omega^2_{K0}}{(\omega^2 - \Omega^2_{K0})^3}\right). \tag{104}$$

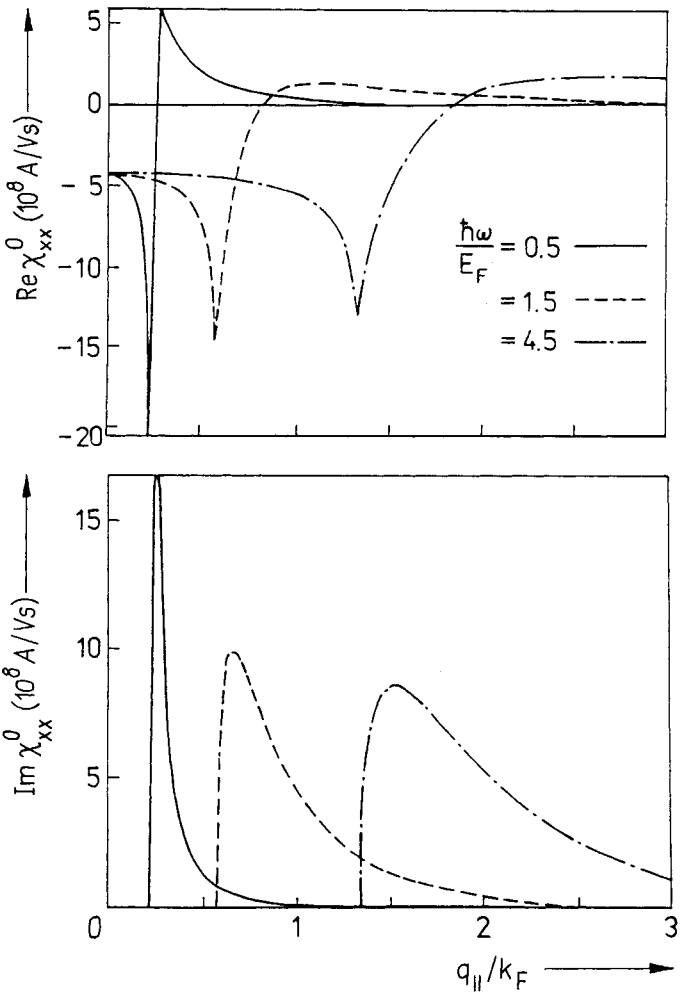

Fig. 5. Plot of the intrasubband contributions Re $\chi^0_{xx}(\boldsymbol{q}_{\parallel}, \omega)$ and Im $\chi^0_{xx}(\boldsymbol{q}_{\parallel}, \omega)$ of the xx component of the RPA polarization tensor for three different frequencies

All the other components are zero,

$$\chi^K_{xy}(\boldsymbol{q}_{\parallel}, \omega) = \chi^K_{yx}(\boldsymbol{q}_{\parallel}, \omega) = \chi^K_{yz}(\boldsymbol{q}_{\parallel}, \omega) = \chi^K_{zy}(\boldsymbol{q}_{\parallel}, \omega) = 0\,.$$

In Fig. 5 to 10 are shown the calculated nonzero components of the RPA polarization tensor $\chi^K_{\alpha\beta}(\boldsymbol{q}_{\parallel}, \omega)$ for $K = 0$ and $K = 1$.

The components of the polarization tensor show a similar peak structure as the polarization function if the boundaries ω_1^{00}, ω_2^{00}, ω_3^{00}, ω_1^{10}, and ω_2^{10} of the single-particle continua are crossed.

Note that $\chi^0_{xz}(\boldsymbol{q}_{\parallel}, \omega)$, $\chi^0_{zx}(\boldsymbol{q}_{\parallel}, \omega)$, and $\chi^0_{zz}(\boldsymbol{q}_{\parallel}, \omega)$ are zero. Because of the definition of $\chi^K_{\alpha\beta}(\boldsymbol{q}_{\parallel}, \omega)$ in (87) the xz component has a real and an imaginary part which are opposite in character in comparison to the other components. We note that $\chi_K(\boldsymbol{q}_{\parallel}, \omega)$ and $\chi^K_{\alpha\beta}(\boldsymbol{q}_{\parallel}, \omega)$ have no singularities.

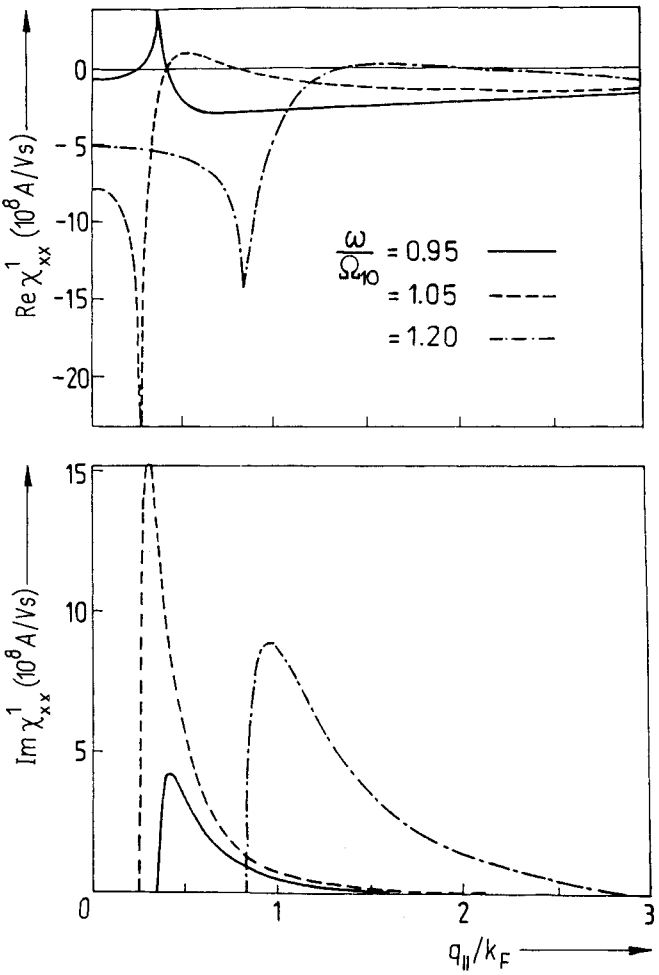

Fig. 6. Plot of the (1–0) intersubband contributions Re $\chi^1_{xx}(\boldsymbol{q}_{\parallel}, \omega)$ and Im $\chi^1_{xx}(\boldsymbol{q}_{\parallel}, \omega)$ of the xx component of the RPA polarization tensor for three different frequencies

4.4 Relation between the polarization function and the components of the polarization tensor

To compare the results of the density-response with that of the current-response it is necessary to have a unique relation between the density-response function and the components of the current-response tensor.

From the point of view of the macroscopic electrodynamics it is necessary to have the same dielectric tensor in electrostatics as well as in electrodynamics. Using (18) and (35) we obtain

$$P(\boldsymbol{x}, \boldsymbol{x}' \mid \omega) = -\frac{1}{\omega^2} \sum_{\alpha,\beta} \frac{\partial^2}{\partial x_\alpha \, \partial x'_\beta} P_{\alpha\beta}(\boldsymbol{x}, \boldsymbol{x}' \mid \omega) \,. \tag{105}$$

On the other hand, from the point of view of quantum mechanics it is possible to show (see Appendix C) that the following equation of continuity for the operators of the charge

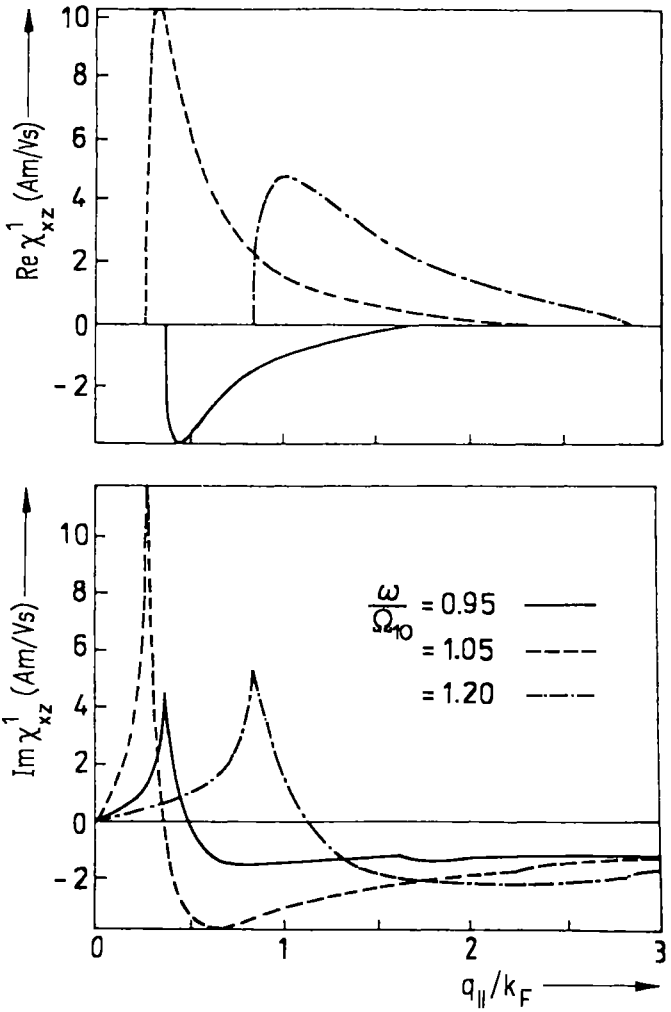

Fig. 7. Plot of the (1–0) intersubband contributions Re $\chi^1_{xz}(\boldsymbol{q}_\parallel, \omega)$ and Im $\chi^1_{xz}(\boldsymbol{q}_\parallel, \omega)$ of the xz component of the RPA polarization tensor for three different frequencies

and current density is valid:

$$\frac{\partial}{\partial t}\hat{\varrho}(\boldsymbol{x}, t) + \sum_\alpha \frac{\partial}{\partial x_\alpha}\hat{j}_\alpha(\boldsymbol{x}, t) = 0\,. \tag{106}$$

Starting with this equation we can derive the relation

$$\frac{\partial^2}{\partial t\,\partial t'}[\hat{\varrho}(\boldsymbol{x}, t), \hat{\varrho}(\boldsymbol{x}', t')] = \sum_{\alpha,\beta}\frac{\partial^2}{\partial x_\alpha\,\partial x'_\beta}[\hat{j}_\alpha(\boldsymbol{x}, t), \hat{j}_\beta(\boldsymbol{x}', t')]\,. \tag{107}$$

From this equation the relation between the polarization function and the components of the polarization tensor follows after multiplication of (107) by $-i/\hbar\hat{\varrho}_G\theta(t - t')$ and taking

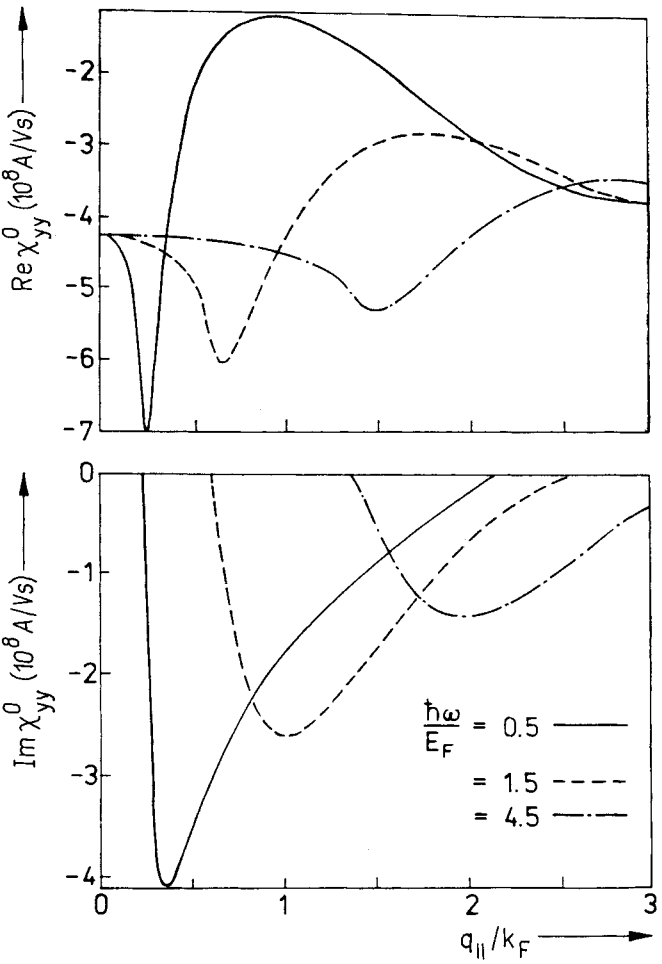

Fig. 8. Plot of the intrasubband contributions Re $\chi^0_{yy}(\boldsymbol{q}_{\parallel}, \omega)$ and Im $\chi^0_{yy}(\boldsymbol{q}_{\parallel}, \omega)$ of the yy component of the RPA polarization tensor for three different frequencies

into account the trace

$$\frac{\partial^2}{\partial t\, \partial t'} P(\boldsymbol{x}, \boldsymbol{x}' \mid t - t') = - \sum_{\alpha,\beta} \frac{\partial^2}{\partial x_\alpha\, \partial x'_\beta} P_{\alpha\beta}(\boldsymbol{x}, \boldsymbol{x}' \mid t - t') . \tag{108}$$

It is important to note that this general relation is not restricted to the RPA and, hence, it is also valid for real interacting electronic systems.

For the p-polarized modes [90] of an arbitrary SQW we have with $\boldsymbol{q}_{\parallel} = (q_x, 0, 0)$

$$P(\boldsymbol{q}_{\parallel}; z, z' \mid \omega) = - \frac{q_{\parallel}^2}{\omega^2} \left\{ P_{xx}(\boldsymbol{q}_{\parallel}; z, z' \mid \omega) + \frac{1}{iq_{\parallel}} \frac{\partial}{\partial z} P_{zx}(\boldsymbol{q}_{\parallel}; z, z' \mid \omega) - \frac{1}{iq_{\parallel}} \frac{\partial}{\partial z'} P_{xz}(\boldsymbol{q}_{\parallel}; z, z' \mid \omega) \right.$$
$$\left. + \frac{1}{q_{\parallel}^2} \frac{\partial^2}{\partial z\, \partial z'} P_{zz}(\boldsymbol{q}_{\parallel}; z, z' \mid \omega) \right\} . \tag{109}$$

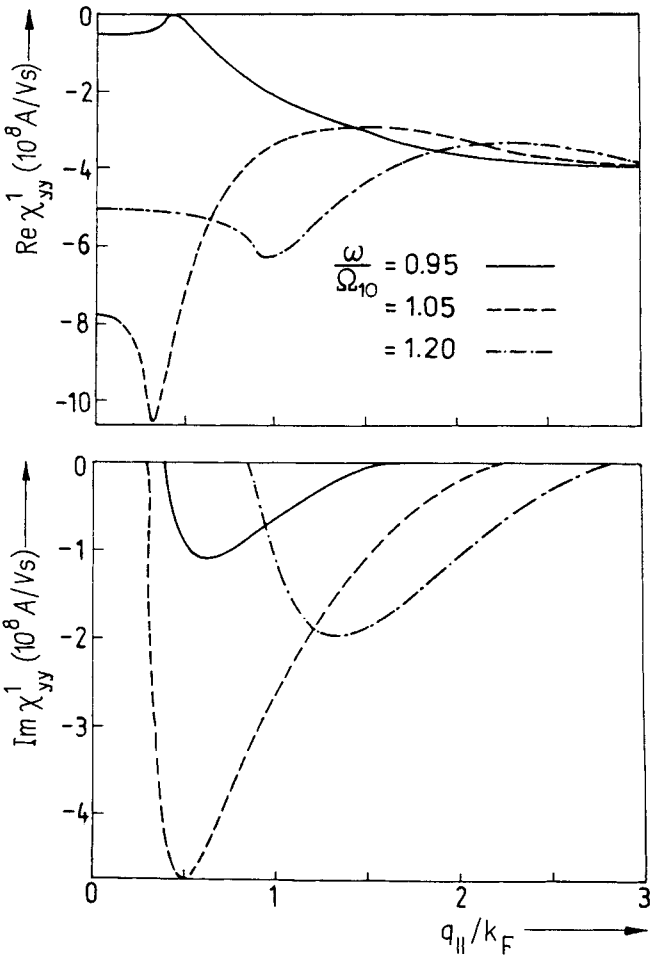

Fig. 9. Plot of the (1–0) intersubband contributions Re $\chi^1_{yy}(\boldsymbol{q}_{\parallel}, \omega)$ and Im $\chi^1_{yy}(\boldsymbol{q}_{\parallel}, \omega)$ of the yy component of the RPA polarization tensor for three different frequencies

Under the assumption of the EQL, (109) can be written in the form

$$\chi_K(\boldsymbol{q}_{\parallel}, \omega) = -\frac{q_{\parallel}^2}{\omega^2}\left\{\chi^K_{xx}(\boldsymbol{q}_{\parallel}, \omega) + \frac{2m\Omega_{K0}}{i\hbar q_{\parallel}}\left(\chi^K_{zx}(\boldsymbol{q}_{\parallel}, \omega) - \chi^K_{xz}(\boldsymbol{q}_{\parallel}, \omega)\right) + \left(\frac{2m\Omega_{K0}}{\hbar q_{\parallel}}\right)^2 \chi^K_{zz}(\boldsymbol{q}_{\parallel}, \omega)\right\}. \tag{110}$$

Using this relation it can be seen that the dispersion relation of the collective excitations of the Q2DEG of the density-response (60) and the dispersion relation for the p-polarization of the current-response (89) differ from each other. This result is different from the well-known case of a homogeneous 3DEG of an isotropic solid for which the density response gives a correct description of the longitudinal modes, the plasmons. But for a Q2DEG, the longitudinal and the transverse field components are coupled and, hence, all

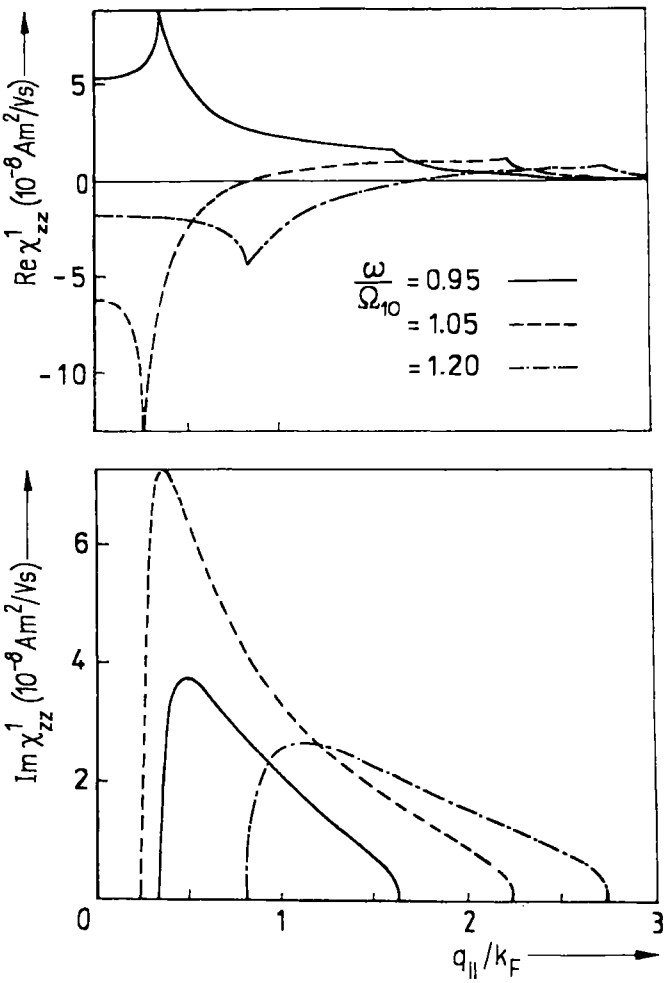

Fig. 10. Plot of the (1–0) intersubband contributions Re $\chi^1_{zz}(\boldsymbol{q}_{\|}, \omega)$ and Im $\chi^1_{zz}(\boldsymbol{q}_{\|}, \omega)$ of the zz component of the RPA polarization tensor for three different frequencies

modes are influenced by retardation. Taking the unretarded limit, i.e. $c \to \infty$ of (89), we have

$$\det \left\{ \delta_{KL} - \mu_0 \tilde{D}^{KL}_{xx}(\boldsymbol{q}_{\|}, \omega) \left[\chi^L_{xx}(\boldsymbol{q}_{\|}, \omega) + \frac{2m\Omega_{L0}}{i\hbar q_{\|}} \chi^L_{zx}(\boldsymbol{q}_{\|}, \omega) \right.\right.$$
$$\left.\left. - \frac{2m\Omega_{L0}}{i\hbar q_{\|}} \chi^L_{xz}(\boldsymbol{q}_{\|}, \omega) + \left(\frac{2m\Omega_{L0}}{\hbar q_{\|}} \right)^2 \chi^L_{zz}(\boldsymbol{q}_{\|}, \omega) \right] \right\} = 0 . \tag{111}$$

Herein $\tilde{D}^{KL}_{xx}$ is D^{KL}_{xx} for $c \to \infty$. Using (110) it follows that the dispersion relation of the plasmon-polaritons in the unretarded limit (111) is the same as (60) for the plasmons of the density-response. Hence, for the p-polarization the density- and the current-response give the same collective excitations. But in the case of the density-response all modes are

unretarded. That means, in contrast to a 3DEG, the results of the density-response are only correct if the condition $q_{\|}^2 \gg \varepsilon_{b1}\omega^2/c^2$ is valid. This can be seen explicitly from (116) and (122) for 2D plasmons and 2D plasmon-polaritons which we derive later.

5. Collective Excitations: Intra- and Intersubband Plasmons and Plasmon-Polaritons

5.1 General consideration

The excitations of a Q2DEG can be separated in collective and single-particle excitations. The collective excitations are plasma oscillations which are coupled to photons in the case of the current-response and hence, plasmon-polaritons, or are not in the case of the density-response. The single-particle excitations are transitions of single electrons from states below the Fermi surface to an empty state above it. Because of the size-quantization on the electron states in the quantum well, collective as well as single-particle excitations can be separated into intra- and intersubband excitations. The intrasubband excitations are transitions of electrons from the states below the Fermi surfaces into the empty states above it within one subband. The intersubband excitations, however, are transitions of electrons from the states in a subband K below the Fermi surface into the empty states above it in a different subband K'. Within the EQL the single-particle excitations exist in the regions of the ω–$q_{\|}$ plane for which $\operatorname{Im}\chi_K(\boldsymbol{q}_{\|}, \omega) \neq 0$, $\operatorname{Im}\chi_{xx}^K(\boldsymbol{q}_{\|}, \omega) \neq 0$, $\operatorname{Im}\chi_{yy}^K(\boldsymbol{q}_{\|}, \omega) \neq 0$, $\operatorname{Im}\chi_{zz}^K(\boldsymbol{q}_{\|}, \omega) \neq 0$, $\operatorname{Re}\chi_{xz}^K(\boldsymbol{q}_{\|}, \omega) \neq 0$, and $\operatorname{Re}\chi_{zx}^K(\boldsymbol{q}_{\|}, \omega) \neq 0$. In Fig. 2 we have plotted these regions which are given by

$$v_F q_{\|}\,(-1 + q_{\|}/(2k_F)) + \Omega_{K0} < \omega < v_F q_{\|}\,(1 + q_{\|}/(2k_F)) + \Omega_{K0}\,.$$

The condition for the existence of self-sustaining collective excitations is given by the dispersion relation. This means that the dispersion relation represents a resonance condition which defines the eigenfrequencies $\omega = \omega_j(\boldsymbol{q}_{\|})$ of the collective excitations having an infinite lifetime. Therefore, the dispersion relations of Sections 4.2 and 4.3 are valid under the conditions $\operatorname{Im}\chi_K = 0$ and $\operatorname{Im}\chi_{xx}^K = 0$, $\operatorname{Im}\chi_{yy}^K = 0$, $\operatorname{Im}\chi_{zz}^K = 0$, $\operatorname{Re}\chi_{xz}^K = 0$, $\operatorname{Re}\chi_{zx}^K = 0$, respectively. Within the single-particle intra- and intersubband continua the dispersion relations (60), (88), and (89) lose their meaning strictly speaking. The collective excitations are not well defined because they are no longer true normal modes of the system. This is related to the fact that regarding damping processes the solutions ω and $q_{\|}$ of the dispersion relation in general will be complex quantities because $\chi_K(\boldsymbol{q}_{\|}, \omega)$ and $\chi_{\alpha\beta}^K(\boldsymbol{q}_{\|}, \omega)$ become complex. The solutions look quite different for the different possibilities occurring when we choose the additional conditions on ω and $q_{\|}$. Which condition is appropriate is determined by the experiment. In an earlier paper we have discussed some consequences in detail [98]. Collective excitations inside the single-particle continua are highly damped by the collisionless and resonant mechanism of the Landau damping [45]. That means the Q2D plasmons are able to decay into single electron–hole pairs.

In Fig. 11 we have plotted the ω–$q_{\|}$ plane in the region of small wave vectors in which the retardation effects become important ($q_{\|}^2 \approx \varepsilon_{b1}\omega^2/c^2$). The regions in the ω–$q_{\|}$ plane where the different types of plasmon-polaritons of the current-response exist are limited by zeros $\alpha_0 = 0$ (that is the dispersion relation of light in vacuum $q_{\|}^2 = \omega^2/c^2$), $\alpha_{1,2} = 0$ (that is the dispersion relation of light in a medium with $\varepsilon_{b1,2}$: $q_{\|}^2 = \varepsilon_{b1,2}\omega^2/c^2$). A source point in layer $\nu = 1$ can produce the following four types of fields (see Appendix A):

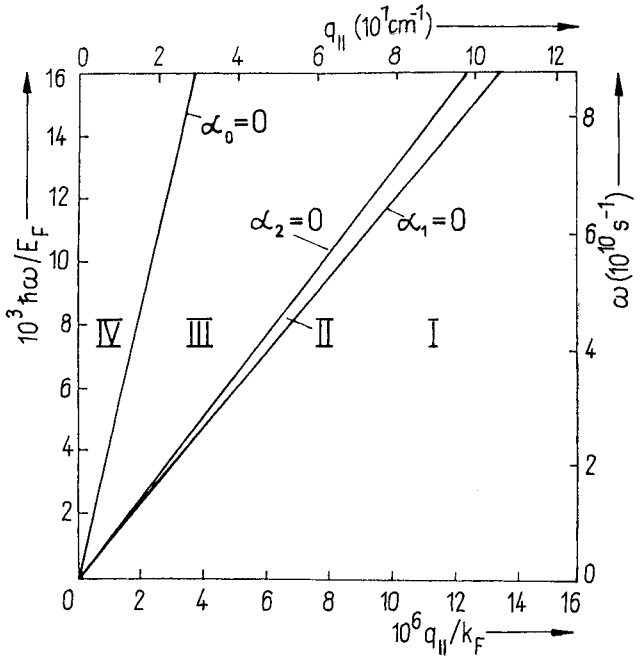

Fig. 11. Regions in the ω–$q_{\parallel}$ plane where the different types of plasmon-polaritons exist

(i) the field decays from each heterointerface into the media (region I);

(ii) the field has the character of a standing wave inside layer $\nu = 1$ but decays exponentially from the interfaces outside of the layer (region II);

(iii) the field has the character of a standing wave in the layers $\nu = 1$ and $\nu = 2$, decays exponentially into the vacuum, and is an outgoing radiative wave inside the substrate ($\nu = 3$) (region III); and

(iv) the field is in contrast to (iii) also an outgoing radiative wave in the vacuum (region IV).

Hence, inside regions I and II we have normal modes and inside the regions III and IV we have so-called leaky waves caused by radiative loss. Because we investigate normal modes of the Q2DEG these must be non-radiative. That means the plasmon-polaritons are characterized by the fields decaying exponentially when moving into the vacuum for $z > a + b$ or below the Q2DEG for $0 > z$. Therefore, α_0 and α_2 are positive and real or $q_{\parallel}^2 > \omega^2/c^2$ and $q_{\parallel}^2 > \varepsilon_{b2}\omega^2/c^2$, respectively. The dispersion curves of the plasmon-polaritons lie to the right of the dispersion curve of light in medium $\nu = 2$. The character of the fields of the plasmon-polaritons (see Appendix A) in the regions of the ω–$q_{\parallel}$ plane is distinguished by the value of α_1 if $\varepsilon_{b1} > \varepsilon_{b2}$:

(i) If α_1 is real or $q_{\parallel}^2 > \varepsilon_{b1}\omega^2/c^2$ the plasmon-polaritons have fields decaying exponentially from each heterointerface into the media. Thus is true in region I.

(ii) If α_1 is purely imaginary or $q_{\parallel}^2 < \varepsilon_{b1}\omega^2/c^2$, i.e. $\varepsilon_{b2}\omega^2/c^2 < q_{\parallel} < \varepsilon_{b2}\omega^2/c^2$, the plasmon-polaritons are characterized by fields having the character of a standing wave inside the layer $\nu = 1$. This is true in region II.

From the dispersion relation (89), we can see that the p-polarized plasmon-polaritons can exists in regions I and II. The s-polarized plasmon-polaritons are described by (88). For

TE-modes the electric field is parallel to the interface and it is directed along the y-direction. In the Q2DEG of the DHS a charge density is only induced for electron motion in x- and z-direction. Hence, s-polarized fields do not induce a time-dependent charge density. This can be easily seen from the equation of continuity, because of the vanishing y-dependence of the current density for our geometry. Therefore, the formation of an s-polarized excitation is only possible by means of a magnetic force (Lorentz force) acting on the induced current density. But this force is very weak, of the order of $v_F/c \ll 1$, in comparison to the electrical force acting on the charge density. If one solves (88) in the long-wavelength approximation there is a weak resonance slightly below Ω_{K0}. This weak resonance was also found by other authors [34, 35]. The frequency of the excitation lies inside the single-particle continuum. Therefore, a strong Landau damping arises and it is not possible to call this resonance a normal mode. In the numerical investigations with the full RPA polarization tensor the resonances do not occur outside the single-particle continuum in the case of s-polarized waves.

For numerical work we have chosen a GaAs-$Ga_{1-x}Al_xAs$ DHS. The material constants are taken to be [99] for GaAs: $\varepsilon_{b1} = 12.87, m = 0.06624m_0$ and for $Ga_{1-x}Al_xAs$: $\varepsilon_{b2} = 10.99$. That means we use the static dielectric constants ε_{sv} for the background dielectric constants ε_{bv}. In the numerical work we concentrate our attention on plasmons and p-polarized plasmon-polaritons occurring in regions I and II.

5.2 Intrasubband plasmons and p-polarized intrasubband plasmon-polaritons

The dispersion relations of the different intrasubband modes will be discussed in the diagonal approximation. For this case the dispersion relation of the (0–0) intrasubband plasmon is given by (62) for $K = 0$ and that of the p-polarized (0–0) intrasubband plasmon-polariton is given by (95). We are concerned with the full RPA spectrum. In our calculations no additional simplifying approximations for the RPA polarization function and polarization tensor are made. Hence, the results are valid for all wave vectors. Fig. 12 to 14 show the dispersion curves of the (0–0) intrasubband plasmons calculated with inclusion of the image effects and without the image effects. The image effects arise from the different polarizabilities of the materials forming the DHS (see Appendix A).

The dispersion curves of the intrasubband plasmons start at $q_{\|} = 0$ and $\omega = 0$ and enter at $q_{\|} = q_{\|}^{c}$ and $\omega = \omega_1$, the single-particle intrasubband continuum. Inside this region the intrasubband plasmons will be Landau damped which we have investigated in detail [45]. It can be seen that the image contribution influences the dispersion curves only in a finite range of the wave vectors. For large wave vectors the image effects vanish (see Fig. 12a). The image contribution to the Coulomb interaction results in an enhancement of the frequency of the mode, especially for low frequencies. From Fig. 13 one can see that with decreasing thickness of the $Ga_{1-x}Al_xAs$ top layer ($\nu = 2$) the image effects on the dispersion curve of the intrasubband plasmon increase. The physical reason for this behaviour is the following. Due to the large difference of the dielectric constants between the $Ga_{1-x}Al_xAs$ top layer and vacuum the most image charges are concentrated at the interface at $z = a + b$. Hence, decreasing b the distance between the Q2DEG and these image charges decreases. An oscillating charge distribution, the plasmon, produces an oscillating image charge in a layered system with materials having different polarizabilities. The image field, which is the homogeneous part of (A12), acts to screen the oscillating charge and, hence, there is an additional force to enhance the frequency of the oscillation. In the case of large wave vectors

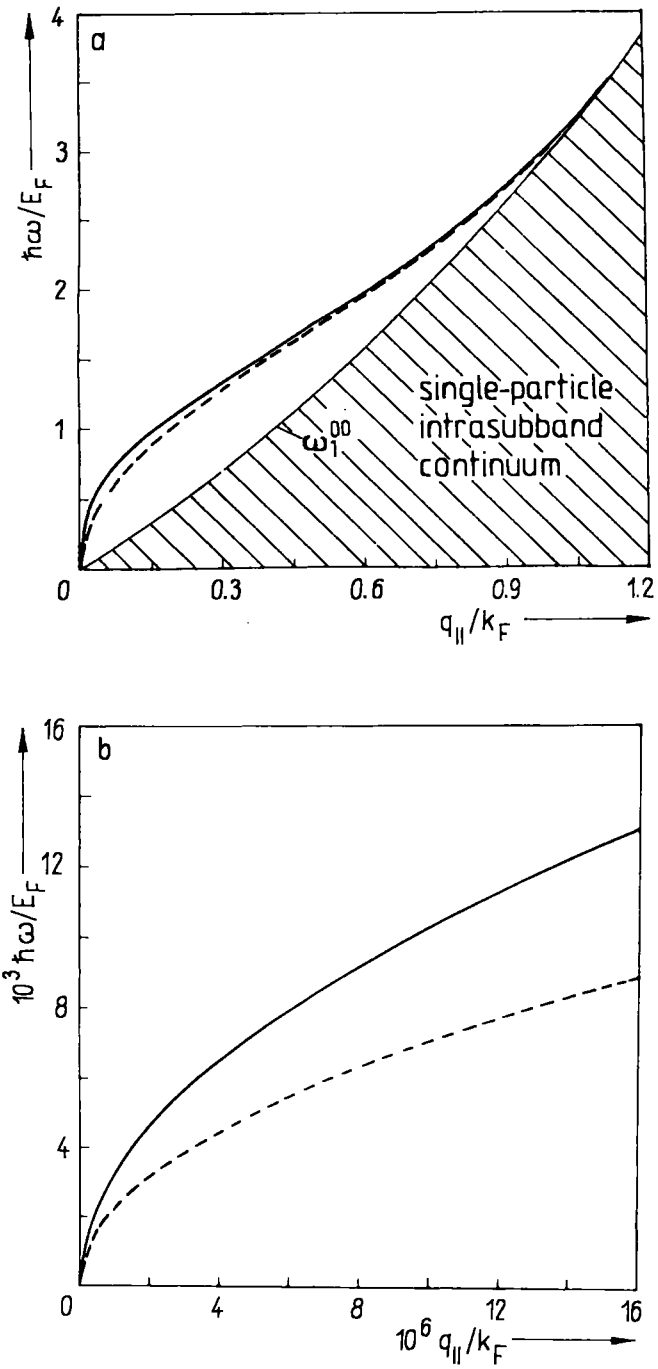

Fig. 12. Dispersion relation of the intrasubband plasmon of the GaAs-$Ga_{1-x}Al_xAs$ DHS with (solid line) and without (dashed line) image effects in a) the whole and b) in the small wave vector region; $n_{2DEG} = 10^{11}\ cm^{-2}$, $a = 20$ nm, $b = 60$ nm

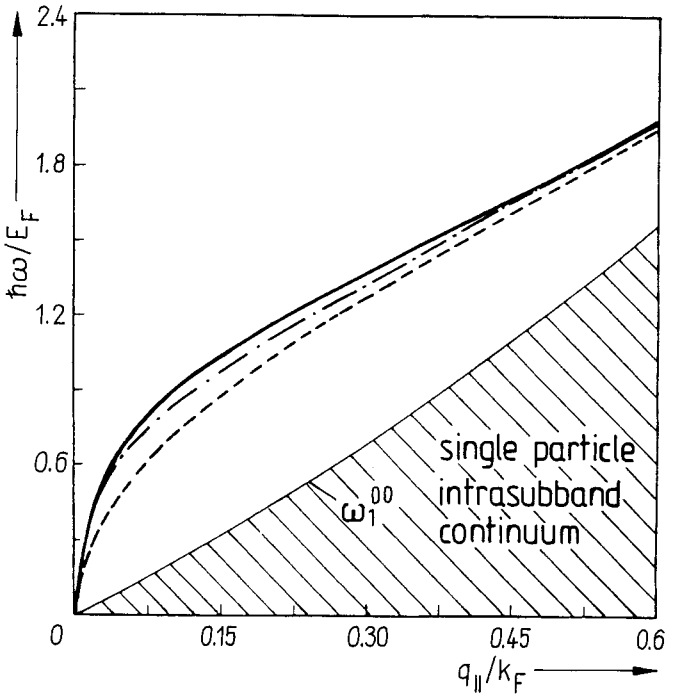

Fig. 13. Dispersion relation of the intrasubband plasmon of the GaAs-$Ga_{1-x}Al_xAs$ DHS with image effects for $b = 20$ nm (solid line) and $b = 60$ nm (dashed-dotted line) and without image effects (dashed line); $n_{2DEG} = 10^{11}$ cm^{-2}, $a = 20$ nm

the image fields are mainly concentrated at the interfaces. Therefore, there is nearly no interaction between the image field and the charge density, induced by the plasmon which is zero at the interfaces of the quantum well. This is the physical reason for the vanishing influence of the image contribution on the dispersion curves of the (0–0) intrasubband plasmon for large wave vectors. as illustrated in Fig. 13 and 14. Further, this result can be seen explicitly if one derives an analytic expression for the dispersion relation of the (0–0) intrasubband plasmon in the long-wavelength limit. With the results of Appendix B the matrix element $D_{xx}^{KK}(\boldsymbol{q}_\parallel, \omega)$, which is necessary in the calculations, reads

$$D_{xx}^{KK}(\boldsymbol{q}_\parallel, \omega) = R_0 \left\{ (\alpha_1 a) \left[\frac{1}{(\alpha_1 a)^2 + \pi^2 (K+2)^2} + \frac{1}{(\alpha_1 a)^2 + (\pi K)^2} \right] \right.$$
$$+ 2(\alpha_1 a)^2 \left[\frac{(2\pi)^2 (K+1)}{((\alpha_1 a)^2 + (\pi K)^2)((\alpha_1 a)^2 + \pi^2 (K+2)^2)} \right]^2$$
$$\times \left[\frac{8 p_2 p_3 (\sinh(\alpha_2 b) + p_1 \cosh(\alpha_2 b))((-1)^K - \cosh(\alpha_1 a))}{\det[I_{ij}]\, e^{\alpha_0 (a+b)}} \right.$$
$$\left. \left. - \frac{4 \sinh(\alpha_1 a)((p_1 p_2 + p_3)\cosh(\alpha_2 b) + (p_1 p_3 + p_2)\sinh(\alpha_2 b))}{\det[I_{ij}]\, e^{\alpha_0 (a+b)}} \right] \right\}. \tag{112}$$

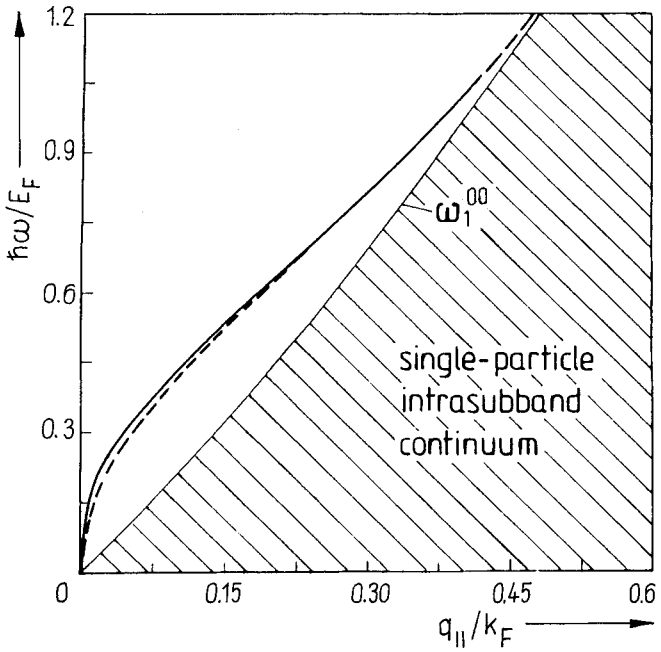

Fig. 14. Dispersion relation of the intrasubband plasmon of the GaAs-$Ga_{1-x}Al_xAs$ DHS with (solid line) and without (dashed line) image effects; $n_{2DEG} = 10^{12}$ cm^{-2}, $a = 20$ nm, $b = 60$ nm

We notice that for $p_1 = p_2 = p_3 = 1$ and $\alpha_v = \alpha_1$ (112) gives the result without image contribution. To compare the result of the current-response with that of the density-response, we calculate both expressions, $D_{xx}^{KK}(\boldsymbol{q}_\parallel, \omega)$ and $D_{KK}(\boldsymbol{q}_\parallel)$. $D_{KK}(\boldsymbol{q}_\parallel)$ is given by (112) if one replaces $R_0 = -c^2\alpha_1/(2\varepsilon_{b1}\omega^2)$ by $R_0 = 1/(2\varepsilon_{b1}q_\parallel)$ and α_v by $q_\parallel$. To obtain explicit dispersion relations it is necessary to expand D_{xx}^{KK} in a power series of α_1 and D_{KK} in a power series of $q_\parallel$. In the case without image contributions we expand D_{KK} to $q_\parallel^2$ and D_{xx}^{KK} to α_1^4.

In the lowest order of $q_\parallel$ the matrix element of the Green's function $D_{00}(\boldsymbol{q}_\parallel)$ including image effects is

$$D_{00}(\boldsymbol{q}_\parallel) = \frac{1}{(1 + \varepsilon_{b2})\, q_\parallel} \tag{113}$$

and without image effects it reads

$$D_{00}(\boldsymbol{q}_\parallel) = \frac{1}{2\varepsilon_{b1} q_\parallel}. \tag{114}$$

Using the LWA expression of the polarization function (66), and the above calculated matrix elements of the Green's function (113) or (114), in the dispersion relation (62) we derive the explicit dispersion relation for the (0–0) intrasubband plasmon. Hence, in the long-wavelength limit including image effects, the dispersion relation is given by

$$\omega_p^{00} = \left(\frac{n_{2DEG} e^2 q_\parallel}{m\varepsilon_0(1 + \varepsilon_{b2})}\right)^{1/2}. \tag{115}$$

If one neglects image effects, then the dispersion reads

$$\omega_{\mathrm{p}}^{00} = \left(\frac{n_{2\mathrm{DEG}} e^2 q_{\|}}{2m\varepsilon_0 \varepsilon_{\mathrm{b1}}} \right)^{1/2} \tag{116}$$

If one compares both results, it can be seen directly that in this limit the Coulomb interaction is screened by the background dielectric constant $\varepsilon_{\mathrm{b2}}$ of the barrier material and by the "vacuum". Neglecting image effects one obtains in the long-wavelength limit the uncorrect result that the Coulomb interaction is screened by the dielectric constant $\varepsilon_{\mathrm{b1}}$ of the host material. Further, one can see that in the long-wavelength limit there is no difference between the (0–0) intrasubband plasmon of a DHS with finite width and a 2D plasmon. Hence, the case of small wave vectors corresponds to the case of small thickness a of the quantum well. For small wave vectors the image field is well extended in z-direction. This implies that the Coulomb interaction is mainly screened by the surrounding media. For small thicknesses of the quantum well nearly all field lines of the Coulomb interaction are within the surrounding media. The induced charge density is given by

$$\begin{aligned} \varrho^{\mathrm{ind}}(\boldsymbol{x}, t) &= \cos(\boldsymbol{q}_{\|}\boldsymbol{x}_{\|} - \omega t)\, \varrho^{\mathrm{ind}}(\boldsymbol{q}_{\|}; z \mid \omega), \\ \varrho^{\mathrm{ind}}(\boldsymbol{q}_{\|}; z \mid \omega) &= \sum_K \varphi_K(z)\, \varphi_0(z)\, \chi_K(\boldsymbol{q}_{\|}, \omega)\, \Phi_{K0}(\boldsymbol{q}_{\|}, \omega), \end{aligned} \tag{117}$$

where $\Phi_{K0}(\boldsymbol{q}_{\|}, \omega)$ is the matrix element of the total scalar potential. For small wave vectors the image potential becomes independent of z and we obtain for the interaction of the plasmon with the image field

$$\int \mathrm{d}z\, \varrho_K^{\mathrm{ind}}(\boldsymbol{q}_{\|}; z \mid \omega)\, \Phi^{\mathrm{im}}(\boldsymbol{q}_{\|}, z) \propto \int \mathrm{d}z\, \varrho_K^{\mathrm{ind}}(\boldsymbol{q}_{\|}; z \mid \omega) \propto \delta_{K0^*} \tag{118}$$

Hence, at small wave vectors only the (0–0) intrasubband plasmon is influenced by the image contributions (see Fig. 12 to 14). In Fig. 14 we have depicted the (0–0) intrasubband plasmons with and without image effects for $n_{2\mathrm{DEG}} = 10^{12}\,\mathrm{cm}^{-2}$. It is to be seen that with increasing electron density the dispersion curves are shifted to higher frequencies.

In Fig. 15 and 16 the dispersion curves of the p-polarized (0–0) intrasubband plasmon-polaritons are plotted, which occur in regions I and II of Fig. 11. From these figures it can be seen that the modes, calculated with or neglecting the image contribution, starts for $q_{\|} = 0$ at $\omega = 0$. If one neglects the image contribution, the dispersion curve for very small wave vector approaches $\alpha_1 = 0$ and is always located to the right of the light line $\alpha_1 = 0$ for all wave vectors (see Fig. 15 and 16b). On the other hand, the dispersion curves calculated including the image contributions start for small wave vectors at $\alpha_2 = 0$. That means, for small wave vectors the intrasubband plasmon-polariton is influenced only by the surrounding media.

This can be seen explicitly if one derives an analytic expression for the dispersion relation of the (0–0) intrasubband plasmon-polariton in the long-wavelength limit. In the lowest order of α_1 the matrix element of the xx component of the Green's tensor $D_{xx}^{00}(\boldsymbol{q}_{\|}, \omega)$ including images effects is

$$D_{xx}^{00}(\boldsymbol{q}_{\|}, \omega) = -\frac{c^2 \alpha_0 \alpha_2}{\omega^2(\alpha_2 + \varepsilon_{\mathrm{b2}}\alpha_0)} \tag{119}$$

and without image effects it reads

$$D_{xx}^{00}(\boldsymbol{q}_{\parallel}, \omega) = -\frac{c^2\alpha_1}{2\omega^2\varepsilon_{b1}}. \tag{120}$$

Using the LWA expression of the xx component of the polarization tensor (98), and the above calculated matrix elements of the xx component of the Green's tensor, (119) or (120), in the dispersion relation (95), we derive the explicit dispersion relation for the (0–0) intrasubband plasmon-polariton. In the small wave vector region $\alpha_2 \ll \varepsilon_{b2}\alpha_0$ is valid and hence, (119) reads $D_{xx}^{00}(\boldsymbol{q}_{\parallel}, \omega) = -c^2\alpha_2/(\omega^2\varepsilon_{b2})$. Consequently one obtains the dispersion relation including image effects in the form

$$q_{\parallel}^2 = \varepsilon_{b2}\frac{\omega^2}{c^2} + \left(\frac{m\varepsilon_0\varepsilon_{b2}\omega^2}{n_{2DEG}e^2}\right)^2. \tag{121}$$

We note that in the vicinity of the light line $\alpha_1 = 0$ there is no difference between the (0–0) intrasubband plasmon-polariton existing in a DHS with finite width and a 2D plasmon-polariton. The dispersion relation depends neither on a nor on b. But it depends on the background dielectric constant of the surrounding media. If we neglect the image effects, the corresponding dispersion relation reads

$$q_{\parallel}^2 = \varepsilon_{b1}\frac{\omega^2}{c^2} + \left(\frac{2m\varepsilon_0\varepsilon_{b1}\omega^2}{n_{2DEG}e^2}\right)^2. \tag{122}$$

It can be seen that now the dispersion relation only depends on the background dielectric constant ε_{b1} of the host material. Taking the unretarded limit, i.e., $c \to \infty$ in (122), we obtain the corresponding dispersion relation (116) of the density-response. If we take this limit for the dispersion relation with image effects (121), we also obtain the corresponding dispersion relation of the density-response (115), with one difference: the form factor $(1 + \varepsilon_{b2})/2$ is replaced by $\varepsilon_{b2}/2$ as a result of the approximation used in deriving (121). Inside region II of the ω–$q_{\parallel}$ plane of Fig. 11 the (0–0) inrasubband plasmon-polaritons have fields with standing wave character inside the quantum well region (layer $\nu = 1$). For a certain value of frequency and wave vector the dispersion curve crosses the light line $\alpha_1 = 0$. We notice that for very small wave vectors the dispersion relations (115), (116) and (121), (122) are the same as for macroscopic surface plasmons and plasmon-polaritons of a very small layer with the background dielectric constant ε_{b1} surrounded by a medium with ε_{b2} if we include image effects or with ε_{b1} if we omit image effects [100]. The image contribution further results, as in the case of the density response, in the increase of the frequency of the plasmon-polariton. The frequency increases with decreasing thickness b of the $Ga_{1-x}Al_xAs$ layer (not drawn in Fig. 15 because of the plotted small wave vector region). For larger values of the wave vector the dispersion curves of the p-polarized intrasubband plasmon-polaritons reach those of the intrasubband plasmons. The retardation only influences the small wave vector region. This is plotted in Fig. 16.

5.3 Intersubband plasmons and p-polarized intersubband plasmon-polaritons

As in the case of intrasubband modes the dispersion relation of the different (1–0) intersubband modes will be discussed in the diagonal approximation. Then the dispersion relation of the (1–0) intersubband plasmon is given by (62) for $K = 1$ and that of the

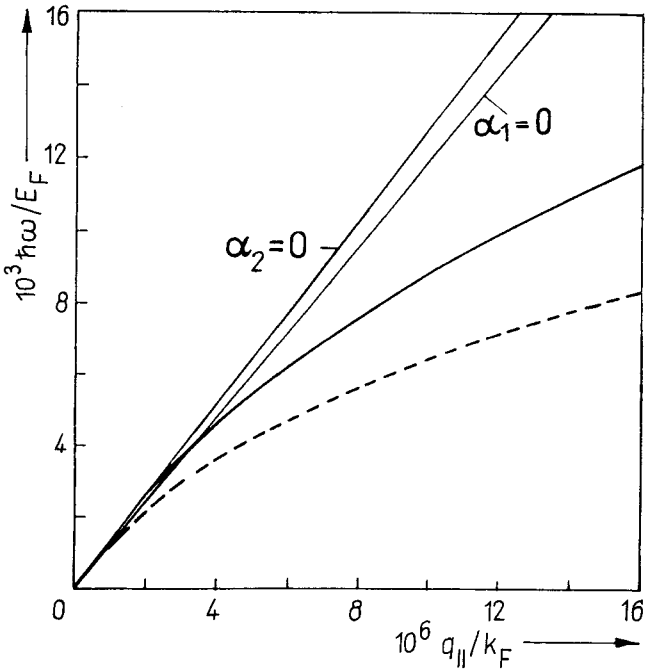

Fig. 15. Dispersion relation of the p-polarized intrasubband plasmon-polariton of the GaAsGa$_{1-x}$Al$_x$As DHS with (solid line) and without (dashed line) image effects; $n_{2DEG} = 10^{11}$ cm^{-2}, $a = 20$ nm

p-polarized (1–0) intersubband plasmon-polariton is given by (96). Note that for the investigated intersubband processes χ^1_{xz} and χ^1_{zz} are different from zero in difference to the intrasubband case where both χ^0_{xz} and χ^0_{zz} are equal to zero in the whole ω–$q_{\parallel}$ plane. As in the case of the intrasubband modes no simplifying approximations for the RPA polarization function and polarization tensor are made. We note that the here considered diagonal approximation is an exact solution for a two-subband model ($K = 0, 1$) where according symmetry of the DHS the (0–0) intrasubband plasmon (symmetric mode) is not coupled with the (1–0) intersubband plasmon (antisymmetric mode). In Fig. 17a the dispersion curves of the (1–0) intersubband plasmons are plotted. They are calculated including image effects and neglecting the image effects.

The (1–0) intersubband plasmon starts for $q_{\parallel} = 0$ at $\omega = (\Omega^2_{10} + \frac{5}{3}\omega_0^2)^{1/2}$ (cf. (143) and (144)). This is true in both cases: with and without image contribution. The image contribution to the Coulomb interaction results in an enhancement of the frequency of the mode only for $q_{\parallel} > 0$. This enhancement increases with decreasing thickness b of the Ga$_{1-x}$Al$_x$As top layer. Hence, the image effects alter only the terms proportional $q_{\parallel}$ and $q^2_{\parallel}$ of (62). This agrees well with (118) for the interaction of the (1–0) intersubband plasmon with the image field. Hence, the depolarization shift [101, 102], which is the energy difference between the single-particle excitation $\hbar\Omega_{10}$ and the collective excitation in RPA at $q_{\parallel} = 0$, is not altered by the image contributions. The depolarization shift arises because each electron feels a field which is different from an external field by the field of the other electrons polarized by the external field (resonance screening) and hence, the electrons have an energy different from the single-particle transition energy due to the collective motion. Therefore, the collective (1–0) intersubband excitation has a frequency higher than Ω_{10}. There is still

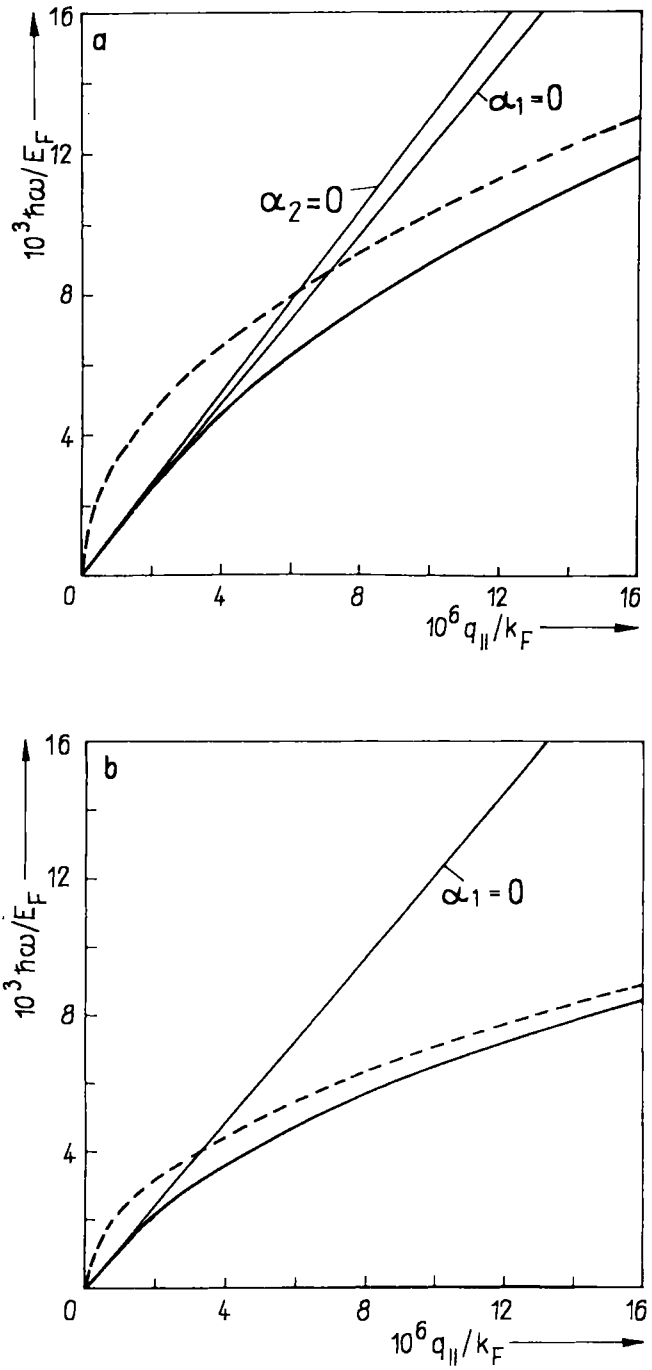

Fig. 16. Dispersion relation of the intrasubband plasmon (dashed line) and p-polarized intrasubband plasmon-polariton (solid line) of the GaAs-$Ga_{1-x}Al_xAs$ DHS a) with and b) without image effects; $n_{2DEG} = 10^{11}$ cm^{-2}, $a = 20$ nm, $b = 60$ nm

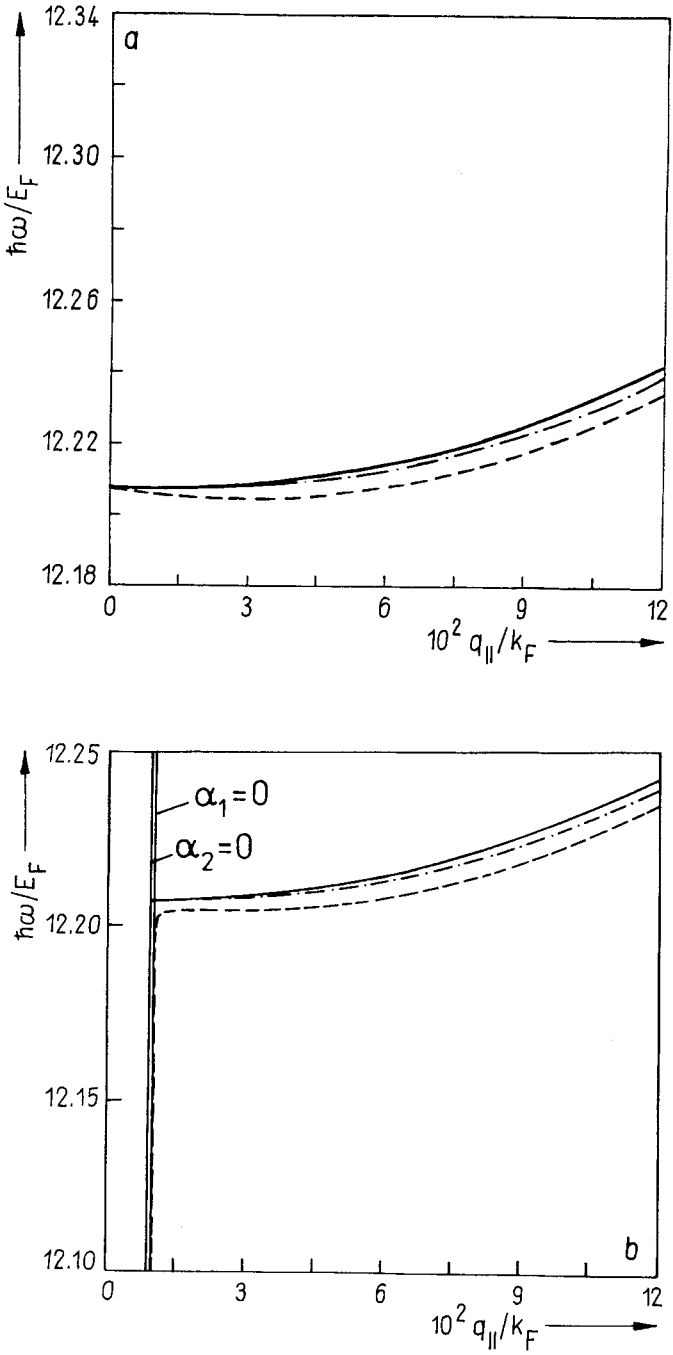

Fig. 17. Dispersion relation of a) the (1–0) intersubband plasmon and b) the p-polarized (1–0) intersubband plasmon-polariton of the GaAs-$Ga_{1-x}Al_xAs$ DHS with image effects for $b = 20$ nm (solid line) and $b = 60$ nm (dashed-dotted line) and without image effects (dashed line); $n_{2DEG} = 10^{11}$ cm^{-2}, $a = 20$ nm

a further frequency shift, caused by exchange and correlation effects [103] (final-state interaction, excitonic shift) and hence it is beyond the RPA. For usual carrier densities this shift is negligibly small, but can cause the dispersion curves to be below Ω_{10} for very low carrier densities [47].

In Fig. 17b the dispersion curves for the p-polarized (1–0) intersubband plasmon-polariton are depicted. It can be seen that the dispersion curve calculated without image contributions starts at the light line $\alpha_1 = 0$ of medium $\nu = 1$. In the near vicinity of this line the dispersion curve shows strong dispersion. In contrast to this behaviour, the dispersion curve calculated with image contributions starts at the light line $\alpha_2 = 0$ of medium $\nu = 2$. In this case the dispersion curve is quite dispersionless. To understand the physics of this behaviour it is necessary to investigate in more detail the long-wavelength approximation of the dispersion relation of the intersubband plasmon-polariton in the diagonal approximation. To obtain explicit dispersion relations it is necessary to expand D_{xx}^{KK} in a power series of α_1 and D_{KK} in a power series of $q_\parallel$. In the case without image contributions we expand D_{KK} to $q_\parallel^2$ and D_{xx}^{KK} to α_1^4. Further, we expand the polarization function χ_K to $q_\parallel^0$. According to (110) we have to include only the component χ_{zz}^K to $q_\parallel^0$ in the case of the current-response. If one includes the image contribution, the problem is more complex. This is because the p_i also contain α_1. Therefore, in this case we expand D_{xx}^{KK} in such a manner that the resulting dispersion relation reduces for $c \to \infty$ to that of the intersubband plasmon and for $\varepsilon_{b\nu} \to \varepsilon_{b1}$, $\alpha_\nu \to \alpha_1$ to that of the intersubband plasmon-polariton without image contributions. Under these conditions we obtain for $D_{KK}(\boldsymbol{q}_\parallel)$ the following results:

$$D_{KK}(\boldsymbol{q}_\parallel) = \bar{\alpha}_{KK} - \bar{\mu}_{KK} q_\parallel - \bar{\gamma}_{KK} q_\parallel^2 + O(q_\parallel^3) \tag{123}$$

which gives, including image effects,

$$\bar{\alpha}_{KK} = \frac{a}{2\varepsilon_{b1}} \frac{K^2 + (K+2)^2}{\pi^2 K^2 (K+2)^2}, \tag{124}$$

$$\bar{\mu}_{KK} = \frac{\varepsilon_{b2} a^2}{\varepsilon_{b1}^2 (1 + \varepsilon_{b2})} \frac{32(K+1)^2 (1 - (-1)^K)}{\pi^4 K^4 (K+2)^4}, \tag{125}$$

and

$$\bar{\gamma}_{KK} = \frac{a^3}{2\varepsilon_{b1}} \frac{K^4 + (K+2)^4 + 32(K+1)^2}{\pi^4 K^4 (K+2)^4} + \frac{32(K+1)^2}{\pi^4 K^4 (K+2)^4} ((-1)^K - 1) \times \left\{ \frac{a^3 \varepsilon_{b2} (\varepsilon_{b1}^2 + \varepsilon_{b2})}{\varepsilon_{b1}^3 (1 + \varepsilon_{b2})^2} - \frac{a^2 b \varepsilon_{b2} (\varepsilon_{b2} - 1)}{\varepsilon_{b1}^2 (\varepsilon_{b2} + 1)} \right\}. \tag{126}$$

If one neglects image effects it follows:

$$\bar{\alpha}_{KK} = -\frac{1}{2\varepsilon_{b1}} \int \mathrm{d}z \int \mathrm{d}z' \, \eta_{K0}(z) |z - z'| \, \eta_{K0}(z'), \tag{127}$$

$$\bar{\mu}_{KK} = \frac{1}{2\varepsilon_{b1}} z_{K0}^2; \qquad z_{K0} = \int \mathrm{d}z \, z \, \eta_{K0}(z), \tag{128}$$

$$\bar{\gamma}_{KK} = \frac{1}{12\varepsilon_{b1}} \int \mathrm{d}z \int \mathrm{d}z' \, \eta_{K0}(z) |z - z'|^3 \, \eta_{K0}(z') \tag{129}$$

with the results

$$\bar{\alpha}_{KK} = \frac{a}{2\varepsilon_{b1}} \frac{K^2 + (K+2)^2}{\pi^2 K^2 (K+2)^2}, \tag{130}$$

$$\bar{\mu}_{KK} = \frac{a^2}{\varepsilon_{b1}} \frac{16(K+1)^2 (1 - (-1)^K)}{\pi^4 K^4 (K+2)^4}, \tag{131}$$

and

$$\bar{\gamma}_{KK} = \frac{a^3}{2\varepsilon_{b1}} \frac{K^4 + (K+2)^4 + 32(K+1)^2 (-1)^K}{\pi^4 K^4 (K+2)^4}. \tag{132}$$

The corresponding result for $D_{xx}^{KK}(\boldsymbol{q}_{\|}, \omega)$ reads

$$D_{xx}^{KK}(\boldsymbol{q}_{\|}, \omega) = \bar{\lambda}_{KK}\alpha_1^2 - \bar{\nu}_{KK}\alpha_1^3 - \bar{\varkappa}_{KK}\alpha_1^4 + O(\alpha_1^5), \tag{133}$$

where including image contributions the coefficients of the above written expansion are given by

$$\bar{\lambda}_{KK} = -\frac{c^2 a}{2\varepsilon_{b1}\omega} \frac{K^2 + (K+2)^2}{\pi^2 K^2 (K+2)^2}, \tag{134}$$

$$\bar{\nu}_{KK} = 0, \tag{135}$$

and

$$\begin{aligned} \bar{\varkappa}_{KK} = -\frac{c^2}{2\varepsilon_{b1}\omega^2} \Bigg\{ & \frac{32a^2\varepsilon_{b2}}{\varepsilon_{b1}(\alpha_0\varepsilon_{b2} + \alpha_2)} \frac{(1 - (-1)^K)(K+1)^2}{\pi^4 K^4 (K+2)^4} \\ & + a^3 \frac{K^4 + (K+1)^4 + 32(K+1)^2}{\pi^4 K^4 (K+2)^4} + \frac{64((-1)^K - 1)(K+1)^2}{\pi^4 K^4 (K+2)^4} \\ & \times \left(\frac{a^3 \varepsilon_{b2}(\varepsilon_{b1}^2 \alpha_0 \alpha_2 + \varepsilon_{b2}\alpha_1^2)}{\varepsilon_{b1}^2 (\varepsilon_{b2}\alpha_0 + \alpha_2)^2} - \frac{a^2 b \varepsilon_{b2}(\varepsilon_{b1}\alpha_0 - \alpha_2)}{\varepsilon_{b1}(\varepsilon_{b2}\alpha_0 + \alpha_2)} \right) \Bigg\}. \end{aligned} \tag{136}$$

These coefficients are given for the case neglecting image effects by the following expressions:

$$\bar{\lambda}_{KK} = \frac{c^2}{2\varepsilon_{b1}\omega^2} \int \mathrm{d}z \int \mathrm{d}z' \, \eta_{K0}(z) |z - z'| \, \eta_{K0}(z'), \tag{137}$$

$$\bar{\nu}_{KK} = -\frac{c^2}{2\varepsilon_{b1}\omega^2} z_{K0}^2, \tag{138}$$

$$\bar{\varkappa}_{KK} = -\frac{c^2}{12\varepsilon_{b1}\omega^2} \int \mathrm{d}z \int \mathrm{d}z' \, \eta_{K0}(z) |z - z'|^3 \, \eta_{K0}(z') \tag{139}$$

with the results

$$\bar{\lambda}_{KK} = -\frac{ac^2}{2\varepsilon_{b1}\omega^2} \frac{K^2 + (K+2)^2}{\pi^2 K^2 (K+2)^2}, \tag{140}$$

$$\bar{\nu}_{KK} = -\frac{a^2 c^2}{\varepsilon_{b1}\omega^2} \frac{16(K+1)^2 (1 - (-1)^K)}{\pi^4 K^4 (K+2)^2}, \tag{141}$$

$$\varkappa_{KK} = -\frac{a^3c^2}{2\varepsilon_{b1}\omega^2}\frac{K^4 + (K+2)^4 + 32(K+1)^2(-1)^K}{\pi^4K^4(K+2)^4}. \tag{142}$$

Using the above given expansions for $D_{KK}(q_\parallel)$ and the LWA result for $\chi_K(q_\parallel, \omega)$, the long-wavelength approximation of the $(K-0)$ intersubband plasmon without image contribution is derived from (62) in the form

$$\omega_p^{K0} = \left\{\Omega_{K0}^2 + \omega_0^2\left(\frac{K^2 + (K+2)^2}{2K(K+2)} + \frac{16(K+1)^2((-1)^K - 1)}{\pi^2K^3(K+2)^3}(q_\parallel a) - \frac{K^4 + (K+2)^4 + 32(K+1)^2(-1)^K}{2\pi^2K^3(K+2)^3}(q_\parallel a)^2\right)\right\}^{1/2}, \tag{143}$$

where $\omega_0^2 = n_{2DEG}e^2/(\varepsilon_0\varepsilon_{b1}ma)$ is the plasma frequency. With image contribution the result is

$$\omega_p^{K0} = \left\{\Omega_{K0}^2 + \omega_0^2\left(\frac{K^2 + (K+2)^2}{2K(K+2)} + \frac{32(K+1)^2((-1)^K - 1)}{\pi^2K^3(K+2)^3} \times \frac{\varepsilon_{b2}}{\varepsilon_{b1}(1+\varepsilon_{b2})}(q_\parallel a) - \frac{K^4 + (K+2)^4 + 32(K+1)^2}{2\pi^2K^3(K+2)^3}(q_\parallel a)^2 - \frac{32(K+1)^2((-1)^K - 1)}{\pi^2K^3(K+2)^3}\left(\frac{\varepsilon_{b2}(\varepsilon_{b1}^2 + \varepsilon_{b2})}{\varepsilon_{b1}^2(1+\varepsilon_{b2})^2}(q_\parallel a)^2 - \frac{\varepsilon_{b2}(\varepsilon_{b2} - 1)}{\varepsilon_{b1}(1+\varepsilon_{b2})}(q_\parallel^2 ab)\right)\right)\right\}^{1/2}. \tag{144}$$

In the terms $\propto q_\parallel^0$ the deviation from Ω_{K0}^2 represents the depolarization shift. If one compares (143) with (144) one can see that the image forces vanish for $q_\parallel = 0$ in the case of intersubband plasmons. This is valid for all K. In the case of the current-response we obtain from (96) for the $(K-0)$ intersubband plasmon-polariton without image contribution the following long-wavelength approximation to the dispersion relation:

$$\omega = \left\{\Omega_{K0}^2 + \omega_0^2\left(\frac{K^2 + (K+2)^2}{2K(K+2)} + \frac{16(K+1)^2((-1)^K - 1)}{\pi^2K^2(K+2)^3}\frac{q_\parallel}{\alpha_1}(q_\parallel a) - \frac{K^4 + (K+2)^4 + 32(K+1)^2(-1)^K}{2\pi^2K^3(K+2)^3}(q_\parallel a)^2\right)\right\}^{1/2} \tag{145}$$

and with image contribution we obtain

$$\omega = \left\{\Omega_{K0}^2 + \omega_0^2\left(\frac{K^2 + (K+2)^2}{2K(K+2)} + \frac{32(K+1)^2((-1)^K - 1)}{\pi^2K^3(K+2)^3} \times \frac{\varepsilon_{b2}q_\parallel}{\varepsilon_{b1}(\alpha_2 + \varepsilon_{b2}\alpha_0)}(q_\parallel a) - \frac{K^4 + (K+2)^4 + 32(K+1)^2}{2\pi^2K^3(K+2)^3}(q_\parallel a)^2 - \frac{32(K+1)^2((-1)^K - 1)}{\pi^2K^3(K+2)^3}\left(\frac{\varepsilon_{b2}(\varepsilon_{b1}^2\alpha_0\alpha_2 + \varepsilon_{b2}\alpha_1^2)}{\varepsilon_{b1}^2(\alpha_2 + \varepsilon_{b2}\alpha_0)^2}(q_\parallel a)^2 - \frac{\varepsilon_{b2}(\varepsilon_{b2}\alpha_0 - \alpha_2)}{\varepsilon_{b1}(\alpha_2 + \varepsilon_{b2}\alpha_0)}(q_\parallel^2 ab)\right)\right)\right\}^{1/2}. \tag{146}$$

We notice that the terms $\propto q_{\parallel}^0$ are neither influenced by the image forces nor by the retardation. But (145) and (146) are valid only in the regions $q_{\parallel}^2 > \varepsilon_{b1}\omega^2/c^2$ and $q_{\parallel}^2 > \varepsilon_{b2}\,\omega^2/c^2$, respectively, and are implicit equations of the frequency. Now it is possible to understand the behaviour of the dispersion curves near $\alpha_1 = 0$ and $\alpha_2 = 0$. Let us start to explain the strong dispersion of the intersubband plasmon-polaritons in the vicinity of $\alpha_1 = 0$ if we neglect the image contributions. Equation (145) for $K = 1$ reads in the vicinity of $\alpha_1 = 0$

$$\omega = \left\{\Omega_{10}^2 + \frac{5}{3}\,\omega_0^2\left(1 - \frac{128}{45\pi^2}\,\frac{q_{\parallel}}{\alpha_1}\,(q_{\parallel}a) + \frac{23}{45\pi^2}\,(q_{\parallel}a)^2\right)\right\}^{1/2}. \tag{147}$$

From this equation one can see that the term proportional to $q_{\parallel}a$ causes a strong dispersion of the dispersion curve near $\alpha_1 = 0$. Note that (147) is implicit because it contains α_1 on the right-hand side. In the expansion of D_{xx}^{KK} in a power series of α_1, (133), the term proportional to α_1^3 depends on z_{K0} (128). The quantity enters the term proportional to $q_{\parallel}a$ of (127). Hence, only if z_{K0} is different from zero, the dispersion curve of the $(K-0)$ intersubband plasmon-polariton calculated without image contributions shows a strong dispersion in the vicinity of $\alpha_1 = 0$. In the case of our model of the Q2DEG $z_{K0} \neq 0$ for odd K and $z_{K0} = 0$ for even K is valid. Dahl and Sham [34] took into account only the first term of the expansion of D_{xx}^{KK}. In this order no differences between the intersubband plasmons and the intersubband plasmon-polaritons occur. Eguiluz and Maradudin [35] investigated the (1–0) intersubband plasmon-polariton numerically in the long-wavelength approximation. For their wave functions $z_{10} = 0$ is valid. Therefore, they found quite dispersionless dispersion curves of the (1–0) intersubband plasmon-polariton.

In Fig. 18 the (1–0) intersubband modes of density- and current-response are compared for two different sheet carrier concentrations neglecting image contributions. It can also be seen that for large values of the wave vector the dispersion curve of the intersubband plasmon-polariton approaches that of the intersubband plasmon. In the vicinity of $\alpha_1 = 0$ the retardation significantly influences the depolarization shift of the (1–0) intersubband plasmon.

Now we look at the case of the (1–0) intersubband plasmon-polariton in the vicinity of $\alpha_2 = 0$ including the image contributions. In this region for $K = 1$ (146) reads

$$\begin{aligned}\omega = \Bigg\{\Omega_{10}^2 + \omega_0^2\Bigg(&\frac{5}{3} - \frac{256}{27\pi^2}\,\frac{\varepsilon_{b2}q_{\parallel}}{\varepsilon_{b1}(\alpha_2 + \varepsilon_{b2}\alpha_0)}\,(q_{\parallel}a) \\ &- \frac{105}{27\pi^2}\,(q_{\parallel}a)^2 + \frac{256}{27\pi^2}\Bigg[\frac{\varepsilon_{b2}(\varepsilon_{b1}^2\alpha_0\alpha_2 + \varepsilon_{b2}\alpha_1^2)}{\varepsilon_{b1}^2(\alpha_2 + \varepsilon_{b2}\alpha_0)^2}\,(q_{\parallel}a)^2 \\ &- \frac{\varepsilon_{b2}(\varepsilon_{b2}\alpha_0 - \alpha_2)}{\varepsilon_{b1}(\varepsilon_{b2}\alpha_0 + \alpha_2)}\,(q_{\parallel}^2ab)\Bigg]\Bigg)\Bigg\}^{1/2}.\end{aligned} \tag{148}$$

In (148) there is no term proportional to $q_{\parallel}/\alpha_1$. Such a term would arise in (148) if one neglects the different dielectric properties of the media. Image contributions make the resonance in (147) vanishing for all subbands. Considerations of the exact matrix element $D_{xx}^{KK}(\boldsymbol{q}_{\parallel}, \omega)$ (see (112)) show its real character in region II of Fig. 11 in contrast to the case of neglecting image polarizations, when D_{xx}^{KK} becomes complex if $\alpha_1^2 < 0$ is valid. Hence, the dispersion curve reaches the light line $\alpha_2 = 0$ nearly dispersionless. In comparison with the dispersion relation of the (1–0) intersubband plasmon

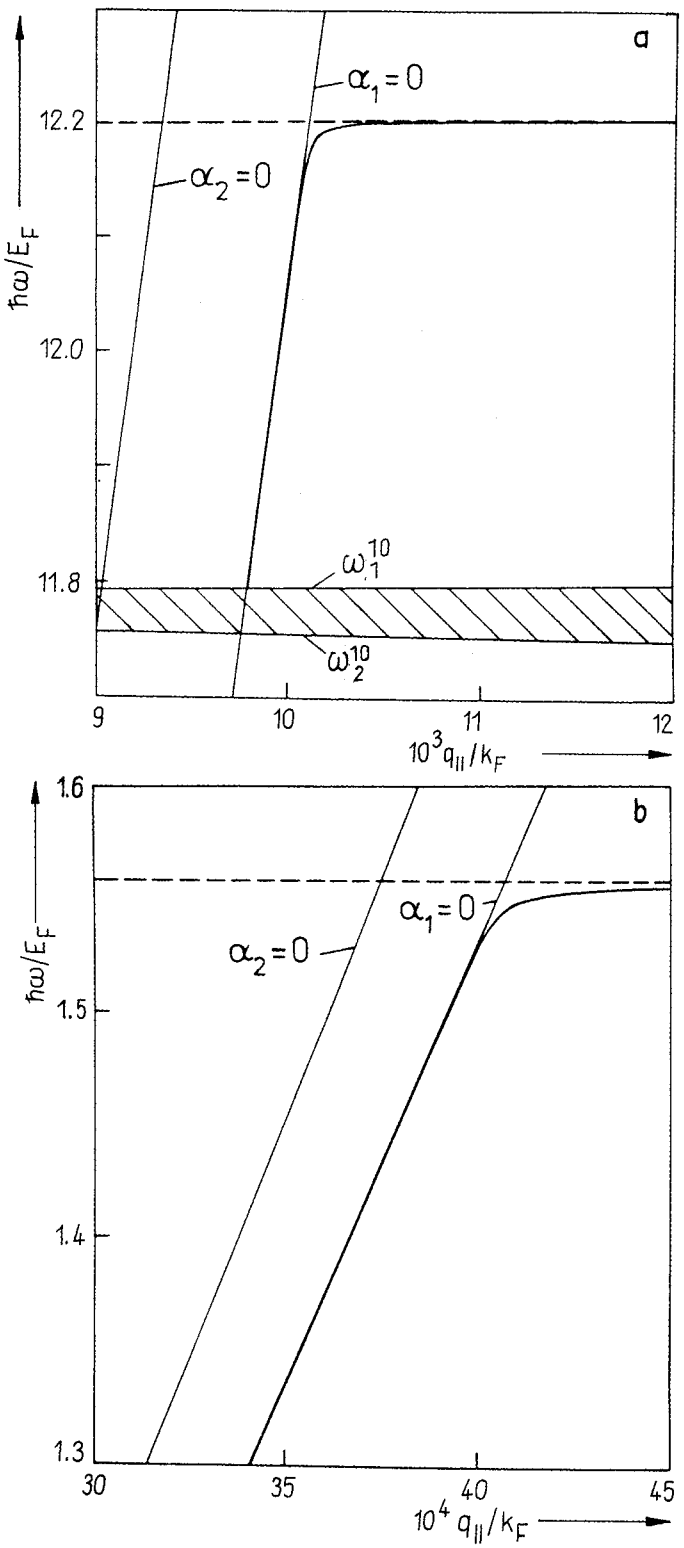

Fig. 18. Dispersion relation of the (1–0) intersubband plasmon (dashed line) and p-polarized (1–0) intersubband plasmon-polariton (solid line) of the GaAs-$Ga_{1-x}Al_xAs$ DHS for a) $n_{2DEG} = 10^{11}\,cm^{-2}$ and b) $n_{2DEG} = 10^{12}\,cm^{-2}$ without image effects; $a = 20$ nm

(from (144)),

$$\omega_p^{10} = \left\{\Omega_{10}^2 + \omega_0^2\left(\frac{5}{3} - \frac{256}{27\pi^2}\frac{\varepsilon_{b2}}{\varepsilon_{b1}(1+\varepsilon_{b2})}(q_\parallel a) - \frac{105}{27\pi^2}(q_\parallel a) + \frac{256}{27\pi^2}\left[\frac{\varepsilon_{b2}(\varepsilon_{b1}^2+\varepsilon_{b2})}{\varepsilon_{b1}^2(1+\varepsilon_{b2})^2}(q_\parallel a)^2 - \frac{\varepsilon_{b2}(\varepsilon_{b2}-1)}{\varepsilon_{b1}(1+\varepsilon_{b2})}(q_\parallel^2 ab)\right]\right)\right\}^{1/2}, \tag{149}$$

there are also differences between plasmons and plasmon-polaritons if the image contribution is taken into account. But these differences are much smaller than in the case without image influence.

Another interesting result holds if not only χ_{zz}^K but also χ_{xx}^K is used in the dispersion relation. Both components are non-zero in the long-wavelength limit. But we note that the inclusion of χ_{xx} and χ_{zz} in the lowest order of $q_\parallel$ in the dispersion relation does not mean that the polarization tensor is included in the lowest order of $q_\parallel$. This is true because of the relation (110) between the polarization function χ_K and the components of the polarization tensor $\chi_{\alpha\beta}^K$. From this relation it follows that an expansion of χ_{zz} to $q_\parallel^3$ corresponds to an expansion of χ_{xx} to $q_\parallel^0$. Consequently, the inclusion of both χ_{xx}^K and χ_{zz}^K in the lowest order of $q_\parallel$ as done in [35] has no physical sense in the small wave vector region. But to compare the results obtained here with those of [33] we give the analytical result for this case. Instead of (147) in the same order of α_1, in the case of neglecting image contributions we obtain

$$(\Omega_{10}^2 - \omega^2)\left\{\Omega_{10}^2 - \omega^2 + \frac{5}{3}\omega_0^2\left(1 - \frac{128}{45\pi^2}\frac{q_\parallel}{\alpha_1}(q_\parallel a) + \frac{23}{45\pi^2}(q_\parallel a)^2\right)\right\} = \frac{25}{36}\varepsilon_{b1}\left(\omega_0^2\frac{v_F}{c}\right)^2 \tag{150}$$

for the (1–0) intersubband plasmon-polariton. In this approximation two branches of the polariton occur. In the shorter-wavelength case, if both branches are well separated, the upper solution, ω_+ is approximately given by (147). The lower one, ω_- lies slightly below Ω_{10},

$$\omega_+ \approx \left\{\Omega_{10}^2 + \frac{5}{3}\omega_0^2\left(1 - \frac{128}{45\pi^2}\frac{q_\parallel}{\alpha_1}(q_\parallel a) + \frac{23}{45\pi^2}(q_\parallel a)^2\right)\right\}^{1/2}, \qquad \omega_- \approx \Omega_{10}. \tag{151}$$

The term on the right-hand side of (150) is proportional to $(v_F/c)^2$ and, therefore, it is very small. In regions where ω_+ and ω_- are well separated from each other this term only leads to small deviations of the dispersion curves given by (151) to higher (ω_+) or lower (ω_-) frequencies. In the case of vanishing z_{K0}, or if the image contributions are taken into account, the two branches are separated everywhere. This results in two quite dispersionless dispersion curves near the intersubband frequency and near the frequency of the intersubband plasmon. Eguiluz and Maradudin [35] found such a behaviour in their numerical investigations of the (1–0) plasmon-polariton by using both χ_{xx}^K and χ_{zz}^K. In the case of neglecting the image contribution for $z_{K0} \neq 0$ there is a region where ω_+ and ω_- would cross over. Then, the small term proportional to $(v_F/c)^2$ in (150) leads to the resonance splitting between the two crossing branches. Unfortunately, the long-wavelength expression of the response function

loses its meaning in the vicinity of Ω_{K0}. Without this approximation the response functions χ^K_{xx} and χ^K_{zz} become complex in the single-particle continuum of the K-th subband and the modes become strongly damped by Landau damping. In our opinion, the lower branch of the p-polarized intersubband plasmon-polariton has no physical sense, because of the invalidation of the approximation used to find it inside the single-particle continuum.

We remark that if we would use for the background dielectric constants the dipole-active lattice dielectric functions, $\varepsilon_{by}(\omega)$, (144) and (146) will have further resonances at $\varepsilon_{b1} = 0$, $1 + \varepsilon_{b2} = 0$, and at $\alpha_2 + \varepsilon_{b2}\alpha_0 = 0$ which describe bulk phonons, surface phonons, and surface phonon-polaritons or guided wave phonon-polaritons 104. This is the simplest way to incorporate the coupling of the plasmons and plasmon-polaritons to the optical phonons of the system. If we neglect the image effects we only obtain the coupling to 3D bulk phonons ($\varepsilon_{b1} = 0$) and to phonon-polaritons ($\alpha_1 = 0$) which are the corresponding resonances of (143) and (145). We notice that the well-known confinement effects of the longitudinal-optical phonons [44, 50] are not described in such a simplified calculation.

The different behaviour of intrasubband and intersubband plasmon-polaritons with and without image contributions in the long-wavelength limit may be explained in the following way. For small wave vectors the intrasubband modes exhibit only a current flowing in the direction of the wave propagation. This current may be interpreted as an oscillating dipole momentum. As is well-known, such oscillating dipoles may emit and absorb electromagnetic waves. Therefore, the intrasubband modes are strongly influenced by retardation. The dipole momentum of the image polarization is directed perpendicular to the dipole momentum of the current. Compensation of the two kinds of dipoles cannot occur and, consequently, intrasubband plasmon-polaritons are strongly retarded with or without image contributions. Intersubband modes in the long-wavelength limit only form a current in z-direction perpendicular to the plane of Q2DEG. Only subbands with odd parity form a dipole momentum interacting with optical waves (see Appendix D). Such modes with odd subband index are influenced by retardation in the case without image contributions. For intersubband modes the dipole momentum formed by the image charges is directed antiparallel to the dipole momentum of the current. Therefore, in this case the image dipoles compensate the dipoles produced by the current density. All intersubband modes are only very weakly influenced by retardation if image polarizations are considered. The difference between the intersubband plasmons and the plasmon-polaritons in higher orders of $(q_{\|}a)$ is produced by higher-order multipoles of the combination of current density and image polarization. Such a behaviour agrees with the results obtained by King-Smith and Inkson [93]. The authors investigated the plasmon-polaritons of a superlattice neglecting image effects. In such a configuration Q2DEG's in different slabs may screen each other. In a superlattice the current densities of the other slabs play the role of compensating image charges. This process strongly depends on the phase shift between different Q2DEG's. Consequently, in [92] p-polarized intersubband plasmon-polaritons are described with some influence of retardation, depending on the wave vector component in the direction of the superlattice axis which determines the phase shift between different Q2DEG's.

6. Conclusions

In this paper we have presented a detailed survey of the effects of retardation and image forces on the intra- and intersubband plasmons in semiconductor quantum wells. The

modes are calculated using the full RPA response functions of the density- and current-reponse. It is shown analytically that the dispersion curves of all collective excitations of the density-response are only correct for large wave vectors, i.e. in the unretarded limit. The dispersion curves are calculated under the assumption of the electric quantum limit and in the diagonal approximation. Whereas the EQL is fulfilled for most quantum wells containing a Q2DEG, the use of the diagonal approximation needs a comment. In the diagonal approximation the intra- and intersubband excitations are uncoupled. This is only a good approximation if the quantum well is symmetric and thin enough and the response-functions of all the other excitations have no resonances in the near vicinity of the frequency of the considered mode [46, 48]. This is well fulfilled for the chosen thickness of the quantum well and the sheet carrier concentrations. But the intersubband mixing of the modes strongly influences their Landau damping. This is true because the (0–0) intrasubband modes become also damped in the single-particle intersubband continua. For a spatially symmetric quantum well, however, the symmetric modes are not coupled with the antisymmetric modes.

It is shown that the retardation and the image contributions influence the intra- and intersubband modes in a different manner. The intrasubband modes with retardation start always at the corresponding light line with a dispersive dispersion curve. On the other hand, the dispersion curves of the intersubband modes can start at the corresponding light line with or without dispersion. It is shown that if one includes the image contribution, the (1–0) intersubband plasmon-polaritons have a dispersion curve which is nearly dispersionless in the near vicinity of the light line. But, if one neglects the image contributions, the behaviour of the dispersion curves depends on the quantity z_{K0} defined in (148). If this quantity is zero, then the dispersion curve is nearly dispersionless, while for non-zero z_{K0} it shows dispersion. Hence, image and retardation effects influence each other with the result that within the region where retardation effects are important, image effects must be included in the calculation. It makes no sense to consider retardation effects neglecting the image forces.

This circumstance very well agrees with the optical properties of the Q2DEG. In Appendix D we calculated a macroscopic dielectric tensor in the long-wavelength limit. Parallel to the layers the response is that of a doped semiconductor and perpendicular we have the well-known intersubband resonances [34]. From (D9) it can be seen that in the case considered here only transitions $0 \to 2, 4, 6, \ldots$ are possible. This corresponds to $z_{K0} \neq 0$. If one uses the macroscopic dielectric function of the Q2DEG for the calculation of the dispersion curves by standard electrodynamics, the results obtained for the interface modes correspond approximately with the results obtained here. But, we notice that in order to obtain the dispersion behaviour quantitatively correct in the long-wavelength limit, it is necessary to use a microscopic formulation of the type developed in this paper.

The RPA used here should be good enough to describe correctly the effects of retardation and the image forces. But it is necessary to remark that for low densities of the Q2DEG exchange and correlation effects become important. As shown in [47], especially the intersubband mode is influenced appreciably by exchange and correlation effects even in the small wave vector region. For the densities of the Q2DEG used in this paper these effects should not be important.

Finally, we remark that the used configuration and the type of formulation presented in this paper provide the possibility of directly comparing the theoretical results to experiments. The excitation of (0–0) intrasubband plasmons in a GaAs-$Ga_{1-x}Al_xAs$ single heterostructure has been investigated with FIR spectroscopy [70]. In these experiments the sample consists

of a GaAs buffer layer at the bottom, which contains the electron space-charge layer, followed by an undoped $Ga_{0.72}Al_{0.28}As$ spacer layer, by a doped $Ga_{0.72}Al_{0.28}As$ layer, and by a cap layer of GaAs. Grating couplers of highly conducting Ag on the top of the samples couple the normally transmitted FIR radiation with the (0–0) intrasubband plasmons of the electron space-charge layer. A grating of periodicity $d \ll \lambda_{FIR}$ spatially modulates the incident radiation and couples to the collective excitations with wave vectors $q_{\|} = 2\pi m/d$ ($m = 1, 2, 3, \ldots$). But, unfortunately the wave vectors in these experiments ranging from $q_{\|} = (0.72 \text{ to } 2.16) \times 10^5 \text{ cm}^{-1}$ are too large for the investigation of the retardation and image effects on the intrasubband plasmons considered in this paper. In the authors' opinion it would be necessary to perform more detailed experiments on the intersubband plasmons of quantum wells, because these modes are influenced by many physical effects (retardation, image forces, plasmon–phonon coupling, exchange-correlation) in a complicated manner.

Acknowledgement

This work has been supported in part by the Deutsche Forschungsgemeinschaft (DFG), project We 1532/3-1.

Appendix A

Electromagnetic Green's functions

In this appendix we evaluate the electrostatic Green's function of (3) and the electromagnetic Green's tensor of (25). We consider first the Green's function $D(\boldsymbol{x}, \boldsymbol{x}')$ of the Poisson equation (3). This function is defined by

$$\nabla(\varepsilon_b(z) \cdot \nabla D(\boldsymbol{x}, \boldsymbol{x}')) = -\delta(\boldsymbol{x} - \boldsymbol{x}'), \tag{A1}$$

where according to symmetry

$$D(\boldsymbol{x}, \boldsymbol{x}') = \frac{1}{A} \sum_{\boldsymbol{q}_{\|}} e^{i\boldsymbol{q}_{\|}(\boldsymbol{x}_{\|} - \boldsymbol{x}'_{\|})} D(\boldsymbol{q}_{\|}; z, z') \tag{A2}$$

is valid. Using (A2) in (A1) it follows:

$$\left(\frac{d}{dz} \varepsilon_b(z) \frac{d}{dz} - \varepsilon_b(z) q_{\|}^2\right) D(\boldsymbol{q}_{\|}; z, z') = -\delta(z - z'). \tag{A3}$$

To solve (A3) we need a special solution of the inhomogeneous, D^{dir}, and a general solution of the homogeneous equation, D^{im}. The sum of both must fulfil the boundary conditions. We require continuity of $D(\boldsymbol{q}_{\|}; z, z')$ and $\varepsilon_{bv} \partial D(\boldsymbol{q}_{\|}; z, z')/\partial z$ at the heterointerfaces and vanishing $D(\boldsymbol{q}_{\|}; z, z')$ at $z = \pm\infty$. The special solution of (A3) is

$$D^{dir}(\boldsymbol{q}_{\|}; z, z') = \frac{1}{2\varepsilon_{b1} q_{\|}} e^{-q_{\|}|z - z'|}. \tag{A4}$$

The Green's tensor $D_{\alpha\beta}(\boldsymbol{x}, \boldsymbol{x}' \mid \omega)$ of the inhomogeneous wave equation (25) is defined by

$$\sum_{\gamma} \frac{\partial^2}{\partial x_{\gamma}^2} D_{\alpha\beta}(\boldsymbol{x}, \boldsymbol{x}' \mid \omega) - \frac{\partial}{\partial x_{\alpha}} \sum_{\gamma} \frac{\partial}{\partial x_{\gamma}} D_{\gamma\beta}(\boldsymbol{x}, \boldsymbol{x}' \mid \omega) + \varepsilon_b(z) \frac{\omega^2}{c^2} D_{\alpha\beta}(\boldsymbol{x}, \boldsymbol{x}' \mid \omega)$$
$$= -\delta_{\alpha\beta} \delta(\boldsymbol{x} - \boldsymbol{x}'), \tag{A5}$$

where we have used Fourier transformation according to time. Using the Fourier transformation according to space with $\boldsymbol{q}_{\parallel} = (q_x, 0, 0)$ without loss of generality, we can write (A5) in the form

$$\left(\frac{\partial^2}{\partial z^2} + \varepsilon_{bv}\frac{\omega^2}{c^2}\right) D_{xx}(\boldsymbol{q}_{\parallel}; z, z' \mid \omega) - iq_{\parallel}\frac{\partial}{\partial z} D_{zx}(\boldsymbol{q}_{\parallel}; z, z' \mid \omega) = -\delta(z - z'),$$

$$\left(-\frac{\partial^2}{\partial z^2} - \varepsilon_{bv}\frac{\omega^2}{c^2}\right) D_{xz}(\boldsymbol{q}_{\parallel}; z, z' \mid \omega) + iq_{\parallel}\frac{\partial}{\partial z} D_{zz}(\boldsymbol{q}_{\parallel}; z, z' \mid \omega) = 0,$$

$$\left(q_{\parallel}^2 - \varepsilon_{bv}\frac{\omega^2}{c^2}\right) D_{zx}(\boldsymbol{q}_{\parallel}; z, z' \mid \omega) + iq_{\parallel}\frac{\partial}{\partial z} D_{xx}(\boldsymbol{q}_{\parallel}; z, z' \mid \omega) = 0,$$

$$\left(\frac{\partial^2}{\partial z^2} - q_{\parallel}^2 + \varepsilon_{bv}\frac{\omega^2}{c^2}\right) D_{yy}(\boldsymbol{q}_{\parallel}; z, z' \mid \omega) = -\delta(z - z'),$$

$$\left(-q_{\parallel}^2 + \varepsilon_{bv}\frac{\omega^2}{c^2}\right) D_{zz}(\boldsymbol{q}_{\parallel}; z, z' \mid \omega) - iq_{\parallel}\frac{\partial}{\partial z} D_{xz}(\boldsymbol{q}_{\parallel}; z, z' \mid \omega) = -\delta(z - z'). \quad \text{(A6)}$$

We solve this equation by the same method as (A3). The special solutions of (A6) under the condition $a > z, z' > 0$ are

$$D_{xx}^{dir}(\boldsymbol{q}_{\parallel}; z, z' \mid \omega) = -\frac{c^2}{\varepsilon_{b1}\omega^2}\frac{\alpha_1}{2} e^{-\alpha_1 |z - z'|}, \quad \text{(A7)}$$

$$D_{xz}^{dir}(\boldsymbol{q}_{\parallel}; z, z' \mid \omega) = D_{zx}^{dir}(\boldsymbol{q}_{\parallel}; z, z' \mid \omega) = -i\frac{c^2 q_{\parallel}}{2\varepsilon_{b1}\omega^2} \times (\theta(z - z') - \theta(z' - z)) e^{-\alpha_1 |z - z'|}, \quad \text{(A8)}$$

$$D_{yy}^{dir}(\boldsymbol{q}_{\parallel}; z, z' \mid \omega) = \frac{1}{2\alpha_1} e^{-\alpha_1 |z - z'|}, \quad \text{(A9)}$$

$$D_{zz}^{dir}(\boldsymbol{q}_{\parallel}; z, z' \mid \omega) = -\frac{c^2}{\varepsilon_{b1}\omega^2}\delta(z - z') + \frac{c^2 q_{\parallel}^2}{2\varepsilon_{b1}\omega^2} e^{-\alpha_1 |z - z'|}, \quad \text{(A10)}$$

$$D_{xy}^{dir} = D_{yx}^{dir} = D_{yz}^{dir} = D_{zy}^{dir} = 0. \quad \text{(A11)}$$

Hence, we make the following generalized ansatz for the general solution of (A3) and (A5) under the condition $a > z' > 0$:

$$K(\boldsymbol{q}_{\parallel}; z, z' \mid \omega) = \begin{cases} F_1(z') e^{-\gamma_0 z}; & z > a + b, \\ F_2(z') e^{\gamma_2 z} + F_3(z') e^{-\gamma_2 z}; & a + b > z > a, \\ F_4(z') e^{\gamma_1 z} + F_5(z') e^{-\gamma_1 z} + R_0 e^{-\gamma_1 |z - z'|}; & a > z > 0, \\ F_6(z') e^{\gamma_3 z}; & 0 > z, \end{cases} \quad \text{(A12)}$$

where $K(\boldsymbol{q}_{\parallel}; z, z' \mid \omega) = D(\boldsymbol{q}_{\parallel}; z, z' \mid \omega)$ in the case of electrostatics and $K(\boldsymbol{q}_{\parallel}; z, z' \mid \omega) = D_{xx}(\boldsymbol{q}_{\parallel}; z, z' \mid \omega)$ or $D_{yy}(\boldsymbol{q}_{\parallel}; z, z' \mid \omega)$ in the case of electrodynamics. The matrix ele-

ments D_{xz}, D_{zx}, and D_{zz} are related to D_{xx}. The corresponding relations follow from (A6) to be

$$D_{xz}(\boldsymbol{q}_\parallel; z, z' \mid \omega) = \frac{iq_\parallel}{\alpha_1^2} \frac{\partial}{\partial z'} D_{xx}(\boldsymbol{q}_\parallel; z, z' \mid \omega),$$

$$D_{zx}(\boldsymbol{q}_\parallel; z, z' \mid \omega) = -\frac{iq_\parallel}{\alpha_1^2} \frac{\partial}{\partial z} D_{xx}(\boldsymbol{q}_\parallel; z, z' \mid \omega),$$

and

$$D_{zz}(\boldsymbol{q}_\parallel; z, z' \mid \omega) = \frac{\delta(z - z')}{\alpha_1^2} - \frac{iq_\parallel}{\alpha_1^2} \frac{\partial}{\partial z} D_{xz}(\boldsymbol{q}_\parallel; z, z' \mid \omega). \tag{A13}$$

Further, in (A12) we have $\gamma_v = q_\parallel$ in the case of electrostatics and $\gamma_v = \alpha_v$ in the case of electrodynamics with

$$\alpha_v = \begin{cases} (\boldsymbol{q}_\parallel^2 - \varepsilon_{bv}\omega^2/c^2)^{1/2}; & \boldsymbol{q}_\parallel^2 > \varepsilon_{bv}\omega^2/c^2, \\ i(\varepsilon_{bv}\omega^2/c^2 - q_\parallel^2)^{1/2}; & \boldsymbol{q}_\parallel^2 < \varepsilon_{bv}\omega^2/c^2. \end{cases} \tag{A14}$$

With the ansatz (A12) we must fulfil the boundary conditions. In the case of the full electrodynamics, we require the continuity of the tangential component of $\boldsymbol{E}$, of the normal component of $\boldsymbol{D}$ and of the tangential component of $\boldsymbol{B}$.

At first we consider the p-polarization. From the continuity of the tangential component of $\boldsymbol{E}$ follows the continuity of A_x and from this the continuity of D_{xx}. From both, the continuity of the normal component of $\boldsymbol{D}$ and the tangential component of $\boldsymbol{B}$ follows the continuity of the quantity

$$\frac{\varepsilon_{bv}\omega^2/c^2}{\alpha_v^2} \frac{\mathrm{d}}{\mathrm{d}z} A_x(\boldsymbol{q}_\parallel, z \mid \omega) + \frac{iq_\parallel}{\alpha_v^2} \mu_0 j_z(\boldsymbol{q}_\parallel, z \mid \omega). \tag{A15}$$

Because $j_z(\boldsymbol{q}_\parallel, z \mid \omega)$ vanishes at the heterointerfaces for quantum wells with barriers being infinitely high, (A15) which must be continuous across the heterointerfaces can written in the form

$$\frac{\varepsilon_{bv}\omega^2/c^2}{\alpha_v^2} \frac{\partial}{\partial z} D_{xx}(\boldsymbol{q}_\parallel; z, z' \mid \omega). \tag{A16}$$

For the s-polarization the continuity of both the tangential component of $\boldsymbol{E}$ and the normal component of $\boldsymbol{B}$ result in the continuity of A_y. From the continuity of A_y follows that of D_{yy} across the heterointerfaces. Further, the continuity of the tangential component of $\boldsymbol{B}$ results in the continuity of $\mathrm{d}A_y/\mathrm{d}z$ and from this follows the continuity of $\partial D_{yy}/\partial z$. We require that $D_{\alpha\beta}(\boldsymbol{q}_\parallel; z, z' \mid \omega)$ vanishes at $z = \pm\infty$. The unknown quantities $F_j(z')$ ($j = 1$ to 6) in (A12) are calculated using the appropriate boundary conditions described above. This leads to an algebraic system of six inhomogeneous linear equations,

$$\sum_{j=1}^{6} I_{ij} F_j(z') = R_i(z') \tag{A17}$$

with

$$\mathscr{J} = \begin{pmatrix} e^{-\gamma_0(a+b)} & -e^{\gamma_2(a+b)} & -e^{-\gamma_2(a+b)} & 0 & 0 & 0 \\ p_1 e^{-\gamma_0(a+b)} & e^{\gamma_2(a+b)} & -e^{-\gamma_2(a+b)} & 0 & 0 & 0 \\ 0 & e^{\gamma_2 a} & e^{-\gamma_2 a} & -e^{\gamma_1 a} & -e^{-\gamma_1 a} & 0 \\ 0 & -p_2 e^{\gamma_2 a} & p_2 e^{-\gamma_2 a} & e^{\gamma_1 a} & -e^{-\gamma_1 a} & 0 \\ 0 & 0 & 0 & 1 & 1 & -1 \\ 0 & 0 & 0 & -1 & 1 & p_3 \end{pmatrix} \tag{A18}$$

and

$$\boldsymbol{F}(z') = \begin{pmatrix} F_1(z') \\ F_2(z') \\ F_3(z') \\ F_4(z') \\ F_5(z') \\ F_6(z') \end{pmatrix}, \qquad \boldsymbol{R}(z') = R_0 \begin{pmatrix} 0 \\ 0 \\ e^{-\gamma_1(a-z')} \\ e^{-\gamma_1(a-z')} \\ -e^{-\gamma_1 z'} \\ e^{-\gamma_1 z'} \end{pmatrix}. \tag{A19}$$

This system of equations is solved by standard techniques, e.g. by the Kramers rule. The coefficient $F_i(z')$ is given by

$$F_i(z') = \frac{\det [I_{ij}^{(i)}]}{\det [I_{ij}]} \tag{A20}$$

with $I_{ij}^{(i)}$ the matrix in which the i-th column is replaced by $R_i(z')$. In the considered range $\det [I_{ij}] \neq 0$ is valid. The different determinants are easily calculated and given by

$$\begin{aligned} \det [I_{ij}] = {} & 4e^{-\gamma_0(a+b)} \{(1 + p_1 p_2 p_3) \sinh(\gamma_1 a) \cosh(\gamma_2 b) \\ & + (p_1 + p_2 p_3) \sinh(\gamma_1 a) \sinh(\gamma_2 b) + (p_2 + p_1 p_3) \cosh(\gamma_1 a) \sinh(\gamma_2 b) \\ & + (p_3 + p_1 p_2) \cosh(\gamma_1 a) \cosh(\gamma_2 b)\}, \end{aligned} \tag{A21}$$

$$\det [I_{ij}^{(1)}] = 4R_0\{(1 + p_3) e^{\gamma_1 z'} + (1 - p_3) e^{-\gamma_1 z'}\}, \tag{A22}$$

$$\begin{aligned} \det [I_{ij}^{(2)}] = {} & 2R_0 e^{-(\gamma_0+\gamma_2)(a+b)} \{(1 - p_1)(1 + p_3) e^{\gamma_1 z'} e^{(\gamma_2-\gamma_1) b} \\ & + (1 - p_1)(1 - p_3) e^{-\gamma_1 z'} e^{-(\gamma_2-\gamma_1) b}\}, \end{aligned} \tag{A23}$$

$$\begin{aligned} \det [I_{ij}^{(3)}] = {} & 2R_0 e^{-(\gamma_0-\gamma_2)(a+b)} \{(1 + p_1)(1 + p_3) e^{\gamma_1 z'} e^{(\gamma_2-\gamma_1) b} \\ & + (1 + p_1)(1 - p_3) e^{-\gamma_1 z'} e^{-(\gamma_2-\gamma_1) b}\}, \end{aligned} \tag{A24}$$

$$\begin{aligned} \det [I_{ij}^{(4)}] = {} & R_0 e^{-\gamma_0(a+b)} e^{-\gamma_1 a} \{(1 + p_1)(1 - p_2)(1 + p_3) e^{\gamma_1 z'} e^{\gamma_2 b} \\ & + (1 - p_1)(1 + p_2)(1 + p_3) e^{\gamma_1 z'} e^{-\gamma_2 b} \\ & + (1 + p_1)(1 - p_2)(1 - p_3) e^{-\gamma_1 z'} e^{\gamma_2 b} \\ & + (1 - p_1)(1 + p_2)(1 - p_3) e^{-\gamma_1 z'} e^{-\gamma_2 b}\}, \end{aligned} \tag{A25}$$

$$\begin{aligned} \det [I_{ij}^{(5)}] = {} & R_0 e^{-\gamma_0(a+b)} \{(1 + p_1)(1 - p_2)(1 - p_3) e^{\gamma_1 z'} e^{-\gamma_1 a} e^{\gamma_2 b} \\ & + (1 - p_1)(1 + p_2)(1 - p_3) e^{\gamma_1 z'} e^{-\gamma_1 a} e^{-\gamma_2 b} \\ & + (1 - p_1)(1 - p_2)(1 - p_3) e^{-\gamma_1 z'} e^{\gamma_1 a} e^{-\gamma_2 b} \\ & + (1 + p_1)(1 + p_2)(1 - p_3) e^{-\gamma_1 z'} e^{\gamma_1 a} e^{\gamma_2 b}\}, \end{aligned} \tag{A26}$$

$$\det[I_{ij}^{(6)}] = R_0\{(1+p_1)(1-p_2)\,e^{\gamma_1 z'}\,e^{\gamma_1 b}\,e^{\gamma_2 b} + (1-p_1)(1+p_2)\,e^{\gamma_1 z'}\,e^{\gamma_1 b}\,e^{-\gamma_2 b} + (1+p_1)(1+p_2)\,e^{-\gamma_1 z'}\,e^{-\gamma_1 b}\,e^{\gamma_2 b} + (1-p_1)(1-p_2)\,e^{-\gamma_1 z'}\,e^{-\gamma_1 b}\,e^{-\gamma_2 b}\}\,. \tag{A27}$$

The coefficients in (A18) and (A21) to (A27) are given in Table 1 for $D(\boldsymbol{q}_\parallel; z, z')$, $D_{xx}(\boldsymbol{q}_\parallel; z, z' \mid \omega)$, and $D_{yy}(\boldsymbol{q}_\parallel; z, z' \mid \omega)$.

Table 1

	$D(\boldsymbol{q}_\parallel; z, z')$	$D_{xx}(\boldsymbol{q}_\parallel; z, z' \mid \omega)$	$D_{yy}(\boldsymbol{q}_\parallel; z, z' \mid \omega)$
γ_ν	$q_\parallel$	α_ν	α_ν
p_1	$\dfrac{\varepsilon_{b0}}{\varepsilon_{b2}}$	$\dfrac{\varepsilon_{b0}\alpha_2}{\varepsilon_{b2}\alpha_0}$	$\dfrac{\alpha_0}{\alpha_2}$
p_2	$\dfrac{\varepsilon_{b2}}{\varepsilon_{b1}}$	$\dfrac{\varepsilon_{b2}\alpha_1}{\varepsilon_{b1}\alpha_2}$	$\dfrac{\alpha_2}{\alpha_1}$
p_3	$\dfrac{\varepsilon_{b3}}{\varepsilon_{b1}}$	$\dfrac{\varepsilon_{b3}\alpha_1}{\varepsilon_{b1}\alpha_3}$	$\dfrac{\alpha_3}{\alpha_1}$
R_0	$\dfrac{1}{2\varepsilon_{b1}q_\parallel}$	$-\dfrac{c^2\alpha_1}{2\varepsilon_{b1}\omega^2}$	$\dfrac{1}{2\alpha_1}$

In the case considered here of a GaAs-$Ga_{1-x}Al_xAs$ DHS we have $\varepsilon_{b0} = 1$, $\varepsilon_{b2} = \varepsilon_{b3}$ and hence $\alpha_2 = \alpha_3$.

Appendix B

Matrix elements of the electrodynamic Green's functions

In this appendix we represent the results for the matrix elements

$$D_{KK'}(\boldsymbol{q}_\parallel) = \int_0^a dz \int_0^a dz'\, \eta_{K0}(z)\, D(\boldsymbol{q}_\parallel; z, z')\, \eta_{K'0}(z') \tag{B1}$$

and

$$D_{\alpha\beta}^{KK'}(\boldsymbol{q}_\parallel, \omega) = \int_0^a dz \int_0^a dz'\, \xi_\alpha^{K0}(z)\, D_{\alpha\beta}(\boldsymbol{q}_\parallel; z, z' \mid \omega)\, \xi_\beta^{K'0}(z')\,. \tag{B2}$$

As mentioned in Appendix A the Green's functions consist of a special solution D^{dir} and $D_{\alpha\beta}^{\mathrm{dir}}$ of the inhomogeneous equation and of a general solution of the homogeneous equation D^{im} and $D_{\alpha\beta}^{\mathrm{im}}$, respectively. Because all steps of the calculation for (B1) and (B2) are quite similar, it is convenient to consider the generalized quantity

$$K(\boldsymbol{q}_\parallel; z, z' \mid \omega) = K^{\mathrm{dir}}(\boldsymbol{q}_\parallel; z - z' \mid \omega) + K^{\mathrm{im}}(\boldsymbol{q}_\parallel; z, z' \mid \omega)$$

with

$$K^{\mathrm{dir}}(\boldsymbol{q}_\parallel; z - z' \mid \omega) = R_0\, e^{-\gamma_1 |z - z'|}\,, \tag{B3}$$

$$K^{\mathrm{im}}(\boldsymbol{q}_\parallel; z, z' \mid \omega) = F_4(z')\, e^{\gamma_1 z} + F_5(z')\, e^{-\gamma_1 z} = R_0\{N_1(\boldsymbol{q}_\parallel, \omega)\, e^{\gamma_1 (z+z')} + N_2(\boldsymbol{q}_\parallel, \omega)\, e^{\gamma_1 (z-z')} + N_3(\boldsymbol{q}_\parallel, \omega)\, e^{-\gamma_1 (z-z')} + N_4(\boldsymbol{q}_\parallel, \omega)\, e^{-\gamma_1 (z+z')}\} \tag{B4}$$

with

$$N_1(\boldsymbol{q}_\parallel, \omega) = \{(1 + p_1)(1 - p_2)(1 + p_3)\, e^{-(\gamma_0+\gamma_1)a} e^{-(\gamma_0-\gamma_2)b} + (1 - p_1)(1 + p_2)(1 + p_3)\, e^{-(\gamma_0+\gamma_1)a} e^{-(\gamma_0+\gamma_2)b}\}/\det[I_{ij}], \tag{B5}$$

$$N_2(\boldsymbol{q}_\parallel, \omega) = \{(1 + p_1)(1 - p_2)(1 - p_3)\, e^{-(\gamma_0+\gamma_1)a} e^{(\gamma_2-\gamma_0)b} + (1 - p_1)(1 + p_2)(1 - p_3)\, e^{-(\gamma_0+\gamma_1)a} e^{-(\gamma_0+\gamma_2)b}\}/\det[I_{ij}], \tag{B6}$$

$$N_3(\boldsymbol{q}_\parallel, \omega) = \{(1 + p_1)(1 - p_2)(1 - p_3)\, e^{-(\gamma_0+\gamma_1)a} e^{(\gamma_2-\gamma_0)b} + (1 - p_1)(1 + p_2)(1 - p_3)\, e^{-(\gamma_0+\gamma_1)a} e^{-(\gamma_0+\gamma_2)b}\}/\det[I_{ij}], \tag{B7}$$

$$N_4(\boldsymbol{q}_\parallel, \omega) = \{(1 - p_1)(1 - p_2)(1 - p_3)\, e^{(\gamma_1-\gamma_0)a} e^{-(\gamma_0+\gamma_2)b} + (1 + p_1)(1 + p_2)(1 - p_3)\, e^{(\gamma_1-\gamma_0)a} e^{(\gamma_2-\gamma_0)b}\}/\det[I_{ij}]. \tag{B8}$$

Using (B3) to (B8) in (B1) or (B2), respectively, the matrix elements read

$$K_{KK'}(\boldsymbol{q}_\parallel, \omega) = K^{\mathrm{dir}}_{KK'}(\boldsymbol{q}_\parallel, \omega) + K^{\mathrm{im}}_{KK'}(\boldsymbol{q}_\parallel, \omega) \tag{B9}$$

with

$$K^{\mathrm{dir}}_{KK'}(\boldsymbol{q}_\parallel, \omega) = R_0 \left\{(\gamma_1 a)\left[\frac{\delta_{KK'} - \delta_{K,K'+2}}{(\gamma_1 a)^2 + \pi^2(K' + 2)^2} + \frac{\delta_{KK'} + \delta_{K+K',0} - \delta_{K+2,K'}}{(\gamma_1 a)^2 + (\pi K')^2}\right] - (\gamma_1 a)^2 [1 + (-1)^{K+K'} - ((-1)^K + (-1)^{K'})\, e^{-\gamma_1 a}]\, M_K(\gamma_1)\, M_{K'}(\gamma_1)\right\}; \tag{B10}$$

$$M_K(\gamma_1) = \frac{4\pi^2(K + 1)}{((\gamma_1 a)^2 + (\pi K)^2)((\gamma_1 a)^2 + \pi^2(K + 2)^2)} \tag{B11}$$

and

$$K^{\mathrm{im}}_{KK'}(\boldsymbol{q}_\parallel, \omega) = R_0\{N_1(\boldsymbol{q}_\parallel, \omega)\, H_{KK'}(\gamma_1, \gamma_1) + N_2(\boldsymbol{q}_\parallel, \omega)\, H_{KK'}(\gamma_1, -\gamma_1) + N_3(\boldsymbol{q}_\parallel, \omega)\, H_{KK'}(-\gamma_1, \gamma_1) + N_4(\boldsymbol{q}_\parallel, \omega)\, H_{KK'}(-\gamma_1, -\gamma_1)\}; \tag{B12}$$

$$H_{KK'}(\gamma_1, \gamma_2) = \gamma_1\gamma_2 a^2 (e^{\gamma_1 a}(-1)^K - 1)(e^{\gamma_2 a}(-1)^{K'} - 1)\, M_K(\gamma_1)\, M_{K'}(\gamma_2). \tag{B13}$$

We note that the form factors $f^{\mathrm{dir}}_{KK'}(\boldsymbol{q}_\parallel)$ and $f^{\mathrm{im}}_{KK'}(\boldsymbol{q}_\parallel)$ defined in (61) are given by $f^{\mathrm{dir}}_{KK'}(\boldsymbol{q}_\parallel) = 2\varepsilon_{b1} q_\parallel D^{\mathrm{dir}}_{KK'}(\boldsymbol{q}_\parallel)$ and $f^{\mathrm{im}}_{KK'}(\boldsymbol{q}_\parallel) = 2\varepsilon_{b1} q_\parallel D^{\mathrm{im}}_{KK'}(\boldsymbol{q}_\parallel)$. For the calculation of the dispersion relation of the intra- and intersubband plasmon-polariton the quantity $C_{KK'}$ defined by (98) is needed. It is easily calculated to be

$$C_{KK'} = \frac{\pi^2}{2a^3}[(K^2 + (K + 2)^2)\,\delta_{KK'} - K(K + 4)\,\delta_{K+2,K'} - (K - 2)(K + 2)\,\delta_{K-2,K'}]. \tag{B14}$$

Appendix C

Gauge invariance of the theory for layered systems

The general expression for the interacting part $\hat{H}_1(t)$ of the Hamiltonian for electrons of the Q2DEG in the presence of an electromagnetic field is

$$\hat{H}_1(t) = \int \mathrm{d}^3x \left(\hat{\varrho}(\boldsymbol{x})\, \boldsymbol{\Phi}(\boldsymbol{x}, t) - \sum_\alpha \hat{j}_\alpha(\boldsymbol{x})\, A_\alpha(\boldsymbol{x}, t) \right) . \tag{C1}$$

From this perturbation follows the induced current density

$$\begin{aligned} j_\alpha^{\mathrm{ind}}(\boldsymbol{x}, t) = \frac{i}{\hbar} \sum_\beta \int \mathrm{d}^3x' \int_{-\infty}^{t} \mathrm{d}t' \,(\mathrm{Tr}\,\{\hat{\varrho}_G[\hat{j}_\alpha(\boldsymbol{x}', t'), \hat{j}_\beta(\boldsymbol{x}, t)]\}\, A_\beta(\boldsymbol{x}', t') \\ - \mathrm{Tr}\,\{\hat{\varrho}_G[\hat{j}_\alpha(\boldsymbol{x}, t), \hat{\varrho}(\boldsymbol{x}', t')]\}\, \Phi(\boldsymbol{x}', t')) + \frac{e}{m} \mathrm{Tr}\,\{\hat{\varrho}_G \hat{\varrho}(\boldsymbol{x}, t)\}\, A_\alpha(\boldsymbol{x}, t) \end{aligned} \tag{C2}$$

and the induced charge density

$$\begin{aligned} \varrho^{\mathrm{ind}}(\boldsymbol{x}, t) = \frac{i}{\hbar} \sum_\alpha \int \mathrm{d}^3x' \int_{-\infty}^{t} \mathrm{d}t' \,(\mathrm{Tr}\,\{\hat{\varrho}_G[\hat{\varrho}(\boldsymbol{x}, t), \hat{j}_\alpha(\boldsymbol{x}', t')]\}\, A_\alpha(\boldsymbol{x}', t') \\ - \mathrm{Tr}\,\{\hat{\varrho}_G[\hat{\varrho}(\boldsymbol{x}, t), \hat{\varrho}(\boldsymbol{x}', t')]\}\, \Phi(\boldsymbol{x}', t')) . \end{aligned} \tag{C3}$$

Because of the possible gauge transformations

$$\boldsymbol{A}(\boldsymbol{x}, t) \to \boldsymbol{A}'(\boldsymbol{x}, t) = \boldsymbol{A}(\boldsymbol{x}, t) + \nabla \Lambda(\boldsymbol{x}, t)$$

and

$$\Phi(\boldsymbol{x}, t) \to \Phi'(\boldsymbol{x}, t) = \Phi(\boldsymbol{x}, t) - \frac{\partial}{\partial t} \Lambda(\boldsymbol{x}, t) \tag{C4}$$

the induced current as well as charge density is transformed according to

$$\begin{aligned} &\boldsymbol{j}^{\mathrm{ind}}(\boldsymbol{x}, t) \to \boldsymbol{j}^{\mathrm{ind}'}(\boldsymbol{x}, t) = \boldsymbol{j}^{\mathrm{ind}}(\boldsymbol{x}, t) + \delta \boldsymbol{j}^{\mathrm{ind}}(\boldsymbol{x}, t) \\ \text{and} \qquad &\varrho^{\mathrm{ind}}(\boldsymbol{x}, t) \to \varrho^{\mathrm{ind}'}(\boldsymbol{x}, t) = \varrho^{\mathrm{ind}}(\boldsymbol{x}, t) + \delta \varrho^{\mathrm{ind}}(\boldsymbol{x}, t) . \end{aligned} \tag{C5}$$

Herein $\delta \boldsymbol{j}^{\mathrm{ind}}$ and $\delta \varrho^{\mathrm{ind}}$ are given by

$$\begin{aligned} \delta j_\alpha^{\mathrm{ind}}(\boldsymbol{x}, t) = \frac{i}{\hbar} \sum_\beta \int \mathrm{d}^3x' \int_{-\infty}^{t} \mathrm{d}t' \Big(\mathrm{Tr}\,\{\hat{\varrho}_G[\hat{j}_\alpha(\boldsymbol{x}, t), \hat{j}_\beta(\boldsymbol{x}', t')]\} \frac{\partial}{\partial x_\beta} \Lambda(\boldsymbol{x}', t') \\ + \mathrm{Tr}\,\{\hat{\varrho}_G[\hat{j}_\alpha(\boldsymbol{x}, t), \hat{\varrho}(\boldsymbol{x}', t')]\} \frac{\partial}{\partial t'} \Lambda(\boldsymbol{x}', t') \Big) \\ + \frac{e}{m} \mathrm{Tr}\,\{\hat{\varrho}_G \hat{\varrho}(\boldsymbol{x}, t)\} \frac{\partial}{\partial x_\alpha} \Lambda(\boldsymbol{x}, t) \end{aligned} \tag{C6}$$

and

$$\delta\varrho^{\mathrm{ind}}(\boldsymbol{x}, t) = \frac{i}{\hbar} \sum_{\alpha} \int_{-\infty}^{t} \mathrm{d}t' \Big(\mathrm{Tr}\,\{\hat{\varrho}_G[\hat{\varrho}(\boldsymbol{x}, t), \hat{j}_\alpha(\boldsymbol{x}', t')]\} \frac{\partial}{\partial x_\alpha} \Lambda(\boldsymbol{x}', t') + \mathrm{Tr}\,\{\hat{\varrho}_G[\hat{\varrho}(\boldsymbol{x}, t), \hat{\varrho}(\boldsymbol{x}', t')]\} \frac{\partial}{\partial t'} \Lambda(\boldsymbol{x}', t') \Big). \tag{C7}$$

We note that only the electromagnetic potentials A and Φ will be affected by the gauge transformation. The operators $\hat{j}$ and $\hat{\varrho}$ do not contain these potentials and hence, they will not be affected by the gauge transformation. The theory developed in Section 4 for layered quantum well structures is gauge invariant, if both $\delta\boldsymbol{j}^{\mathrm{ind}}(\boldsymbol{x}, t)$ and $\delta\varrho^{\mathrm{ind}}(\boldsymbol{x}, t)$ vanish. To show this we start with (C6). If the first summand of this equation is integrated by parts under the condition that $\Lambda - 0$ for $t = -\infty$ and considering Born-von Kármán periodic boundary conditions in the x–y plane and vanishing electron field operators at $z = \pm\infty$, it follows

$$\begin{aligned}\delta j_\alpha^{\mathrm{ind}}(\boldsymbol{x}, t) = \frac{i}{\hbar} \sum_{\beta} \int \mathrm{d}^3x' \int_{-\infty}^{t} \mathrm{d}t' \Big(\mathrm{Tr} \Big\{ \hat{\varrho}_G \Big[\hat{j}_\alpha(\boldsymbol{x}, t), -\frac{\partial}{\partial x_\beta} \hat{j}_\beta(\boldsymbol{x}', t') \\ - \frac{\partial}{\partial t'} \hat{\varrho}(\boldsymbol{x}', t') \Big] \Big\} \Lambda(\boldsymbol{x}', t') \Big) \\ + \frac{i}{\hbar} \int \mathrm{d}^3x'\, \mathrm{Tr}\,\{\hat{\varrho}_G[\hat{j}_\alpha(\boldsymbol{x}, t), \hat{\varrho}(\boldsymbol{x}', t)]\}\, \Lambda(\boldsymbol{x}', t) \\ + \frac{e}{m} \mathrm{Tr}\,\{\hat{\varrho}_G \hat{\varrho}(\boldsymbol{x}, t)\} \frac{\partial}{\partial x_\alpha} \Lambda(\boldsymbol{x}, t)\,. \end{aligned} \tag{C8}$$

With the equation of motion

$$\frac{\partial}{\partial t} \hat{\varrho}(\boldsymbol{x}, t) = \frac{i}{\hbar} [\hat{H}_0, \hat{\varrho}(\boldsymbol{x}, t)]\,, \tag{C9}$$

where $\hat{H}_0$ is given by (45) one can derive

$$\frac{\partial}{\partial t} \hat{\varrho}(\boldsymbol{x}, t) + \sum_{\alpha} \frac{\partial}{\partial x_\alpha} \hat{j}_\alpha(\boldsymbol{x}, t) = 0\,. \tag{C10}$$

With (C10) the first term of (C8) vanishes. For the second term of (C8) it follows

$$\begin{aligned} &\frac{i}{\hbar} \int \mathrm{d}^3x'\, \mathrm{Tr}\,\{\hat{\varrho}_G[\hat{j}_\alpha(\boldsymbol{x}, t), \hat{\varrho}(\boldsymbol{x}', t)]\}\, \Lambda(\boldsymbol{x}', t) \\ &= -\frac{e}{m} \mathrm{Tr}\,\{\hat{\varrho}_G \hat{\varrho}(\boldsymbol{x}, t)\} \frac{\partial}{\partial x_\alpha} \Lambda(\boldsymbol{x}, t)\,. \end{aligned} \tag{C11}$$

Hence, $\delta\boldsymbol{j}^{\mathrm{ind}}$ vanishes identically. It is possible to show by the same steps that $\delta\varrho^{\mathrm{ind}}$ also vanishes identically. Consequently, the theory is gauge invariant for any layered structure.

We note that $\boldsymbol{j}^{\mathrm{ind}}(\boldsymbol{x}, t)$ and $\varrho^{\mathrm{ind}}(\boldsymbol{x}, t)$ given in (C2) and (C3) satisfy the equation of continuity which is easily shown.

Appendix D

The optical limit of the macroscopic dielectric tensor

In this appendix we derive from the RPA polarization tensor a macroscopic expression of the dielectric tensor in the optical limit, i.e. for $q_{\parallel} \to 0$. The RPA polarization tensor in the EQL is given by

$$P_{\alpha\beta}(\boldsymbol{q}_{\parallel} \to 0; z, z' \mid \omega) = \sum_{K} \chi^{K}_{\alpha\beta}(\boldsymbol{q}_{\parallel} \to 0 \mid \omega)\, \xi^{K0}_{\alpha}(z)\, \xi^{K0}_{\beta}(z')\,. \tag{D1}$$

Using (98), (100), (102), and (104) it follows

$$P_{xx}(0; z, z' \mid \omega) = -\frac{n_{2DEG}e^2}{m} \sum_{K=0,1,2,\ldots} \left(1 + \frac{v_F k_F}{2} \frac{\Omega_{K0}}{\omega^2 - \Omega^2_{K0}}\right) \eta_{K0}(z)\, \eta_{K0}(z')\,, \tag{D2}$$

$$P_{yy}(0; z, z' \mid \omega) = P_{xx}(0; z, z' \mid \omega)\,, \tag{D3}$$

$$P_{xz}(0; z, z' \mid \omega) = P_{zx}(0; z, z' \mid \omega) = 0\,, \tag{D4}$$

and

$$P_{zz}(0; z, z' \mid \omega) = -\frac{n_{2DEG}e^2}{m} \sum_{K \neq 0} \frac{(\hbar\omega)^2}{2m\Omega_{K0}(\omega^2 - \Omega^2_{K0})}\, g_{K0}(z)\, g_{K0}(z')\,. \tag{D5}$$

Because the wavelength of the light in the relevant region (infrared) is large in comparison to the thickness of the quantum well, it is possible to average the physical quantities over the layer thickness. Then we have for the optically induced current density

$$j^{opt}_{\alpha}(\boldsymbol{q}_{\parallel}; z \mid \omega) = \sum_{\beta} A^{opt}_{\beta}(\boldsymbol{q}_{\parallel}; z \mid \omega) \left\{\frac{1}{a} \int dz \int dz'\, P_{\alpha\beta}(0; z, z' \mid \omega)\right\}$$

$$\equiv \sum_{\beta} P^{opt}_{\alpha\beta}(\omega)\, A^{opt}_{\beta}(\boldsymbol{q}_{\parallel}; z \mid \omega) \tag{D6}$$

with

$$P^{opt}_{xx}(\omega) = P^{opt}_{yy}(\omega) = -\frac{n_{2DEG}e^2}{ma} \tag{D7}$$

and

$$P^{opt}_{zz}(\omega) = -\frac{n_{2DEG}e^2}{ma} \sum_{K \neq 0} \frac{\omega^2 f_{K0}}{\omega^2 - \Omega^2_{K0}}\,. \tag{D8}$$

Herein f_{K0} denotes the oscillator strength given by

$$f_{K0} = (1 - (-1)^K)^2\, \frac{64(K+1)^2}{\pi^2 K^3 (K+2)^3}\,. \tag{D9}$$

Because of the symmetry the selection rule $f_{20} = f_{40} = f_{60} = \ldots = 0$ is valid. In the calculation of (D7) and (D8) we have used

$$\int_0^a dz\, \eta_{K0}(z) = \delta_{K0} \tag{D10}$$

and

$$\int_0^a \mathrm{d}z\, g_{K0}(z) = \frac{8}{a}\frac{K+1}{K(K+2)}\left(1-(-1)^K\right). \tag{D11}$$

With the standard relation between the polarization tensor and the dielectric tensor (35), the local macroscopic dielectric tensor in the optical limit is given by

$$\varepsilon_{xx}(\omega) = \varepsilon_{yy}(\omega) = \varepsilon_{b1}\left(1 - \frac{\omega_0^2}{\omega^2}\right), \tag{D12}$$

$$\varepsilon_{zz}(\omega) = \varepsilon_{b1}\left(1 - \sum_{K\neq 0}\frac{\omega_0^2 f_{K0}}{\omega^2 - \Omega_{K0}^2}\right), \tag{D13}$$

$$\varepsilon_{xy}(\omega) = \varepsilon_{yx}(\omega) = \varepsilon_{xz}(\omega) = \varepsilon_{zx}(\omega) = 0 \tag{D14}$$

with the plasma frequency $\omega_0^2 = n_{2DEG}e^2/(\varepsilon_0\varepsilon_{b1}ma)$.

References

[1] T. Ando, A. B. Fowler, and F. Stern, Rev. mod. Phys. **54**, 437 (1982).
[2] T. Mimura, S. Hiyamizu, T. Fujii, and K. Nambu, Japan. J. appl. Phys. **19**, L225 (1980).
[3] K. von Klitzing, G. Dorda, and M. Pepper, Phys. Rev. Letters **45**, 494 (1980).
[4] D. C. Tsui, H. L. Störmer, and A. C. Gossard, Phys. Rev. Letters **48**, 1559 (1982).
[5] R. Dingle, W. Wiegmann, and C. H. Henry, Phys. Rev. Letters **33**, 827 (1974).
[6] A. B. Fowler, A. Hartstein, and R. A. Webb, Phys. Rev. Letters **48**, 196 (1982).
[7] B. J. van Wees, H. van Houten, C. W. J. Beenakker, J. G. Williamson, L. P. Kouwenhoven, D. van der Marel, and C. T. Foxon, Phys. Rev. Letters **60**, 848 (1988).
[8] D. A. Wharam, T. J. Thornton, R. Newbury, M. Pepper, H. Ahmed, J. E. F. Frost, D. G. Hasko, D. C. Peacock, D. A. Ritchie, and G. A. C. Jones, J. Phys. C **21**, L209 (1988).
[9] R. H. Ritchie, Phys. Rev. **106**, 874 (1957).
[10] R. A. Ferrell, Phys. Rev. **111**, 1214 (1958).
[11] F. Stern, Phys. Rev. Letters **18**, 546 (1967).
[12] H. Ehrenreich and M. H. Cohen, Phys. Rev. **115**, 786 (1959).
[13] A. V. Chaplik, Zh. eksper. teor. Fiz. **62**, 746 (1972) (Soviet Phys. – J. exper. theor. Phys. **35**, 395 (1972)).
[14] P. B. Visscher and L. M. Falicov, Phys. Rev. B **3**, 2541 (1971).
[15] A. L. Fetter, Ann. Phys. (USA) **81**, 367 (1973); **88**, 1 (1974).
[16] M. Apostol, Z. Phys. B **22**, 13 (1975).
[17] G. F. Giuliani and J. J. Quinn, Phys. Rev. Letters **51**, 919 (1983).
[18] J. K. Jain, Phys. Rev. B **32**, 5456 (1985).
[19] D. Grecu, J. Phys. C **8**, 2627 (1975).
[20] J. K. Jain and P. B. Allen, Phys. Rev. Letters **54**, 2437 (1985).
[21] K. W. Chiu and J. J. Quinn, Phys. Rev. B **9**, 4724 (1974).
[22] N. J. M. Horing and M. M. Yildiz, Ann. Phys. (USA) **97**, 216 (1976).
[23] C. Kallin and B. I. Halperin, Phys. Rev. B **30**, 5655 (1984).
[24] A. H. MacDonald, J. Phys. C **18**, 1003 (1985).
[25] M. Kobayashi, J. Mizuno, and I. Yokota, J. Phys. Soc. Japan **39**, 18 (1975).
[26] S. Das Sarma and J. J. Quinn, Phys. Rev. B **25**, 7603 (1982).
[27] W. L. Bloss and E. M. Brody, Solid State Commun. **43**, 523 (1982).
[28] A. C. Tselis and J. J. Quinn, Phys. Rev. B **29**, 3318 (1984).
[29] W. Gasser and U. C. Täuber, Z. Phys. B **69**, 87 (1987).
[30] A. Caillé, M. Banville, and M. J. Zuckermann, Solid State Commun. **24**, 805 (1977).
[31] Wu Xiaoguang, F. M. Peeters, and J. T. Devreese, Phys. Rev. B **32**, 6982 (1985).

[32] F. M. PEETERS, WU XIAOGUANG, and J. T. DEVREESE, Phys. Rev. B **36**, 7518 (1987).
[33] W. P. CHEN, Y. J. CHEN, and E. BURSTEIN, Surface Sci. **58**, 263 (1976).
[34] D. DAHL and L. J. SHAM, Phys. Rev. B **16**, 651 (1977).
[35] A. EGUILUZ and A. A. MARADUDIN, Ann. Phys. (USA) **113**, 29 (1978).
[36] A. C. TSELIS and J. J. QUINN, Surface Sci. **113**, 362 (1982).
[37] W. L. BLOSS, Solid State Commun. **46**, 143 (1983).
[38] G. GONZALES DE LA CRUZ, A. C. TSELIS, and J. J. QUINN, J. Phys. Chem. Solids **44**, 807 (1983).
[39] P. HAWRYLAK, J. W. WU, and J. J. QUINN, Phys. Rev. B **31**, 7855 (1985).
[40] R. D. KING-SMITH and J. C. INKSON, Phys. Rev. B **33**, 5489 (1986).
[41] W. H. BACKES, F. M. PEETERS, F. BROSENS, and J. T. DEVREESE, Phys. Rev. B **45**, 8437 (1992).
[42] L. WENDLER and R. PECHSTEDT, phys. stat. sol. (b) **138**, 197 (1986).
[43] L. WENDLER and R. PECHSTEDT, Phys. Rev. B **35**, 5887 (1987).
[44] L. WENDLER and R. PECHSTEDT, phys. stat. sol. (b) **141**, 129 (1987).
[45] L. WENDLER, Solid State Commun. **65**, 1197 (1988).
[46] L. WENDLER, R. HAUPT, and V. G. GRIGORYAN, phys. stat. sol. (b) **149**, K123 (1988).
[47] L. WENDLER and V. G. GRIGORYAN, Solid State Commun. **71**, 527 (1989).
[48] L. WENDLER, R. HAUPT, and V. G. GRIGORYAN, Physica (Utrecht) **B167**, 91, 101, 113 (1990).
[49] L. WENDLER and R. PECHSTEDT, J. Phys., Condensed Matter **2**, 8881 (1990).
[50] L. WENDLER, phys. stat. sol. (b) **129**, 513 (1985).
[51] L. WENDLER and R. HAUPT, phys. stat. sol. (b) **141**, 493 (1987).
[52] L. WENDLER and R. HAUPT, phys. stat. sol. (b) **143**, 487 (1987).
[53] S. DAS SARMA, Phys. Rev. B **29**, 2334 (1984).
[54] J. K. JAIN and S. DAS SARMA, Phys. Rev. B **36**, 5949 (1987).
[55] M. JONSON, J. Phys. C **9**, 3055 (1976).
[56] A. K. RAJAGOPAL, Phys. Rev. B **15**, 4264 (1977).
[57] A. CZACHOR, A. HOLAS, S. R. SHARMA, and K. S. SINGWI, Phys. Rev. B **25**, 214 (1982).
[58] J. C. RYAN, Phys. Rev. B **43**, 4499 (1991).
[59] W. HANSEN, M. HORST, J. P. KOTTHAUS, U. MERKT, CH. SIKORSKI, and K. PLOOG, Phys. Rev. Letters **58**, 2586 (1987).
[60] T. DEMEL, D. HEITMANN, P. GRAMBOW, and K. PLOOG, Phys. Rev. B **38**, 12732 (1988).
[61] QUIANG LI and S. DAS SARMA, Phys. Rev. B **40**, 5860 (1989).
[62] A. GOLD and A. GHAZALI, Phys. Rev. B **41**, 7626 (1990).
[63] L. WENDLER, R. HAUPT, and R. PECHSTEDT, Phys. Rev. B **43**, 14669 (1991).
[64] W.-M. QUE and G. KIRCZENOW, Phys. Rev. B **39**, 5998 (1989).
[65] H. L. CUI, X. J. LU, N. J. M. HORING, and X. L. LEI, Phys. Rev. B **40**, 3443 (1989).
[66] C. C. GRIMES and G. ADAMS, Phys. Rev. Letters **36**, 145 (1976).
[67] S. J. ALLEN, JR., D. C. TSUI, and R. A. LOGAN, Phys. Rev. B **38**, 980 (1977).
[68] T. N. THEIS, J. P. KOTTHAUS, and P. J. STILES, Solid State Commun. **24**, 273 (1977).
[69] D. C. TSUI, E. GORNIK, and R. A. LOGAN, Solid State Commun. **35**, 875 (1980).
[70] E. BATKE, D. HEITMANN, and C. W. TU, Phys. Rev. Letters **34**, 6951 (1986).
[71] D. OLEGO, A. PINCZUK, A. C. GOSSARD, and W. WIEGMANN, Phys. Rev. B **25**, 7867 (1982).
[72] R. SOORYAKUMAR, A. PINCZUK, A. C. GOSSARD, and W. WIEGMANN, Phys. Rev. B **31**, 2578 (1985).
[73] G. FASOL, N. MESTRES, H. P. HUGHES, A. FISCHER, and K. PLOOG, Phys. Rev. Letters **56**, 2517 (1986).
[74] A. PINCZUK, M. G. LAMONT, and A. C. GOSSARD, Phys. Rev. Letters **56**, 2092 (1986).
[75] T. N. THEIS, Surface Sci. **98**, 515 (1980).
[76] R. A. HÖPFEL and E. GORNIK, Surface Sci. **142**, 412 (1984).
[77] A. V. CHAPLIK, Surface Sci. Rep. **5**, 289 (1985).
[78] D. HEITMANN, Surface Sci. **170**, 332 (1986).
[79] E. BATKE, Adv. Solid State Phys. **31**, 297 (1991).
[80] M. V. KRASHENINNIKOV, M. B. SULTANOV, and A. V. CHAPLIK, Zh. eksper. teor. Fiz. **77**, 1636 (1979) (Soviet Phys. — J. exper. theor. Phys. **50**, 821 (1979)).
[81] A. V. CHAPLIK and M. V. KRASHENINNIKOV, Solid State Commun. **27**, 1297 (1978).
[82] B. I. HALPERIN, Japan. J. appl. Phys. **26**, Suppl. 26-3, 1913 (1987).
[83] M. SHAYEGAN, T. SAJOTO, M. SANTOS, and C. SILVESTRE, Appl. Phys. Letters **53**, 791 (1988).

[84] E. G. GWINN, R. M. WESTERVELT, P. F. HOPKINS, A. J. RIMBERG, M. SUNDARAM, and A. C. GOSSARD, Phys. Rev. B **39**, 6260 (1989).
[85] V. CELLI and D. N. MERMIN, Phys. Rev. B **140**, A839 (1965).
[86] Z. TESANOVICH and B. I. HALPERIN, Phys. Rev. B **36**, 4888 (1987).
[87] A. H. MACDONALD and G. W. BRYANT, Phys. Rev. Letters **58**, 515 (1987).
[88] A. WIXFORTH, M. SUNDARAM, J. H. ENGLISH, and A. C. GOSSARD, Phys. Rev. B **43**, 10000 (1991).
[89] M. KALOUDIS, K. ENSSLIN, A. WIXFORTH, M. SUNDARAM, J. H. ENGLISH, and A. C. GOSSARD, Phys. Rev. B **46**, 12469 (1992).
[90] L. WENDLER and E. KÄNDLER, Phys. Letters A **146**, 339 (1990).
[91] A. C. TSELIS and J. J. QUINN, Phys. Rev. B **29**, 2021 (1984).
[92] T. TOYODA, V. GUDMUNDSSON, and Y. TAKAHASHI, Physica (Utrecht) **A127**, 529 (1984).
[93] R. D. KING-SMITH and J. C. INKSON, Phys. Rev. B **36**, 4796 (1987).
[94] A. L. FETTER and J. D. WALECKA, Quantum Theory of Many-Particle Systems, McGraw-Hill Publ. Co., New York 1971.
[95] R. KUBO, J. Phys. Soc. Japan **12**, 570 (1957).
[96] G. D. MAHAN, Many-Particle Physics, Plenum Press, New York 1981.
[97] A. A. ABRIKOSOV, L. P. GORKOV, and I. E. DZYALOSHINSKY, Methods of Quantum Field Theory in Statistical Physics, Prentice-Hall, Englewood Cliffs (N. J.) 1963.
[98] L. WENDLER and R. HAUPT, phys. stat. sol. (b) **143**, 131 (1987).
[99] S. ADACHI, J. appl. Phys. **58**, R1 (1985).
[100] L. WENDLER and R. HAUPT, J. appl. Phys. **59**, 3289 (1986).
[101] W. P. CHEN, Y. J. CHEN, and E. BURSTEIN, Surface Sci. **58**, 263 (1976).
[102] S. J. ALLEN, D. C. TSUI, and B. VINTER, Solid State Commun. **20**, 425 (1976).
[103] T. ANDO, J. Phys. Soc. Japan **51**, 3893 (1982).
[104] L. WENDLER, phys. stat. sol. (b) **123**, 469 (1984).

(Received February 26, 1993)